USGS
science for a changing world

The Performance of Nearshore Dredge Disposal at Ocean Beach, San Francisco, California, 2005-2007

By Patrick L. Barnard, Li H. Erikson, Jeff E. Hansen, and Edwin Elias

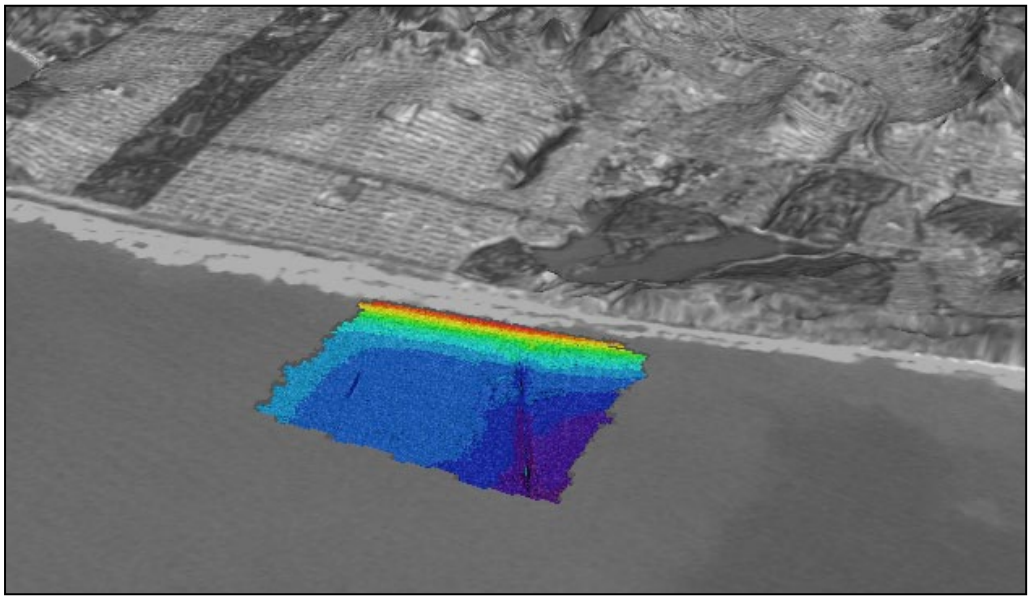

Open-File Report 2008-1347

U.S. Department of the Interior
U.S. Geological Survey

U.S. Department of the Interior
KEN SALAZAR, Secretary

U.S. Geological Survey
Suzette M. Kimball, Acting Director

U.S. Geological Survey, Reston, Virginia 2009

For product and ordering information:
World Wide Web: http://www.usgs.gov/pubprod
Telephone: 1-888-ASK-USGS

For more information on the USGS—the Federal source for science about the Earth,
its natural and living resources, natural hazards, and the environment:
World Wide Web: http://www.usgs.gov
Telephone: 1-888-ASK-USGS

Suggested citation:
Barnard, P.L., Erikson, L.H., Hansen, J.E., and Elias, E., 2009. The Performance of nearshore dredge disposal at Ocean Beach, San Francisco, California, 2005-2007: U.S. Geological Survey Open-File Report 2008-1347, 93 p. [http://pubs.usgs.gov/of/2008/1347/].

Contents

Tables

Figures

The Performance of Nearshore Dredge Disposal at Ocean Beach, San Francisco, California, 2005-2007

By Patrick L. Barnard[1], Li H. Erikson[2], Jeff E. Hansen[3], and Edwin Elias[4]

Executive Summary

Ocean Beach, California, contains an erosion hot spot in the shadow of the San Francisco ebb tidal delta that threatens valuable public infrastructure as well as the safe recreational use of the beach. In an effort to reduce the erosion at this location a new plan for the management of sediment dredged annually from the main shipping channel at the mouth of San Francisco Bay was implemented in May 2005 by the United States Army Corps of Engineers, San Francisco District (USACE). The USACE designated a temporary nearshore dredge disposal site for the annual disposal of about 230,000 m^3 (300,000 yd^3) of sand about 750 m offshore and slightly south of the erosion hot spot, in depths between approximately 9 and 14 m. The site has now been used three times for a total sediment disposal of about 690,000 m^3 (about 900,000 yds^3). The disposal site was chosen because it is in a location where strong tidal currents and open-ocean waves can potentially feed sediment toward the littoral zone in the reach of the beach that is experiencing critical erosion, as well as prevent further scour on an exposed outfall pipe. The onshore migration of sediment from the target disposal location might feed the primary longshore bar or the nearshore zone, and provide a buffer to erosion that peaks during winter months when large waves impact the region. The United States Geological Survey (USGS) has been monitoring and modeling the bathymetric evolution of the test dredge disposal site and the adjacent coastal region since inception in May 2005. This paper reports on the first 2.5 years of this monitoring program effort (May 2005 to December 2007) and assesses the short-term coastal response. Here are the key findings of this report:

- Approximately half of the sediment that has been placed in the nearshore dredge-disposal site during the 2.5 years of this study remains within the dredge focus area.
- In the winter of 2006-7, large waves transported the dredge-mound material onshore.
- High rates of seasonal cross-shore sediment transport mask any potential profile change in the Coastal Profiling System data due to dredge placement.
- Pockets of accretion have been recorded by topographic surveying adjacent to the dredge site, but it is unclear if the accretion is linked to the nourishment.

[1]Research Geologist, Coastal and Marine Geology Team, Santa Cruz, CA, pbarnard@usgs.gov.
[2]Coastal Engineer, Coastal and Marine Geology Team, Santa Cruz, CA, lerikson@usgs.gov.
[3]Department of Earth and Planetary Sciences, University of California, Santa Cruz, jehansen@pmc.ucsc.edu.
[4]Coastal Engineer, Deltares, Delft, The Netherlands, eelias@usgs.gov.

- Cross-shore profile modeling suggests that dredge material must be placed in water depths no greater than 5 m to drive a positive shoreline response.
- Area modeling demonstrates that the new dredge site increases wave dissipation and modifies local sediment-transport patterns, although the effect on the nearshore morphology is largely negligible.
- Any increase in beach width or wave energy-dissipation related to the nourishment is likely to be realized only in the vicinity directly onshore of the nourishment site, which is several hundred meters south of the area of critical erosion.
- Larger waves from the northwest and smaller waves from the west or southwest contribute most to the sediment transport from the dredge mound onshore.

Introduction

Ocean Beach, California, contains an erosion hot spot in the shadow of the San Francisco ebb tidal delta that threatens valuable public infrastructure, as well as the safe recreational use of the beach (fig. 1). In an effort to reduce the erosion at this location, a new plan for the management of sediment dredged annually from the main shipping channel at the mouth of San Francisco Bay was implemented in May 2005 by the United States Army Corps of Engineers, San Francisco District (USACE). The USACE designated a temporary nearshore dredge-disposal site for the annual disposal of about 230,000 m^3 of sand, about 750 m offshore and slightly south of the erosion hot spot, in depths between approximately 9 and 14 m. The site has been used three times for a total sediment disposal of about 690,000 m^3. The site was chosen because it is located where strong tidal currents and open-ocean waves can feed sediment toward the littoral zone in the reach of the beach that is experiencing critical erosion; dredge disposal at this site as helps to prevent further scour on an exposed outfall pipe. The onshore migration of sediment from the target disposal location might feed the primary longshore bar or the nearshore zone and provide a buffer to erosion that peaks during winter months when large waves impact the region. The U.S. Geological Survey (USGS) has been monitoring and modeling the bathymetric evolution of the test dredge-disposal site and the adjacent coastal region since May 2005. This paper reports on the first 2.5 years of this monitoring program effort (May 2005 - December 2007) and assesses the short-term coastal response.

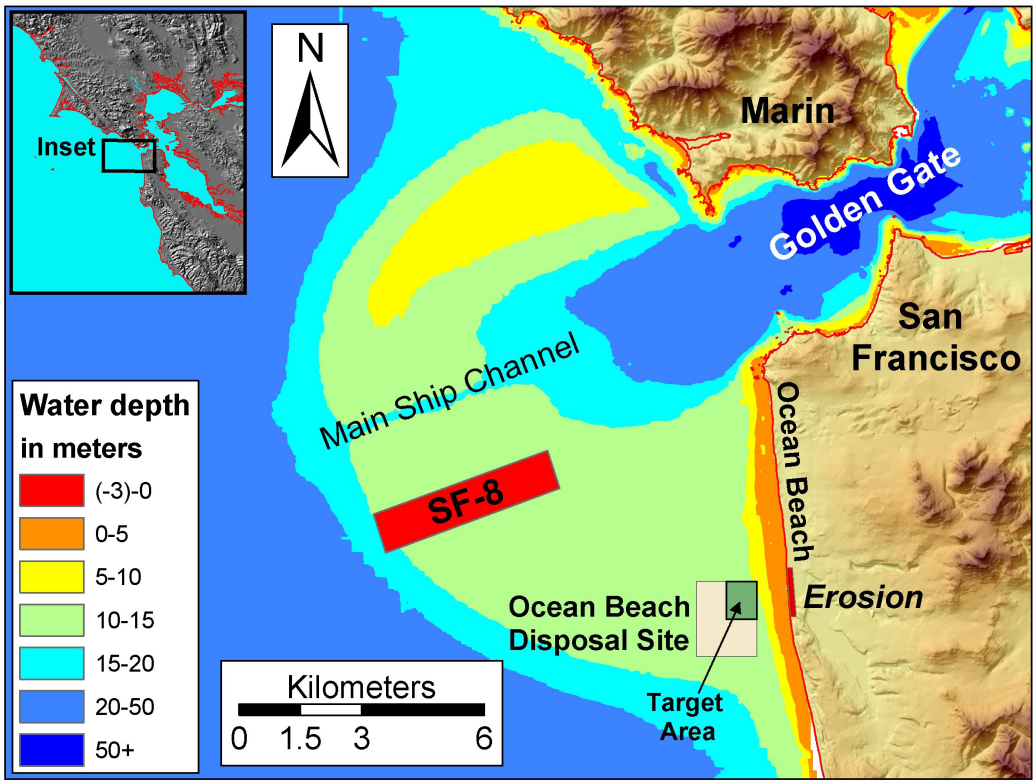

Figure 1. Map of the study area showing the location of the existing dredge- disposal site (SF-8) and the test-dredge disposal site (Ocean Beach Disposal Site, Ocean Beach, San Francisco, California). Bathymetry is from a 1956 National Ocean Service (NOS) survey.

Objectives

The objectives of this report are to

- Evaluate nearshore and beach change in the vicinity of the nearshore dredge-disposal site during a 2.5-year monitoring period,
- Present the results of applied numerical-modeling efforts, and
- Discuss research findings as they relate to coastal-management options.

Background

The USGS has been conducting field research at the mouth of San Francisco Bay, with an emphasis on Ocean Beach, since April 2004 (Barnard, 2005; Barnard and Hanes 2005, 2006, 2007; Barnard and others [2006a, b, 2007a, b]; Erikson and others, 2007; Eshleman and others, 2007; Hanes and Barnard, 2007; Hansen, 2007). Much of this work complements the research described in this report. The Ocean Beach Coastal Processes Study (website: http://walrus.wr.usgs.gov/coastal_processes/) includes monthly topographic-beach surveys, quarterly cross-shore bathymetric profiles, grain-size analyses, numerical modeling, video monitoring, wave and current measurements, and multibeam/side-scan bathymetric surveys in collaboration with the Seafloor Mapping Lab at California State University, Monterey Bay (SFML), and USACE. The goal of this project is to define the dominant sediment-transport pathways at the mouth of San Francisco Bay and to determine the cause of erosion at Ocean Beach. A complete summary of work to date, including detailed descriptions of the methods and data, is available online at http://pubs.usgs.gov/of/2007/1217/.

The southern portion of Ocean Beach has been eroding for decades, anecdotally, with a recent comparison of datum-based shorelines indicating an average retreat rate of about 1.1 m/yr in Reaches 5 and 6 (see fig. 2 and table 1 for reach and profile designations) during the last decade (fig. 3; Barnard and others, 2007a). However, erosion along some sections in the south has become so severe that the mean high water (MHW) line on the planar beach no longer exists and, therefore, cannot be calculated. Although there are local anomalies based on large-scale horn and cusp locations, since1997-8 there is a pronounced trend of accretion in the northern and central portions and of Ocean Beach (profiles 1-80) and erosion in the vicinity of Sloat Boulevard (profile 95) in the southern portion of Ocean Beach (profiles 80-120). Overall, the entire beach MHW line accreted an average of 5.8 m (range = -18.8 - +41.8 m) from October 1997 to October 2004, and 2.7 m from April 1998 to April 2006 (range = -49.4 - +42.1 m). Reach 5 (profiles 89-100) showed the highest amount of erosion along Ocean Beach, with 15.1 m of shoreline retreat as measured from the fall of 1997 to 2006 (Barnard and others, 2007a). Shoreline-change rates determined by Hapke and others (2006) for the Ocean Beach area indicate that the long-term (mid to late 1800's-1998) and short-term (1950s-1998) rates are stable at the northern end (about 0 m/yr) but become strongly erosional toward the south (about 1-2 m/yr).

During multibeam surveys in 2004 and May 2005, large bedforms were mapped with asymmetry measurements indicating pronounced alongshore sediment transport just outside the surf zone at Ocean Beach in water depths of about 10 m (fig. 4*A*). Approximately 2 km north of the erosion hot spot, there is evidence of shoreward migrating, 5-10 m wavelength bedforms (fig. 4*B*). As close as 700 m offshore of the region experiencing erosion, multibeam surveys revealed

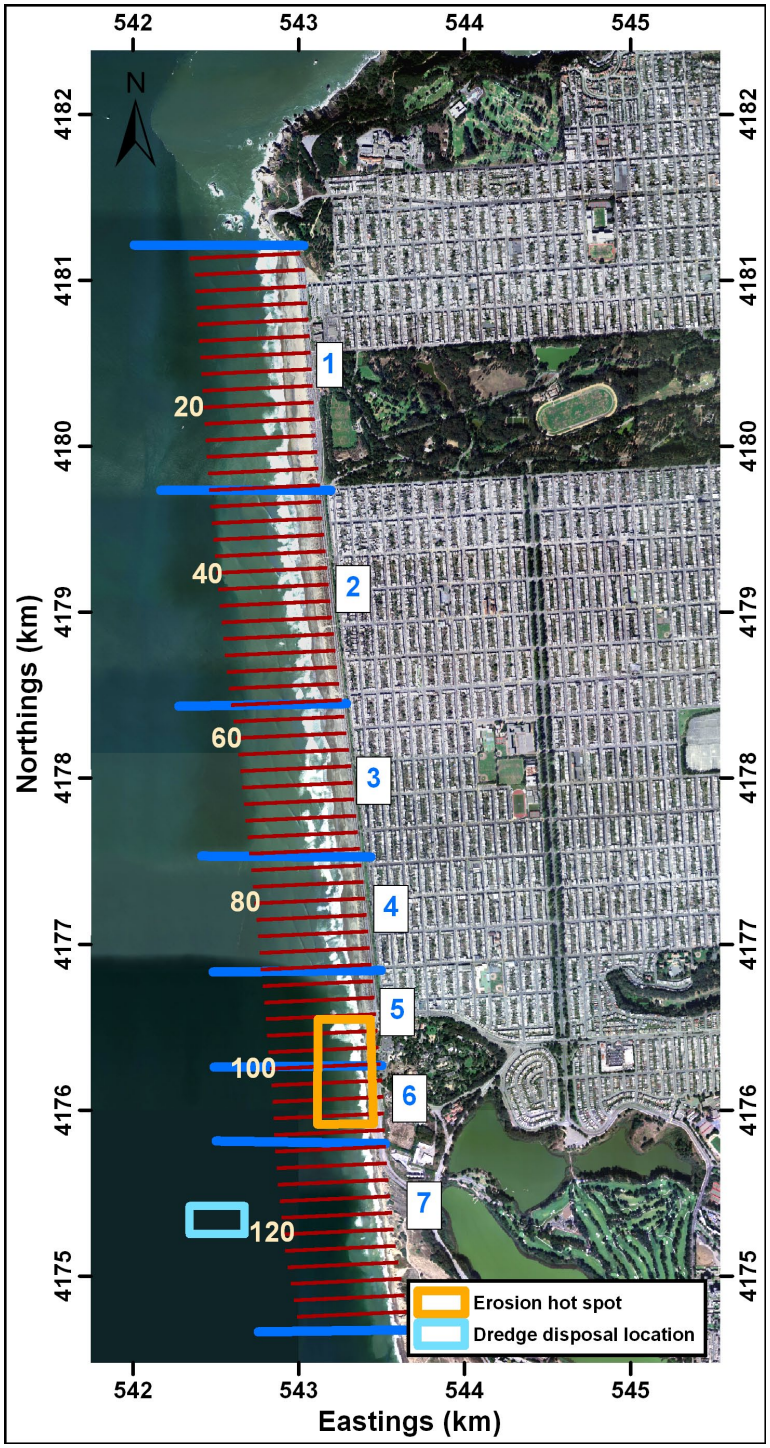

Figure 2. Map of the reach locations (area between blue lines) and profile numbers (red lines [every other line shown], see also table 1) for Ocean Beach, San Francisco, California. The area of chronic erosion is indicated by the orange box located primarily in Reach 5 and 6, the center location of the dredge disposal is indicated by the blue box.

Table 1. Reach designations at Ocean Beach, California.

	Name	Length, in meters	Profile range Start	End
Reach 1	North End/ O'Shougnessy Sea Wall	1,477	1	30
Reach 2	Dune Field- S of Lincoln	1,282	31	56
Reach 3	New Sea Wall	925	57	74
Reach 4	Dune Field- N of Sloat	684	75	88
Reach 5	North of pinch point (N Sloat)	574	89	100
Reach 6	South of pinch point (S Sloat)	467	101	109
Reach 7	Ft. Funston	1,442	110	138

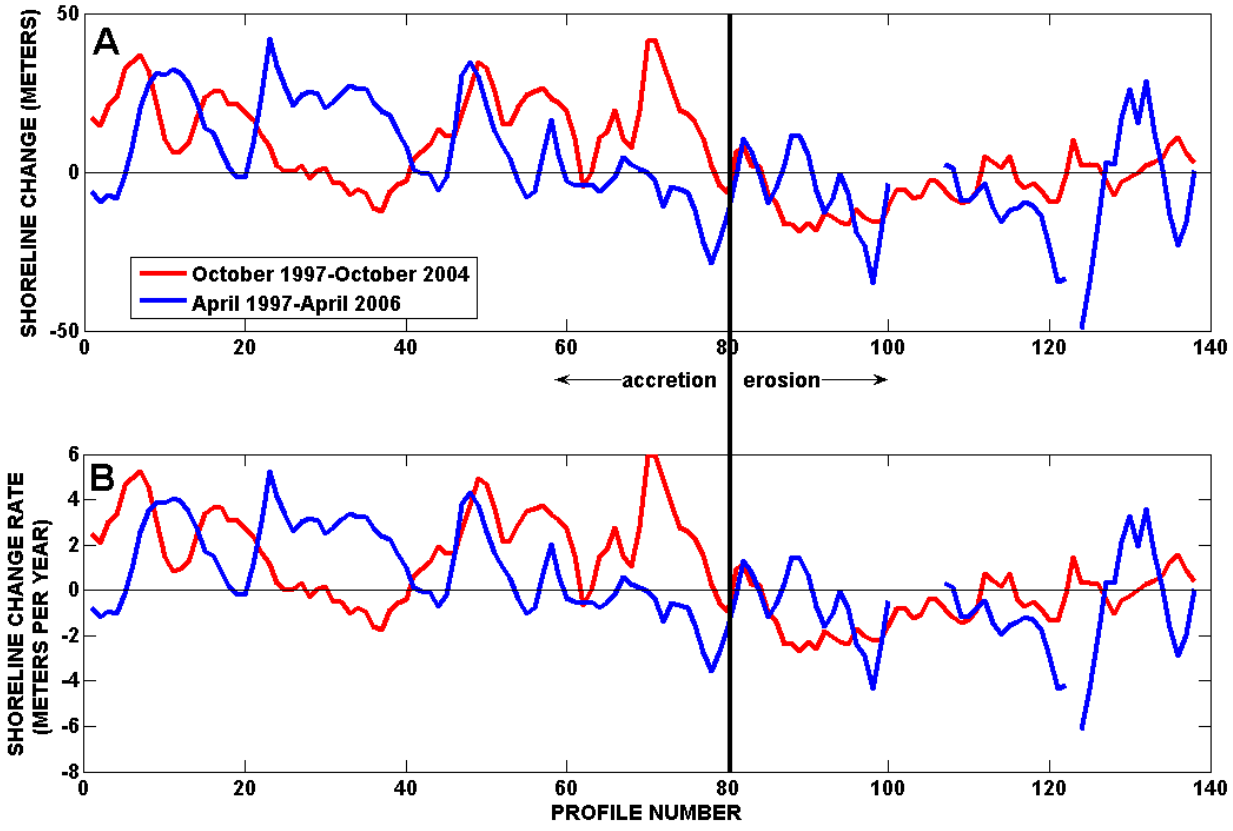

Figure 3. *A* Mean High Water Shoreline change and *B*, rate since LIDAR data was collected in 1997-98. The red line represents the rate as determined from the fall beach (October 1997-October 2004). The blue line represents the rate as determined from the spring beach (April 1997-April 2006).

that sediment covering the Southwest Ocean Outfall, a pipe which transports one-third of the City of San Francisco's treated sewage out to sea, has been scoured by strong tidal currents and the pipe may be severely exposed in water depths ranging from 10 to 14 m (figs. 4*C*, A1, A14). It is unknown whether the structural integrity of the pipe has been compromised. Despite massive amounts of sediment loss at the mouth of San Francisco Bay during the last half-century, in corroboration with anecdotal reports from dredge-ship captains, the multibeam survey also demonstrated significant amounts of accretion at the Main Ship Channel dredge-disposal site, SF-8 (fig. 5; Barnard and others, 2007a). Annual disposal of dredged sediment in this region since 1971 caused steady shoaling to the point that recent navigation had become hazardous, triggering the USACE to seek a new disposal site. The large mounds in and around SF-8 attributed to the annual disposal total 4.3 million m^3 of sediment accretion, an average of 60 cm of shoaling with a maximum of 2 m vertical accretion.

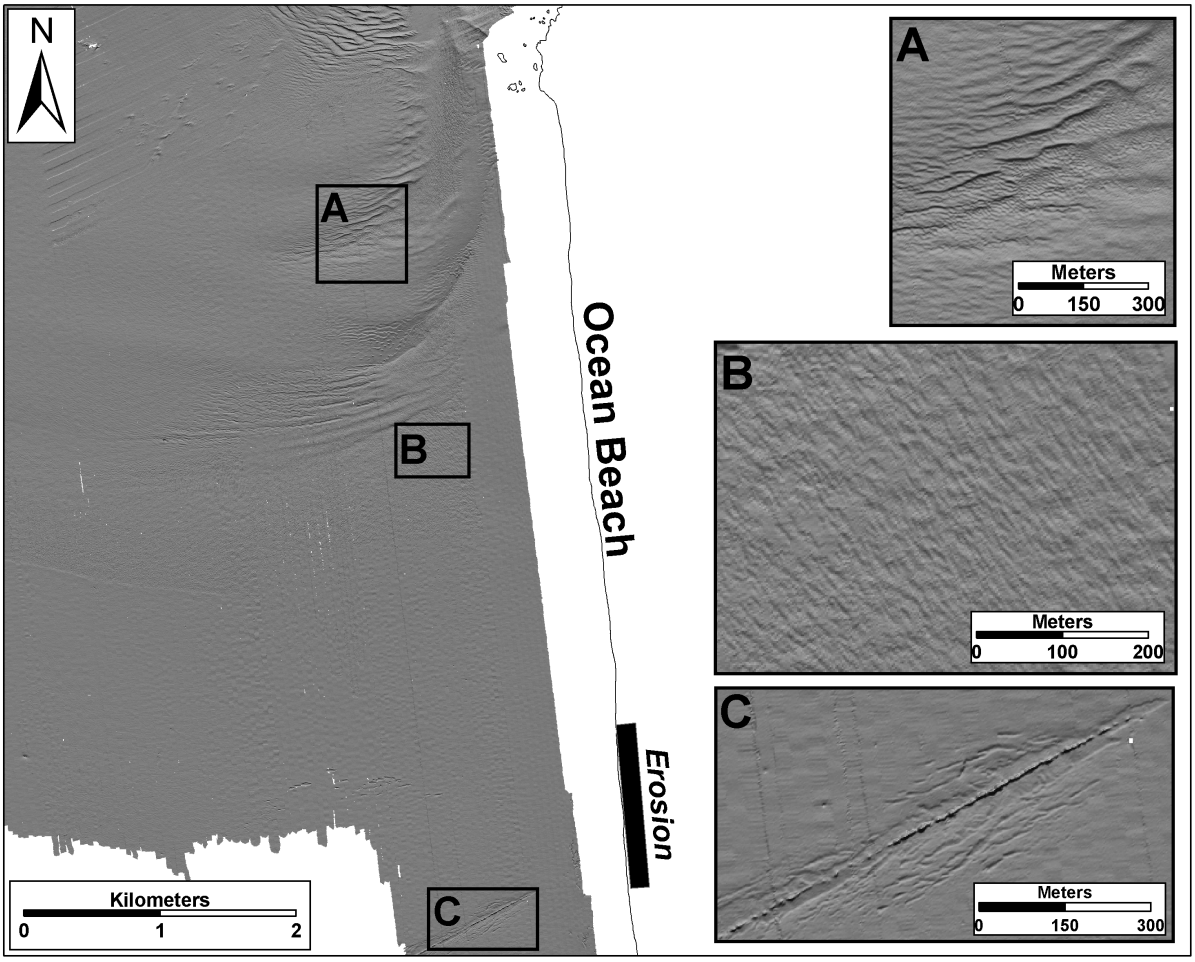

Figure 4. Multibeam survey from 2004 showing *A*, alongshore migrating bedforms, *B*, onshore-directed bedform morphologies north of the disposal site, and *C*, intense scour associated with the outfall pipe, the approximate site of the June 2005 dredge disposal (from Barnard and others, 2007a).

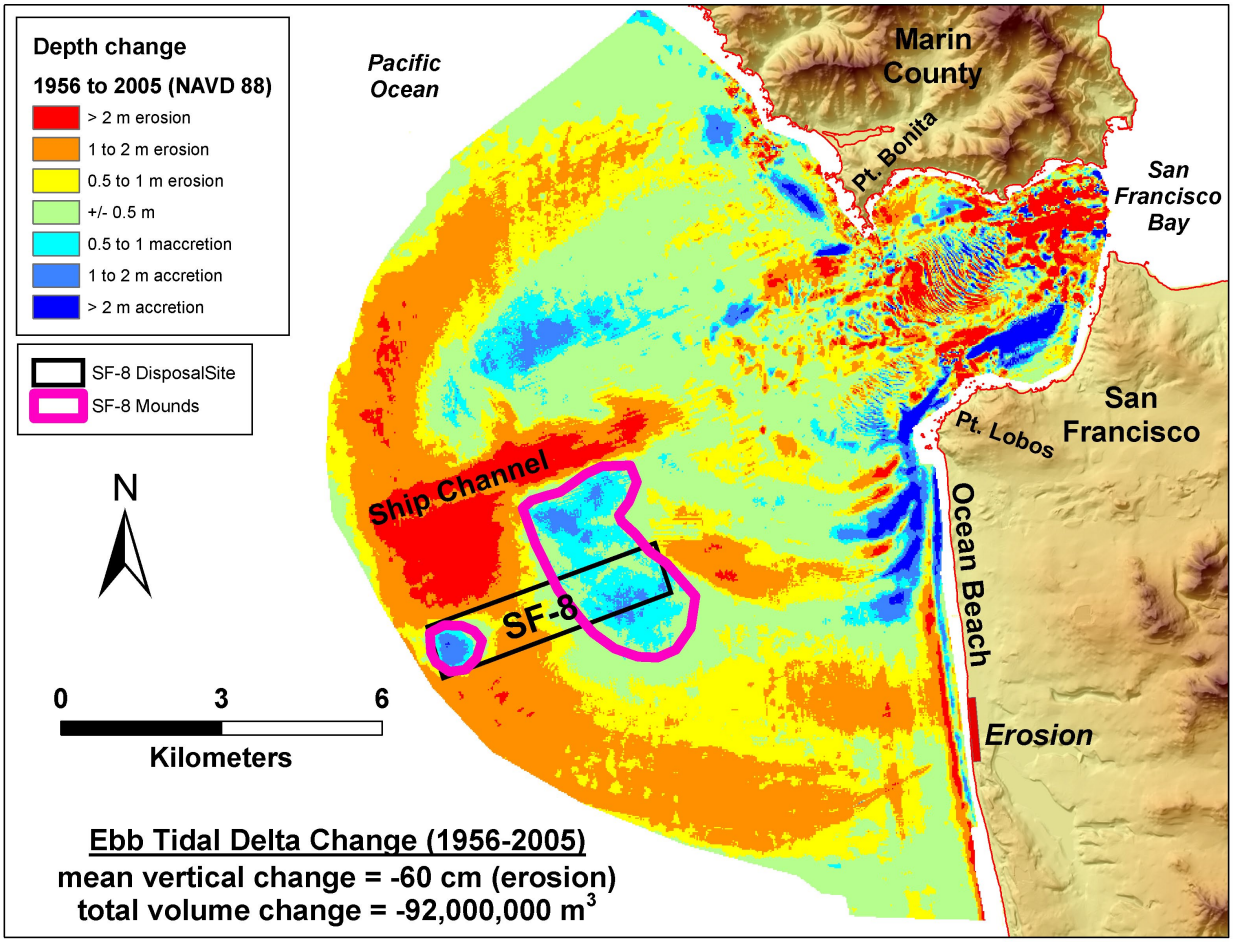

Figure 5. Change between bathymetric surveys conducted in 1956 and 2005. The area designated "SF-8 Mounds" incorporated a net change of +4.3 million m^3.

In May 2005, the USACE established a test disposal site offshore and south of the erosion hot spot at Ocean Beach (fig. 1) to

- Avoid hazardous navigation at SF-8,
- Fill in scour holes on the Southwest Ocean Outfall pipe to mitigate potential structural instability
- Provide wave protection to the chronically eroding stretch of beach, and
- Establish a nearshore nourishment site where dredged sediment could feed into the littoral zone.

Annual channel-maintenance dredge material has been placed at this test disposal site three times (May or June) since 2005. This report summarizes the performance of this program in the context of the morphological evolution of the beach and nearshore regions. A report by

Barnard and Hanes (2005), summarizing just the first year of the dredge-disposal monitoring, can be found online at http://pubs.usgs.gov/of/2006/1140/.

Methods

The USGS monitored and evaluated the morphologic evolution of the test dredge-disposal site and the adjacent coastal region from May 2005 to December 2007. During the dredge disposal monitoring period, survey work has included 12 multibeam surveys by SFML, 10 coastal-profiling surveys, 40 beach-topographic surveys, and 3 beach-grain size surveys. In June 2005, at the onset of the first dredge disposal, and again in January 2006, the USGS deployed several tripods offshore of Ocean Beach, each equipped with a current profiler, to make calculations of the directional wave spectrum, water levels and tidal currents from in place measurements (fig. 6). The USGS conducted eight days of offshore sediment sampling in June and July 2005. A total of 191 stations were sampled by collecting grab samples or employing a digital bed-sediment camera (eyeball) at the mouth of San Francisco Bay, with emphasis immediately on and around the Ocean Beach disposal site (fig. 6). The subsequent sediment analysis was used to determine if the grain size of the dredge disposal (shoreface nourishment) is suitable for bed-load transport under the prevailing hydrodynamic conditions of the area, if it is compatible with sediment on the beach, and as input for numerical modeling efforts. For a complete analysis of these data sets see Barnard and others (2007a) at http://pubs.usgs.gov/of/2007/1217/. Also see the appendix section, Survey Error and Uncertainty, for a more detailed analysis of survey accuracy.

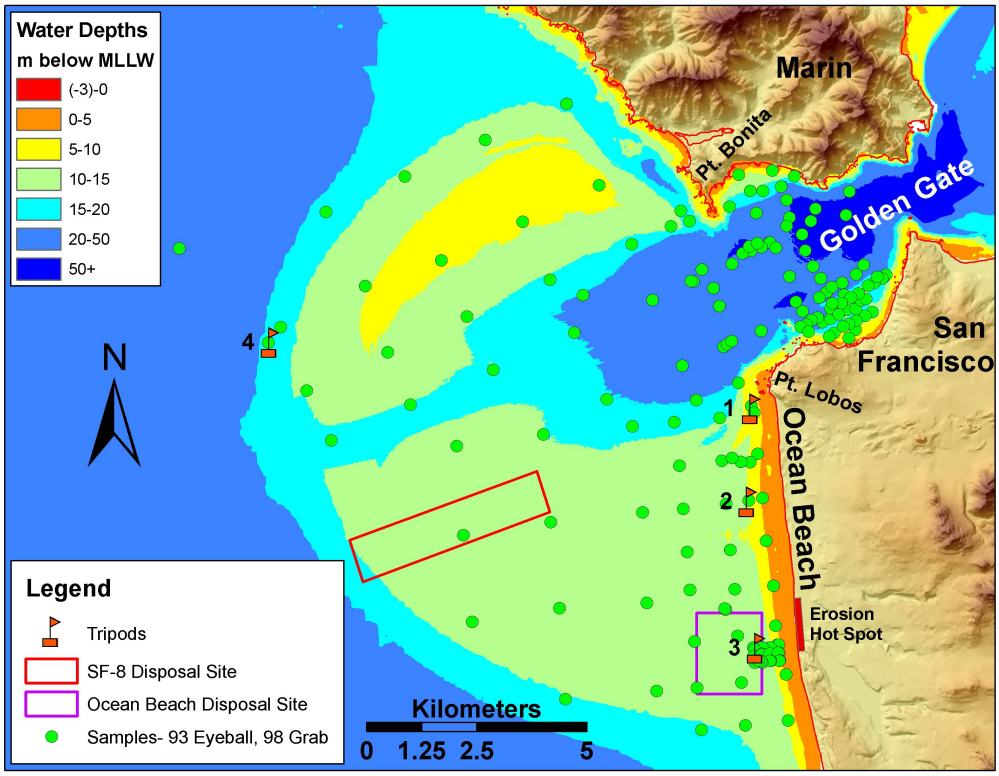

Figure 6. Instrument deployment and sediment-sampling locations during the initial 2005 dredge-disposal monitoring period.

Vertical Difference Maps and Volume Changes

Volume changes within the disposal area were estimated by gridding the multibeam bathymetry data into fine mesh grids of 2 x 2 m and 10 x 10 m, by using a standard inverse-distance weighting algorithm in Fledermaus©. The coarser grid (10 x 10 m) was occasionally employed for performing robust calculations where computer memory became limited. Comparison between volumes calculated with the 2 m and 10 m grids differed by less than 1 percent.

Centroid Calculations

To determine the location of initial dredge placements, the centroid of sediment mounds were inferred from bathymetric difference plots. The centroid was used as a proxy to the mound's center of mass, assuming constant specific gravity and density of the material. Areas and volumes of placement were estimated by subtracting older survey depth measurements from measurements made during a subsequent survey; it was assumed that all sediment remained within the multibeam survey area (taken as the control volume for these calculations), and that no transport of sediments occurred within the control volume between the subsequent surveys. The latter assumptions of conservation of mass and no transport within the survey area were not strictly adhered to because the pre- and post-nourishment surveys were done about 3 weeks apart for the nourishments in 2005 and 2006, and 6 weeks apart for the 2007 nourishment. Nonetheless, this approach was taken to provide an estimate of the initial location of the dredge placements.

Employing bathymetric difference plots between subsequent multibeam surveys, the area was divided into 10 x 10 m grid cells so that the volume of each grid was $10*10*\Delta z$, where Δz is the vertical elevation difference within each grid cell. The centroid coordinates (C_x, C_y, C_z) were then calculated from composites of the total volume such that

$$C_x = \frac{\sum_n V^n C_x^n}{\sum_n V^n}, \quad C_y = \frac{\sum_n V^n C_y^n}{\sum_n V^n}, \quad C_z = \frac{\sum_n V^n C_z^n}{\sum_n V^n} \quad (1)$$

where V is the volume, n is the number of equally sized grid cells, x and y are planar coordinates, z is the vertical coordinate, and C_x^n, C_y^n, and C_z^n are centers of gravity of each of the grid cells. Background accretion or erosion away from the immediate vicinity of the initial dredge mound location was removed prior to calculating the centroid of placed material, and as a consequence, the total number of composites, n, varied between bathymetry difference maps.

Profile Averaging

To assess measured morphologic changes and infer sediment-transport pathways in the vicinity of the nourishment, an area encompassing nourishment sites and extending about one km to the north and south and shoreward to the approximate 3 m contour was subdivided into 21 subsections (fig. 7). The subsections were defined with shore-parallel and shore-normal grid lines to identify cross- and alongshore patterns. Division in the cross-shore direction was based on an estimated cross-shore extent that would allow moving bars to remain within a given subsection (for example, Duin and others, 2004). The nourishment area was divided into three subsections consisting of central, northern and southern parts.

In order to assess cross-shore profile evolution, alongshore morphodynamic phenomena, such as sand waves and rip channels, were smoothed out by averaging cross-shore profiles within each cross-shore subsection (for example, a1-c1, a2-c2…). This was done for each survey by extracting shore-normal transects every 20 m in the alongshore direction and subsequently averaging in the alongshore direction.

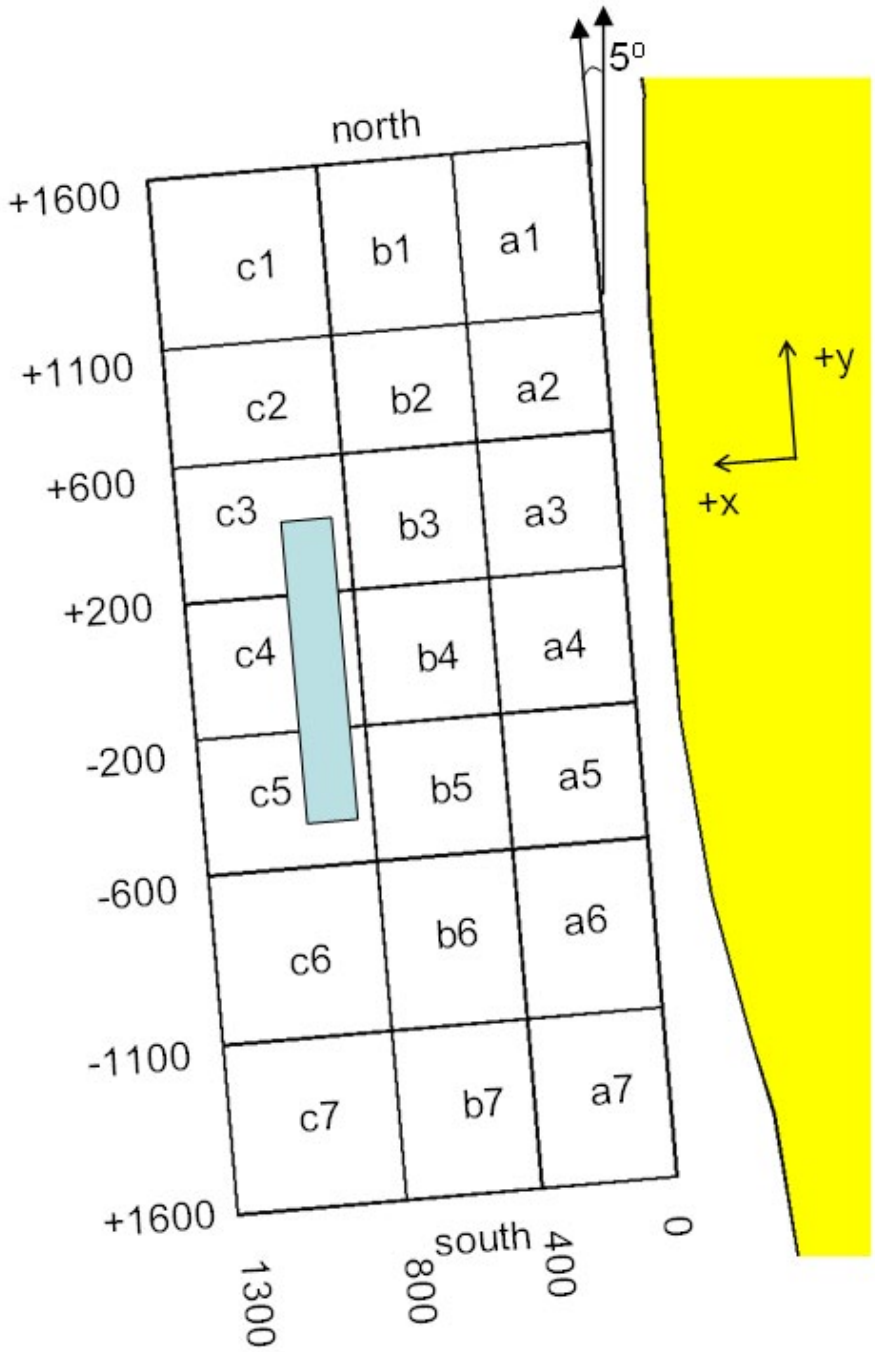

Figure 7. Subsections used to asses measured morphologic changes. Subsections range in area from 0.20 km^2 near the shore to 0.25 km^2 in the offshore cells. The nourishment area is indicated by the blue box in subsections c3 through c5.

Topographic Beach Surveys

As of February 2008, 55 global positioning system (GPS)-based topographic beach surveys have been conducted by the USGS, with at least one survey completed most months since April 2004. The surveys are done by using an all terrain vehicle (ATV) equipped with a GPS receiver and antenna. From April 2004 through February 2007, the surveys were done in differential mode (DGPS), in which a differential correction (recorded at a nearby base station) was applied to the GPS data after the survey was complete. Since March of 2007, the surveys have been conducted by using a Real-Time Kinematic (RTK)-GPS system in which the base station broadcasts the differential correction to the ATV in real-time. A typical survey of the entire 7 km stretch of beach consists of roughly 20,000 individually recorded points, each with a conservatively estimated random error of 0.05 m in both the horizontal and vertical directions. The survey points are gridded to produce a topographic surface of the surveyed area by using standard interpolation techniques in ArcGIS©.

Sediment volume and shoreline position can be extracted from the survey grids, and subsequently, volume and shoreline change can be calculated by comparison of multiple surveys. Correlation between volume change and the position of a shoreline proxy, such as mean sea level (MSL), is high (R^2 values >0.9) for most areas of Ocean Beach, indicating that both analyses provide similar results (Hansen, 2007). The position of MSL (0.975 m above NAVD88; National Oceanic and Atmospheric Administration, 2008b) is used as a proxy for the shoreline in this analysis, and its position was analyzed at the 135 cross-shore profiles, spaced 50 m apart (fig. 2 and table 1). The MSL shoreline was chosen over the MHW shoreline primarily because the data coverage is better for the analysis period, with more profiles intersecting the MSL shoreline than the MHW shoreline. Both beach profiles and shoreline positions were extracted from the topographic grids by using the Digital Shoreline Analysis System (DSAS) in ArcGIS© (Thieler and others, 2005).

Coastal Profiling System Surveys

The Coastal Profiling System (CPS), a hydrographic-surveying system mounted on a personal watercraft (PWC), is used to collect bathymetric data on an approximate quarterly basis at Ocean Beach (fig. 8). The CPS combines the high accuracy positioning of a RTK-GPS and the mobility of a PWC to collect rapid and precise bathymetric profiles. The survey setup for this site consists of 18 cross-shore profiles running from 1.8 km offshore through the surf zone and 2 alongshore profiles parallel to the coastline. For more information on CPS methods see the Appendix and Barnard and others (2007a).

Wave and Current Conditions

Field measurements of waves and currents within the nourishment area were obtained with an acoustic Doppler current profiler (ADCP) deployed at NAD83 Zone 10, Easting 542,475.4 m, Northing 4,175,524.3 m (Lat 37.726N Long 122.518W) in a water depth of about 12 m (fig. 6, Tripod 3) on two separate occasions, to capture summer and winter conditions:

	Deployment date	Recovery date	Duration
Summer conditions	21-Jun-2005 18:50:30	30-Jul-2005 10:40:30	38.66 days
Winter conditions	12-Jan-2006 17:40:30	06-Feb-2006 04:00:30	24.43 days

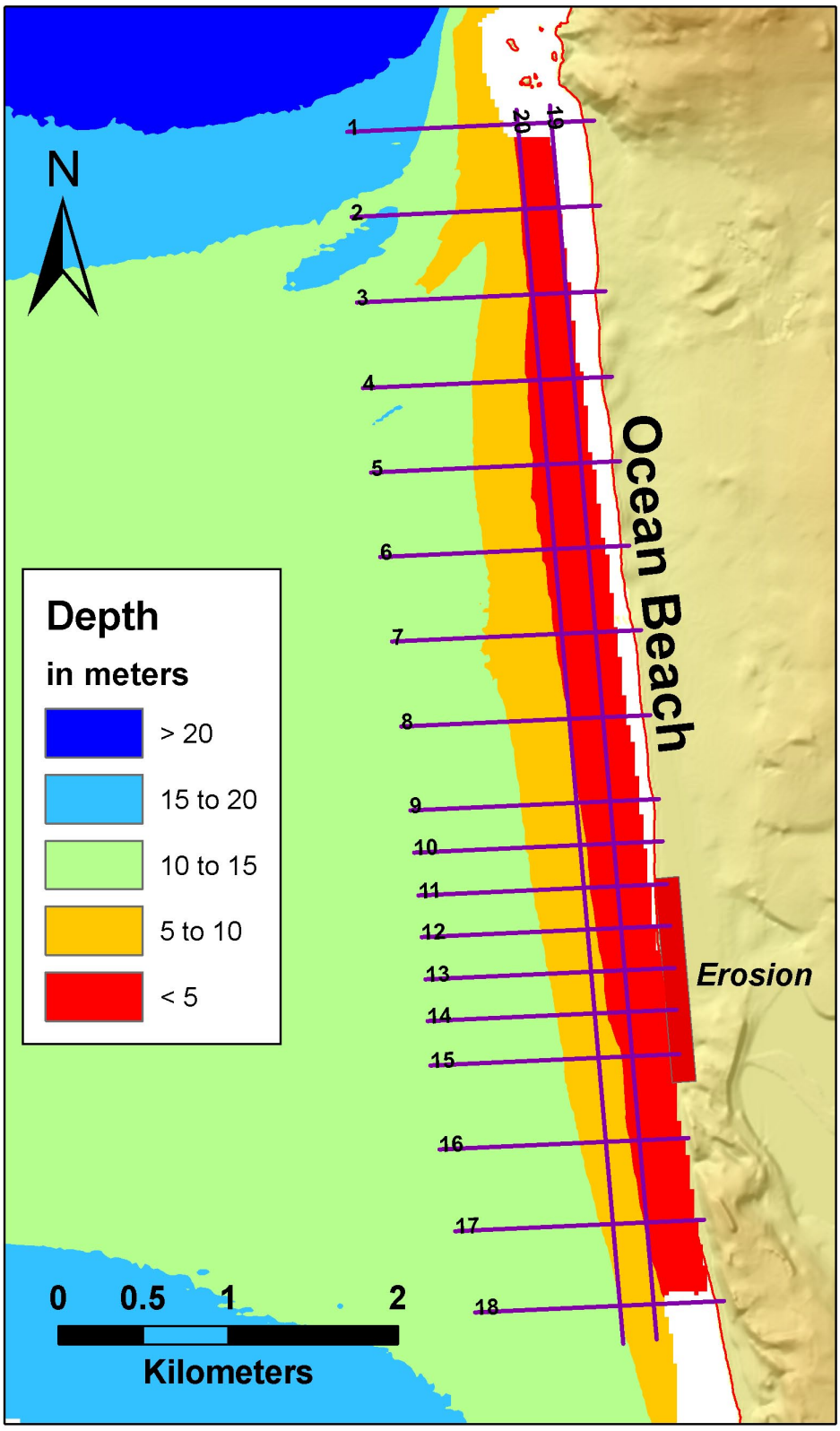

Figure 8. Ocean Beach Coastal Profiling System (CPS) survey lines.

An RD Instrument ADCP Workhorse Sentinel with three 1,200 kHz transducers was deployed. The ADCP was oriented upward and mounted on a weighted aluminum frame, approximately 0.5 m above the seabed. Currents were measured in 1 m bins throughout the water column starting at 1 m from the seabed (after accounting for the blanking distance). Currents were measured at 1Hz with an ensemble averaging length of 1 minute every 10 minutes. Wave conditions were estimated from 68.27-min-long bursts every 2 hours at a sampling rate of 2 Hz. The sampling scheme was set to optimize battery life for the month-long deployments. For more information see Barnard and others (2007a).

Model-Derived Wave and Current Conditions

To ascertain the fate, transport, and overall stability of hypothetical foreshore nourishments, two numerical-modeling approaches were applied. The Delft3D model (Roelvink and van Banning, 1994; Lesser and others, 2004), coupled with SWAN (Simulating Waves Nearshore; Delft University, 2008) was used to compute vertically-averaged currents and simulate transport in an area mode. Tidal constituents determined from a previously calibrated area model were used to force the Delft3D model at distant offshore boundaries. The numerical model SWAN was used to propagate offshore waves to the study area and was forced with offshore wave measurements from the Pt. Reyes CDIP buoy (p029; SCRIPPS, 2008) located approximately 18 nautical miles offshore in 550 m of water. The SWAN model accounts for refraction, propagation, wave-wave interaction, bottom dissipation, depth-induced wave breaking, and when coupled with Delft3D, current dissipation.

The UNIBEST-TC (Bosboom and others 2000) model was used to study sediment transport and morphologic-profile development in the cross-shore direction. The model assumes a sandy, uniform coast and computes cross-shore sediment transports and the resulting profile changes under the combined action of waves and longshore tidal currents (Walstra and Roelvink, 2000). Alongshore tidal currents were generated in the model by using constituents determined with a previously calibrated Delft3D area model. Wave conditions at the open boundary were estimated with SWAN model results.

Sediment-transport formulations described in van Rijn (1993) were used in both models. A distinction is made between bed- and suspended-load sediment transports, where bed-load transport represents the movement of sand particles in close contact with the bed surface. Implementations of the formulations differ slightly. For more detail see Bosboom and others (2000) for the UNIBEST-TC model and Roelvink and van Banning (1994) and Delft3D user manuals (WL Hydraulics/Deltares) for the Delft3D model.

Results and Discussion

Multibeam Surveys

Overall Bathymetric Changes

Multibeam bathymetry was measured by SFML prior to and following placement of dredged material and at intermittent intervals between placements (see Appendix for survey bathymetry and shaded-relief maps). Multibeam collection dates and resolution of grids used in the analyses are listed in table 2. Table 3 lists dredge focus area (target area or control area) change statistics between each of the 12 surveys. Figures. 9-11 illustrate the overall behavior of the nearshore-dredge disposal during the entire monitoring period. Figure 9 shows that the

Table 2. Multibeam survey list.

Survey	Julian Day	Month	Day	Year	Notes	Maximum resolution, in meters	Gridded resolution, in meters
1	136-137	May	16-17	2005	predisposal	1	2, 10
2	159	June	8	2005	postdisposal	1	2, 10
3	190	July	9	2005	postdisposal	1	2, 10
4	292-293	October	19-20	2005	postdisposal	1	2, 10
5	134	May	14	2006	predisposal	1	2, 10
6	153-154	June	2,3	2006	postdisposal	1	2, 10
7	334-339	Nov-Dec	30, 5	2006	postdisposal	1	2, 10
8	23	January	23	2007	postdisposal	1	2, 10
9	145	May	25	2007	predisposal	1	2, 10
10	192	July	11	2007	postdisposal	1	2, 10
11	308	November	4	2007	postdisposal	1	2, 10
12	345	December	11	2007	postdisposal	1	2, 10

Table 3. Volume-change statistics between successive surveys in meters, including successive-survey volume change and the cumulative volume change since surveys began in May 2005 (Survey 1). The highlighted rows represent the surveys immediately after dredge disposal. See table 2 for full survey information.

Survey no.	Max	Min	Mean	Std	Surface area	Volume change	Cumulative change
1	-	-	-	-	-	0	0
2	1.89	-0.52	0.44	0.27	763,943	335,643	335,643
3	1.28	-1.66	-0.24	0.09	794,345	-190,259	145,384
4	0.88	-1.12	-0.03	0.11	796,611	-24,701	120,683
5	0.73	-1.08	0.05	0.17	796,012	43,444	164,127
6	1.62	-0.99	0.12	0.26	794,469	93,368	257,495
7	1.21	-0.75	0.02	0.12	795,885	19,560	277,056
8	1.14	-1.11	0.12	0.20	780,329	94,404	371,459
9	0.68	-0.54	0.00	0.07	780,428	917	372,377
10	1.81	-0.35	0.19	0.23	795,401	151,769	524,146
11	0.41	-1.09	-0.29	0.28	793,732	-233,814	290,332
12	1.36	-0.88	0.13	0.33	794,246	104,803	395,135

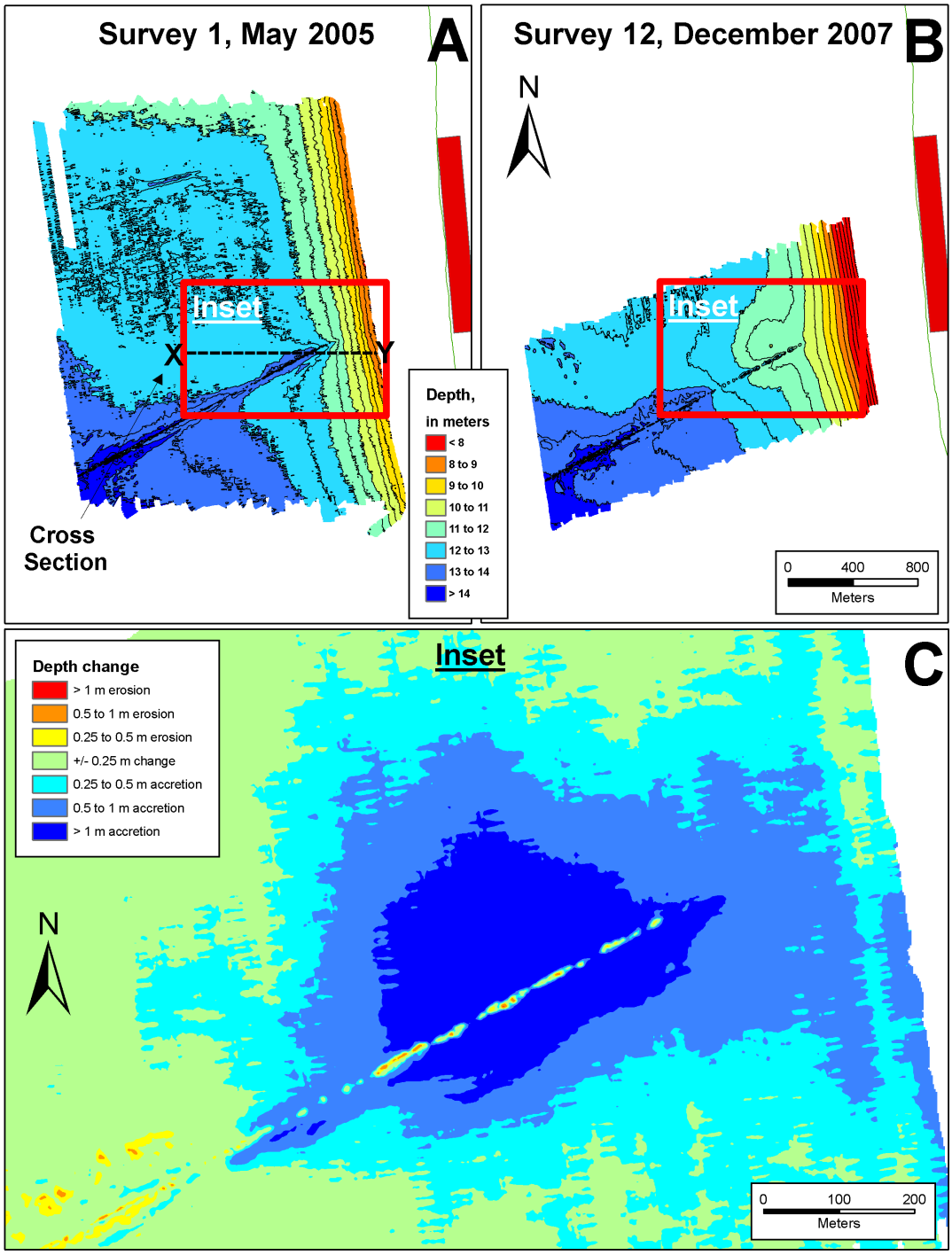

Figure 9. Bathymetric change with respect to May 2005 bathymetry prior to any shoreface nourishment. *A*, Bathymetry from May 2005 prior to initial dredge disposal. Also shown is the location of cross section X-Y in figure 10. *B*, Bathymetry from December 2007 after 3 periods of dredge disposal. Depth is relative to the North American Vertical Datum (NAVD88). *C*, Change between May 2005 and December 2007 showing about 400,000 m^3 of sediment that has remained in the dredge-disposal region since program inception.

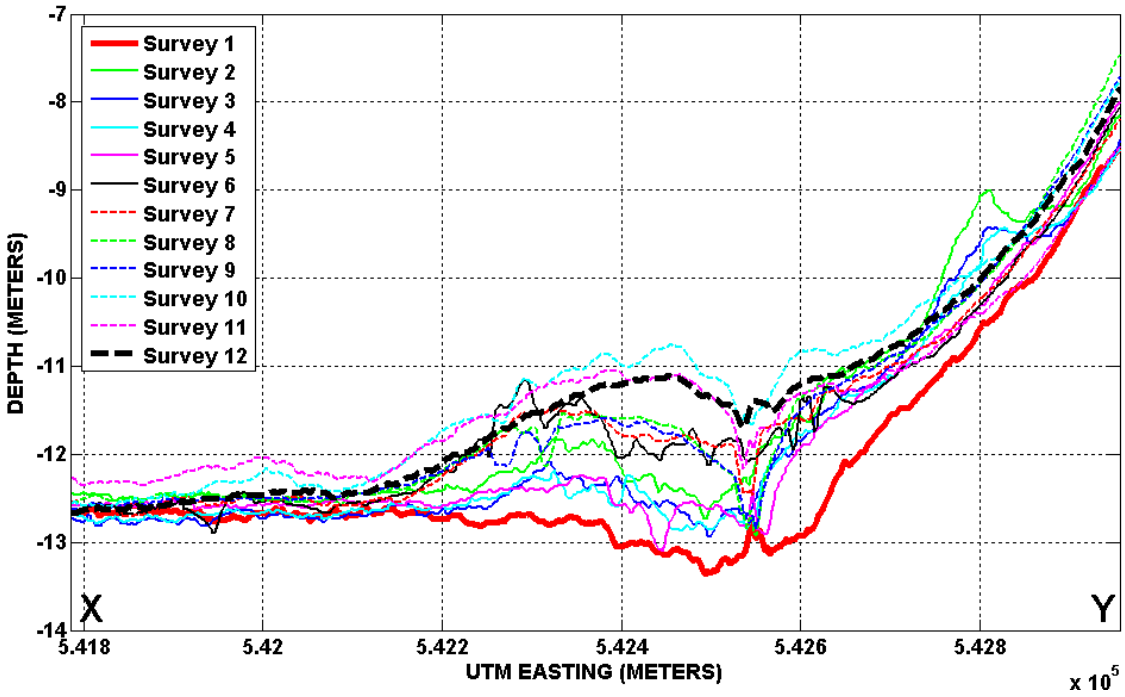

Figure 10. Cross-shore profiles (X-Y in fig. 9) through the center of the dredge-disposal region. The thicker lines represent the first (Survey 1, red) and last (Survey 2, black dashed) surveys. Multibeam survey numbers correspond with those listed in table 2. Depth is relative to the North American Vertical Datum (NAVD88).

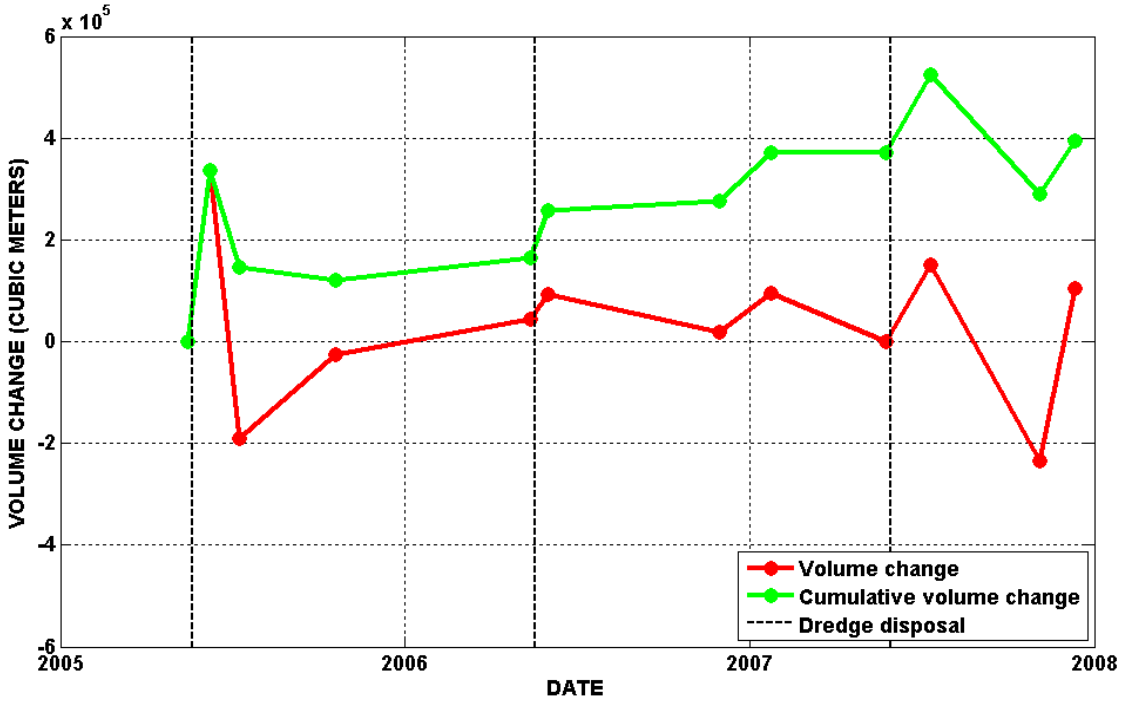

Figure 11. Volume changes as a function of time in the dredge focus area (see fig. 9 for focus-area designation).

bathymetric contours have built out seaward through 3 dredge disposals and 2.5 years of monitoring. However, despite repeated attempts to target disposal on the outfall pipe, sediment is rapidly scoured away, and the pipe appears exposed in each survey (figs. A1-24). A cross-section through the center of the disposal area (fig. 10) demonstrates a progressive, long-term build-up of sediment during the 2.5 year monitoring period. The mound builds significantly after each disposal event, then slowly dissipates until the next annual disposal. Figure 11 and table 3 illustrate that approximately half the dredge material remains within the target area, with a net accumulation of 395,135 m^3 of sediment within the disposal area between May 2005 and December 2007. In figure 11, volumetric changes within the focus area show that a larger portion of the placed material left the control area in 2005 than in subsequent years. The trend of net accretion through the winter months suggests that future placement material may remain in the area, at least for the winter season, and provide a buffer in the form of wave-energy dissipation and a potential source for onshore transport of sediments.

Inferred Mound Placement

Dredge mounds, inferred from multibeam measurements obtained within three and six weeks of each other for the 2005, 2006, and 2007 nourishments are shown in the left column in figure 12. Estimated mound volumes were 265,000 m^3 in June 2005, 58,200 m^3 in June 2006, and 201,000 m^3 in July 2007 (table 4). The substantially lower estimate of the June 2006 placement, in comparison to permit allowances (about 230,000 m^3) and the other two dredge mound volumes, suggests that either considerable dispersal of material took place between the May and June surveys in 2006, the material was spread over a wider area, or less material was placed. Because the amount of sediments lost between pre- and post-nourishment surveys is unknown, the uncertainty of the calculated centroid locations and estimated nourishment volumes is largely unknown. Errors associated with gridding (10 x 10 m) and calculation of the centroid locations is estimated to be ±20m in the horizontal direction.

Calculated mound centroids shown with the red circle in the left-hand panels of figure 12 indicate that the first nourishment in 2005 was placed about 300 m shoreward of the following nourishments. Shore normal profile evolutions through the initial mound centroids, shown on the right-hand side of figure 12, indicate that, although the initial mound dispersed quickly, much of the volume remained in place.

Table 4. Summary of mound volumes and centroid locations as determined from pre- and post-nourishment multibeam measurements, Ocean Beach, California.

Nourishment date	Centroid location			Volume
	Easting, in kilometers	Northing, in kilometers	Vertical, in meters	in cubic meters
June 2005	542.61	4175.31	0.4	2.65E+05
June 2006	542.34	4175.42	0.4	5.82E+04
July 2007	542.39	4175.30	0.2	2.01E+05

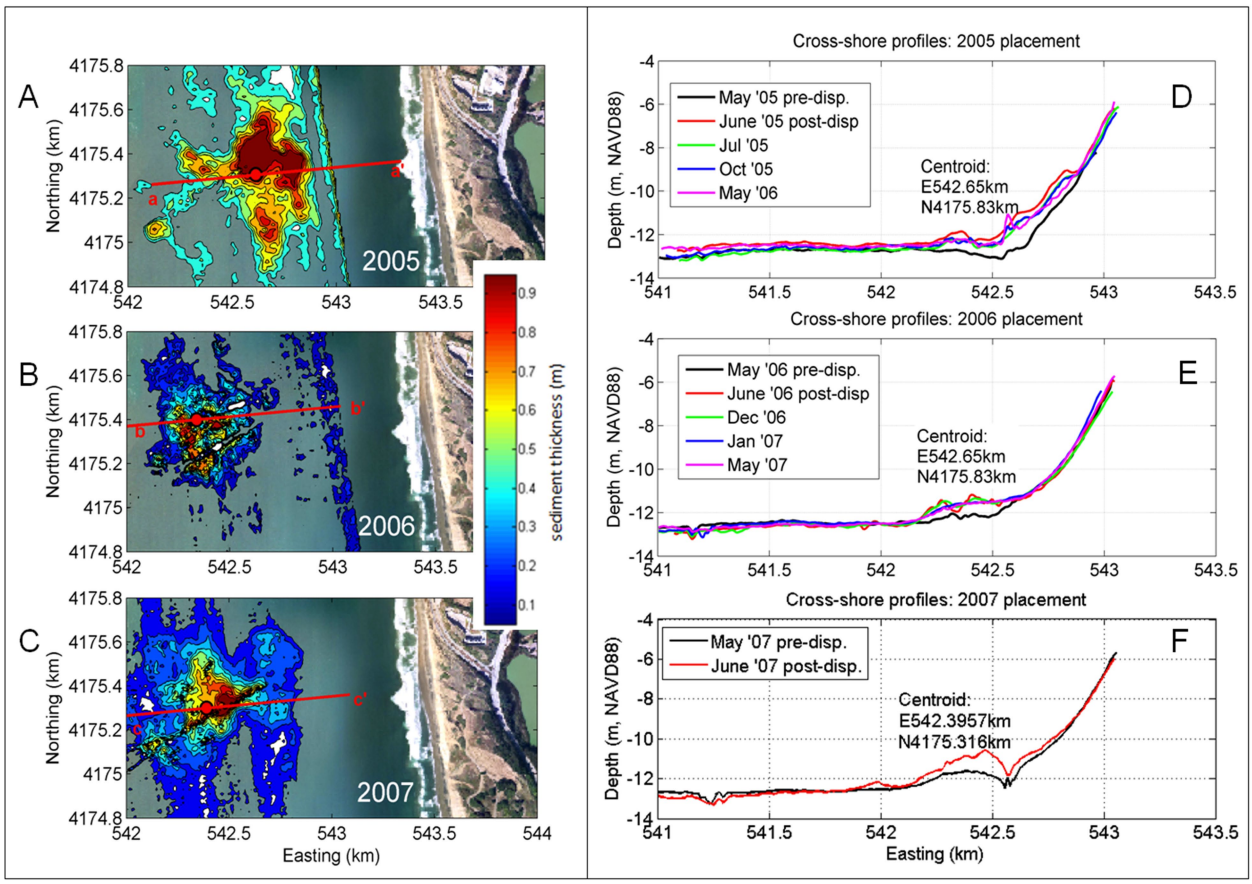

Figure 12. Inferred mound placements and profile evolutions. Mound thickness and location was inferred by subtracting multibeam-bathymetry measurements obtained prior to and following mound placements in *A,* 2005; *B,* 2006; and *C,* 2007. Mound centroid locations are indicated with red circles. Figures on the right side show profile evolution along a cross-shore transect passing through the original centroid and oriented approximately shore-normal.

Centroid Migration

Movement of placed mounds was assessed by locating the centroid of accreted material in subsequent bathymetric difference plots. For the 2005 and 2007 nourishments, there is no clear signal of mound movement. For the 2006 surveys however, a weak signal of potential mound migration can be seen in the vertical difference plot between December and June (fig. 13). Comparisons between the December 2006 and January 2007 plots suggest that material accreted shoreward and south of the initial mound placement, somewhat south of the pipe outlet. It is unclear if the accretion signal at the shoreward end of the measurement area (right-hand plot in fig. 13) is related to the placed material, or from some other source.

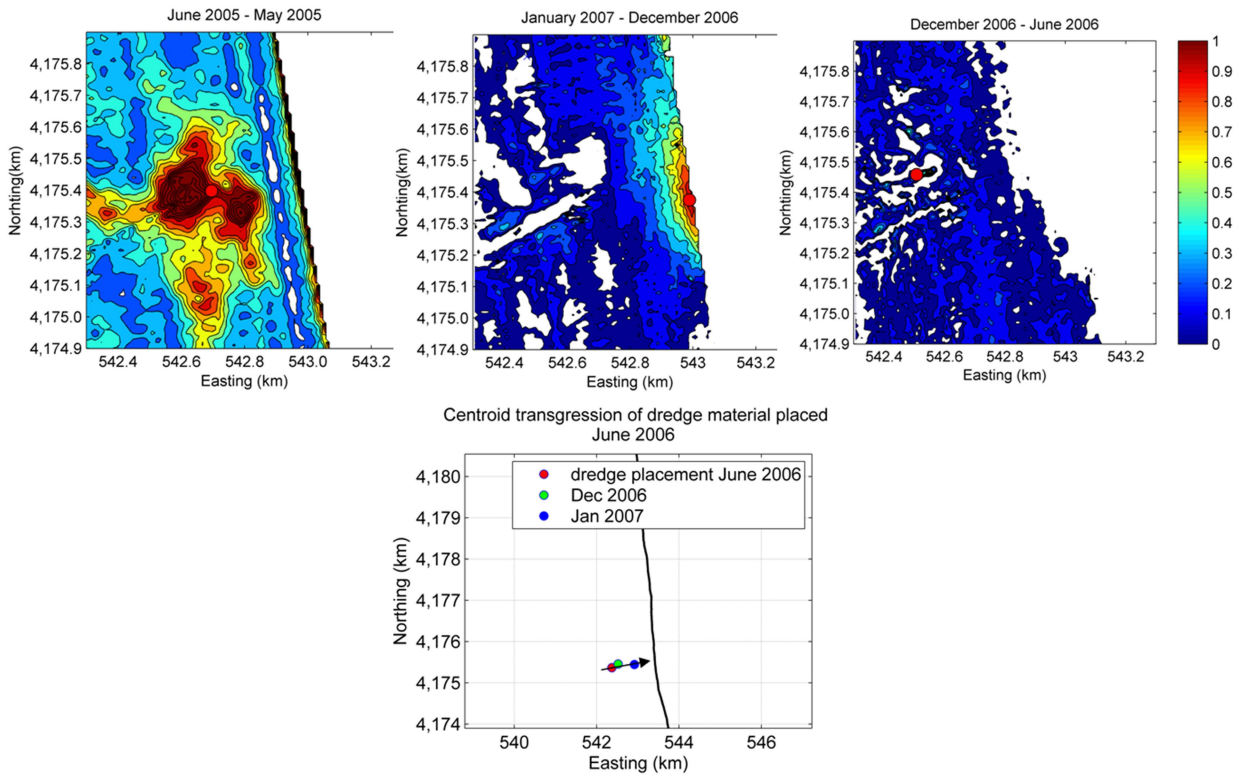

Figure 13. Movement of the mound placed in 2006. Centroids (or center of mass assuming homogenous material) of net accumulated material were calculated to infer mound migration. Accumulated material was estimated by subtracting subsequent bathymetric plots within the survey region extending slightly more than a kilometer fro the location of mound placement in the along-shore direction.

Detailed Depth Changes

Bathymetric difference plots between all subsequent multibeam measurements are presented in figure 14. The right-hand side shows difference plots of the survey area. Cross-shore profiles averaged across alongshore sections a2-c2, a4-c4, and a6-c6 (fig. 6) are shown on the left hand plots in figure 14. Alongshore averaging of cross-shore profiles was done to (1) smooth out irregularities, such as small sandwaves and rip channels; and (2) characterize regions to the north, south, and within the disposal area by one cross-shore profile. Variation of the cross-shore profiles within a given alongshore section is small, as may be inferred from the vertical bars which show the greatest standard deviation to be in the region of mound placement (std = 0.8 m). The wave roses in figure 14*A*-*K* represent model-predicted significant wave heights and directions at E541 km, N4,175.5 km, immediately seaward of the multibeam survey area. Model predictions are from a calibrated SWAN model consisting of four nested wave grids and forced with offshore conditions measured at half hour intervals at the CDIP p029 buoy (Eshleman and

Figure 14. Bathymetric change plots between chronological measurements. Coastal area bathymetric-difference plots are shown on the right side. Alongshore-averaged cross-shore profiles are shown on the left side for subsections a2-c2, a4-c4, and a6-c6 as designated in figure 7. Cross-shore profiles represent an average of 20-m spaced transects with the standard deviation shown by the vertical bars. The wave rose in the center plot is model-predicted wave conditions just offshore of the multibeam survey area at N4,175.5 km, E541 km. The wave model was forced with offshore waves measured by the CDIP buoy 18 nautical miles offshore.

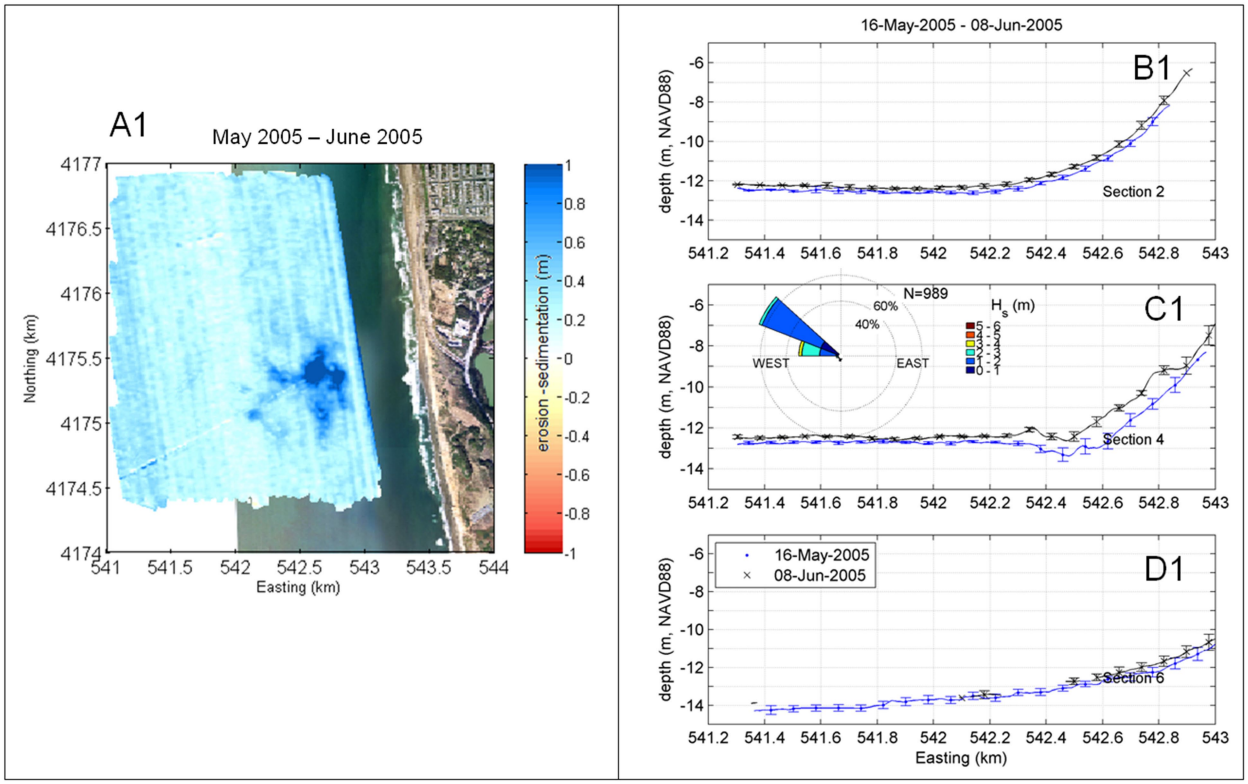

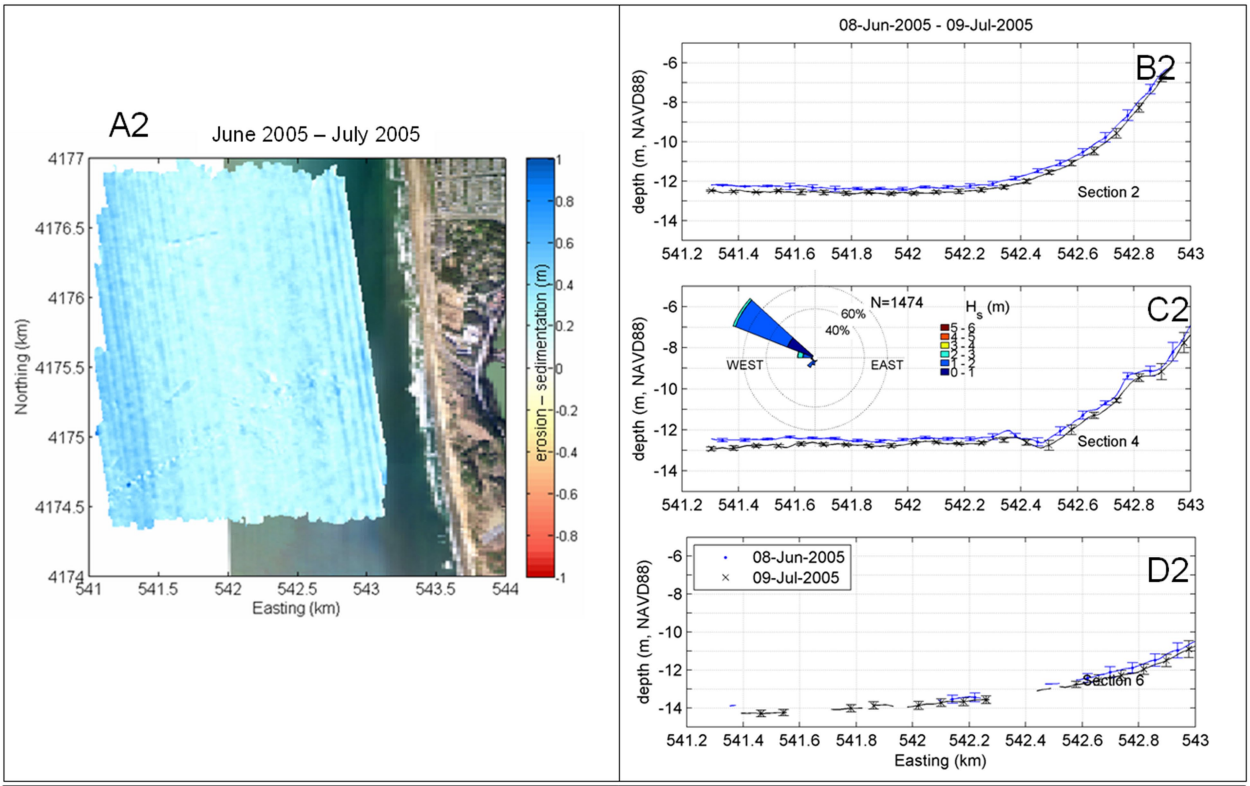
A2
June 2005 – July 2005
Northing (km)
Easting (km)
erosion – sedimentation (m)
08-Jun-2005 - 09-Jul-2005
B2
depth (m, NAVD88)
Section 2
C2
N=1474
H_s (m)
WEST
EAST
Section 4
D2
08-Jun-2005
09-Jul-2005
Section 6
Easting (km)

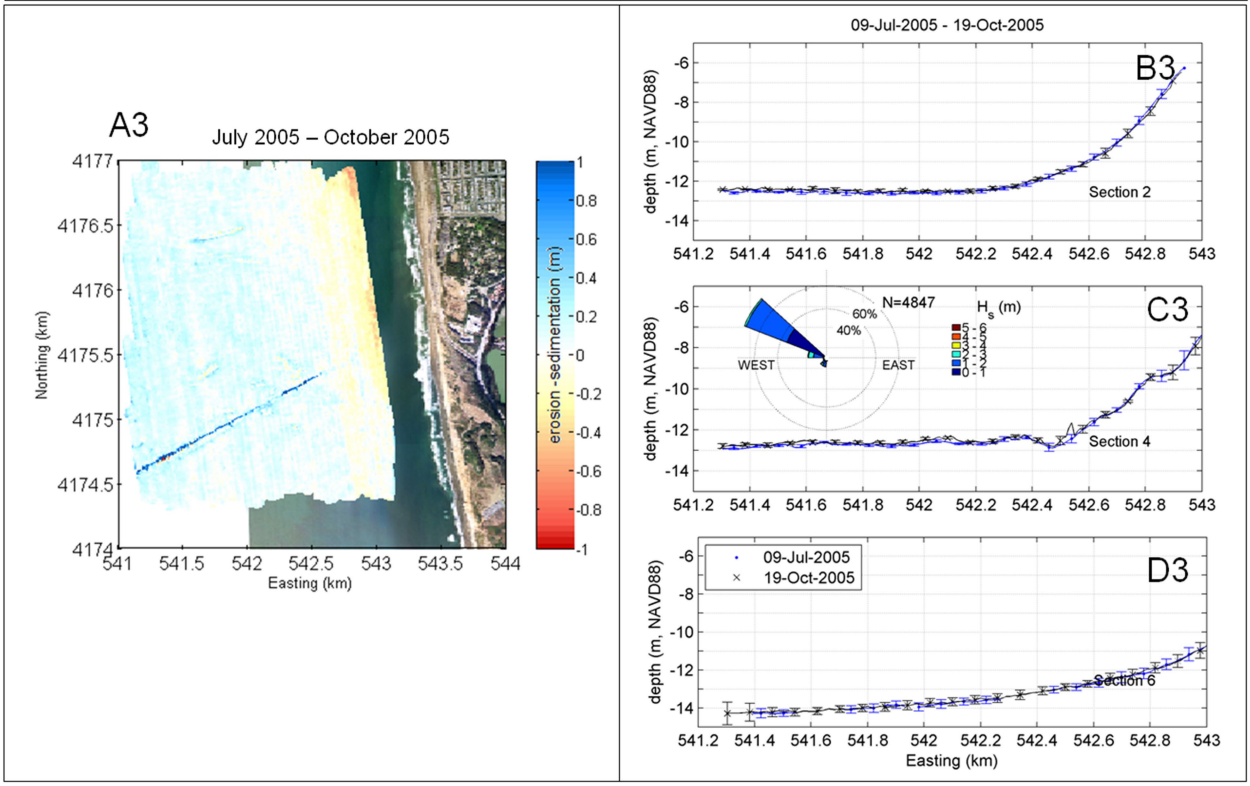
A3
July 2005 – October 2005
Northing (km)
Easting (km)
erosion -sedimentation (m)
09-Jul-2005 - 19-Oct-2005
B3
depth (m, NAVD88)
Section 2
C3
N=4847
H_s (m)
WEST
EAST
Section 4
D3
09-Jul-2005
19-Oct-2005
Section 6
Easting (km)

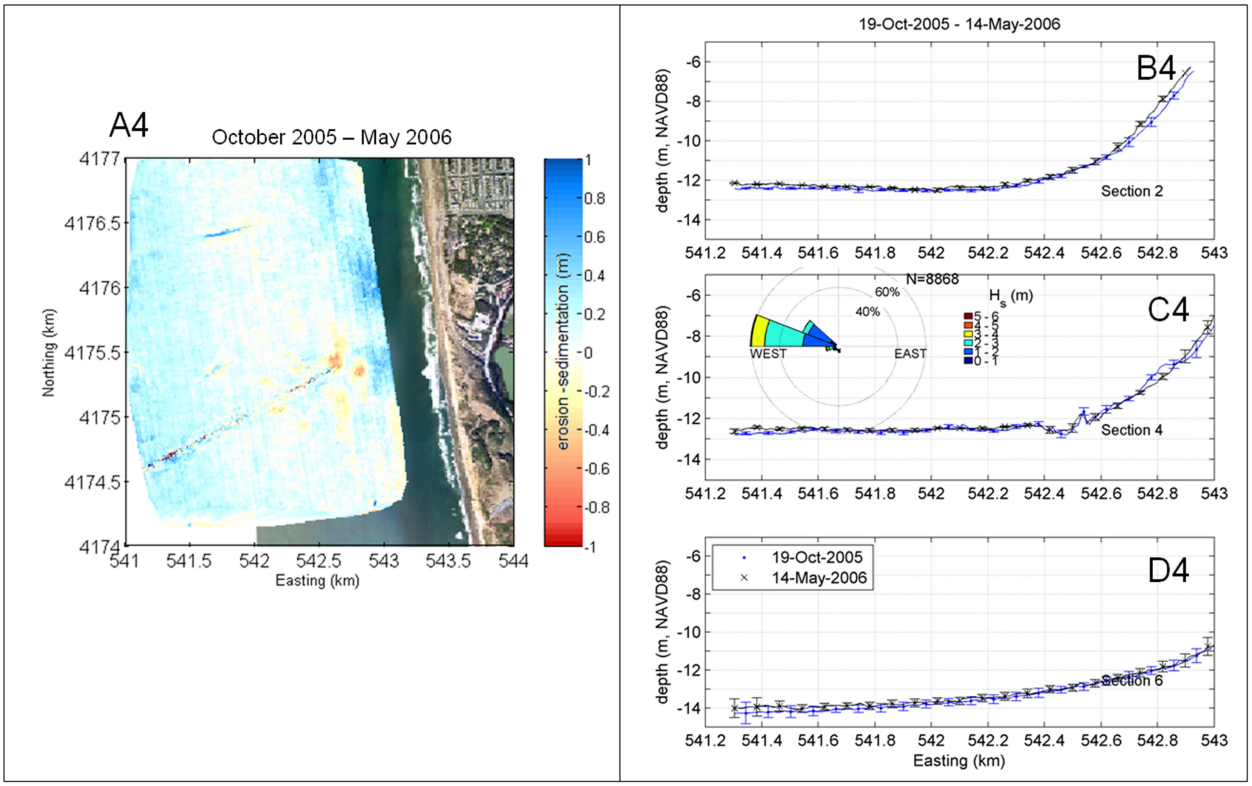
A4
October 2005 – May 2006
Northing (km)
Easting (km)
erosion -sedimentation (m)
19-Oct-2005 - 14-May-2006
B4
Section 2
C4
N=8868
WEST
EAST
Section 4
D4
19-Oct-2005
14-May-2006
Section 6
depth (m, NAVD88)
Easting (km)

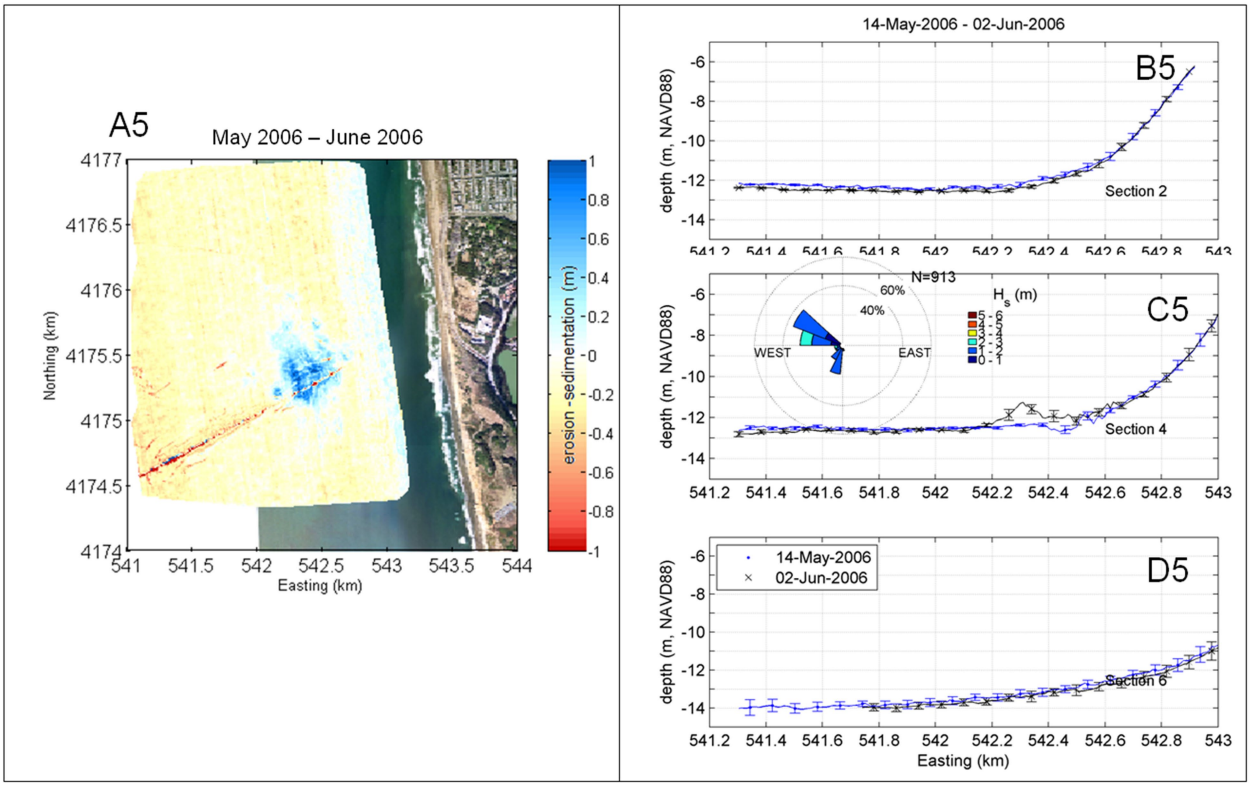
A5
May 2006 – June 2006
Northing (km)
Easting (km)
erosion -sedimentation (m)
14-May-2006 - 02-Jun-2006
B5
Section 2
C5
N=913
WEST
EAST
Section 4
D5
14-May-2006
02-Jun-2006
Section 6
depth (m, NAVD88)
Easting (km)

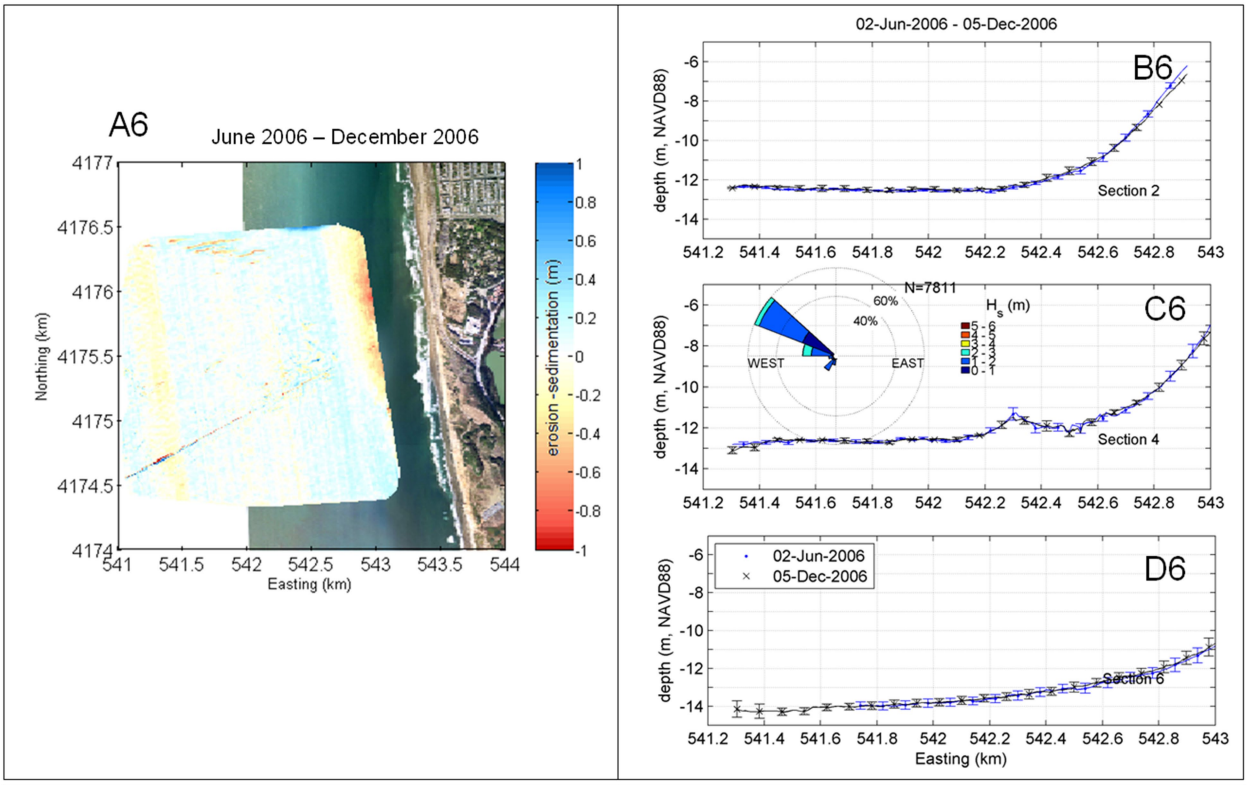
A6
June 2006 – December 2006
Northing (km)
Easting (km)
erosion -sedimentation (m)
02-Jun-2006 - 05-Dec-2006
B6
Section 2
depth (m, NAVD88)
N=7811
C6
Section 4
WEST
EAST
D6
02-Jun-2006
05-Dec-2006
Section 6

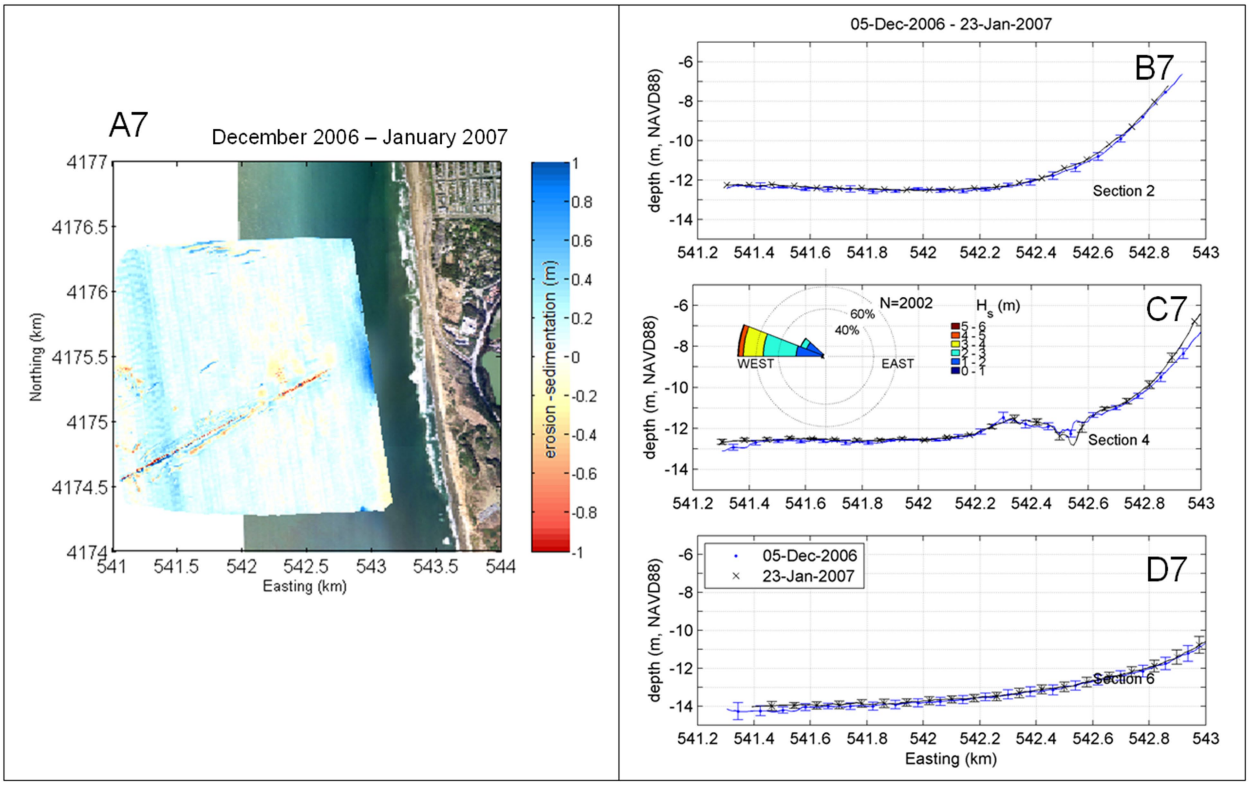
A7
December 2006 – January 2007
Northing (km)
Easting (km)
erosion -sedimentation (m)
05-Dec-2006 - 23-Jan-2007
B7
Section 2
depth (m, NAVD88)
N=2002
C7
Section 4
WEST
EAST
D7
05-Dec-2006
23-Jan-2007
Section 6

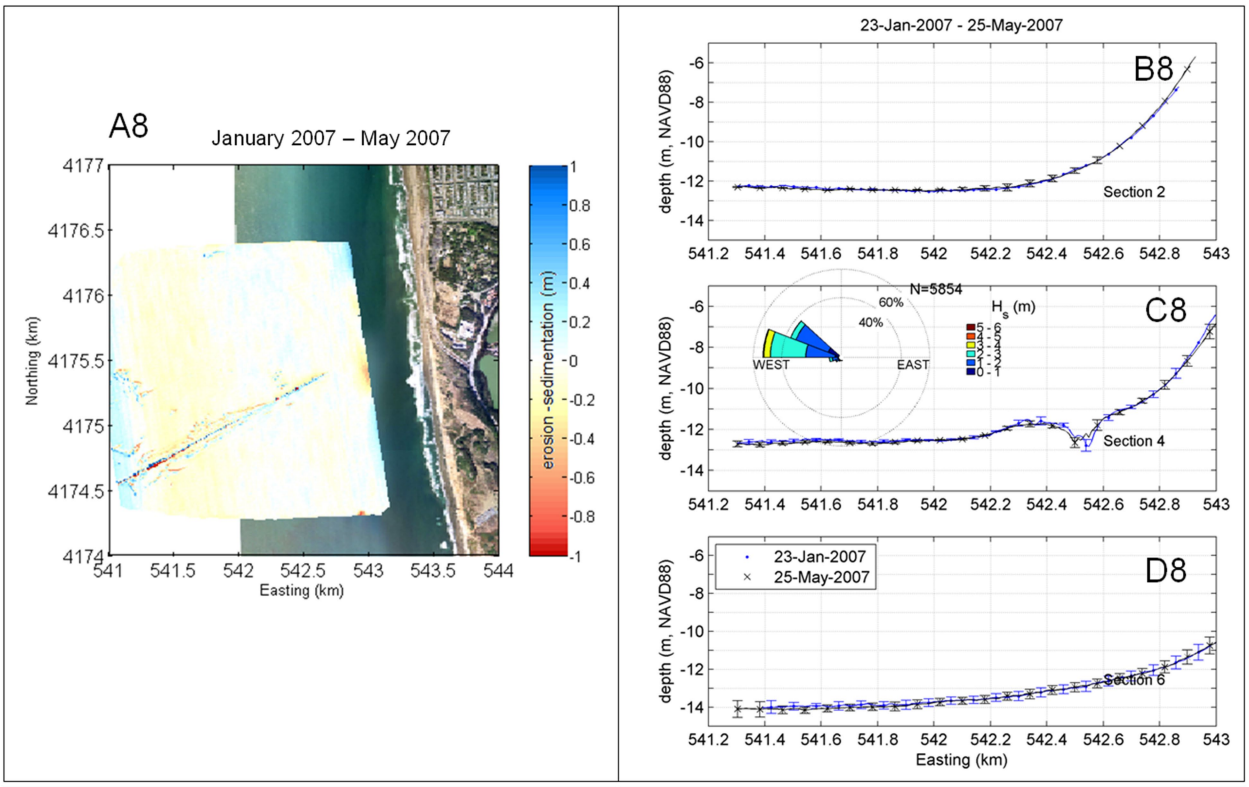
A8
January 2007 – May 2007
Northing (km)
Easting (km)
erosion - sedimentation (m)
23-Jan-2007 - 25-May-2007
B8
Section 2
C8
N=5854
H_s (m)
WEST
EAST
Section 4
D8
23-Jan-2007
25-May-2007
Section 6
depth (m, NAVD88)
Easting (km)

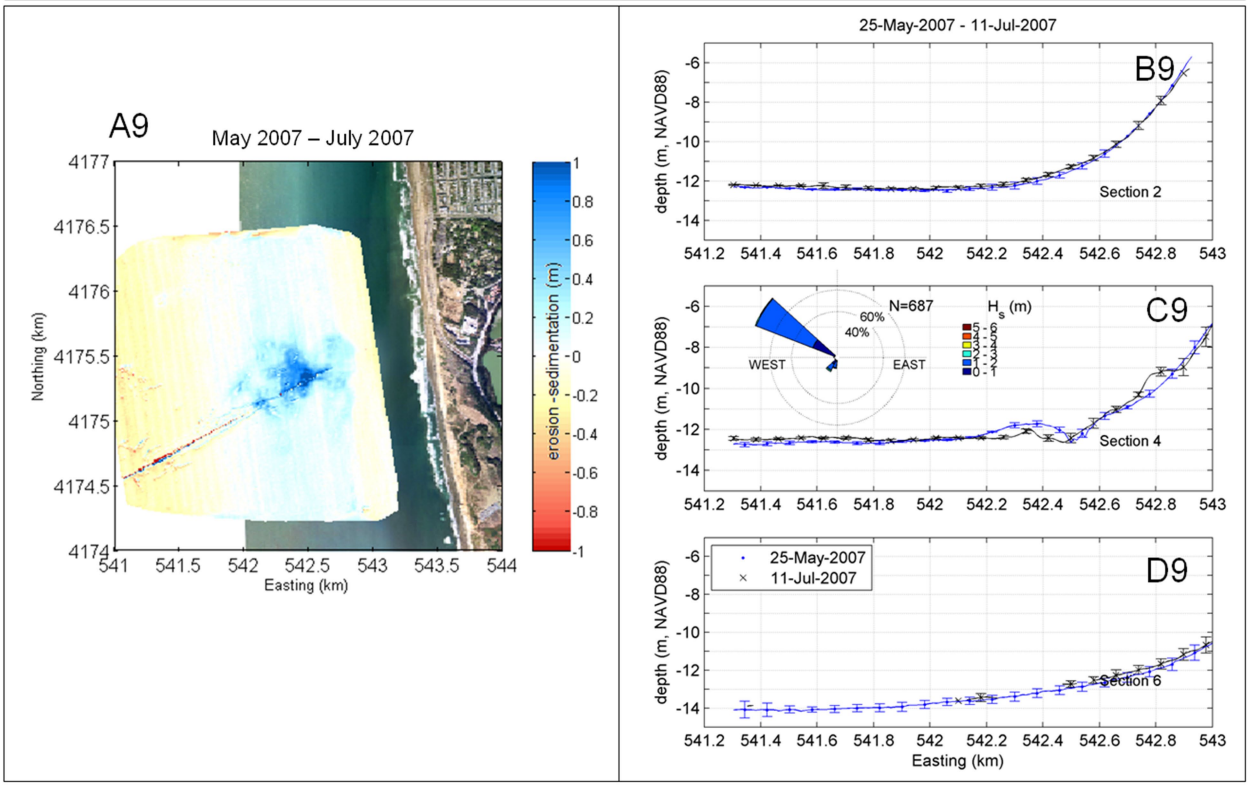
A9
May 2007 – July 2007
Northing (km)
Easting (km)
erosion - sedimentation (m)
25-May-2007 - 11-Jul-2007
B9
Section 2
C9
N=687
H_s (m)
WEST
EAST
Section 4
D9
25-May-2007
11-Jul-2007
Section 6
depth (m, NAVD88)
Easting (km)

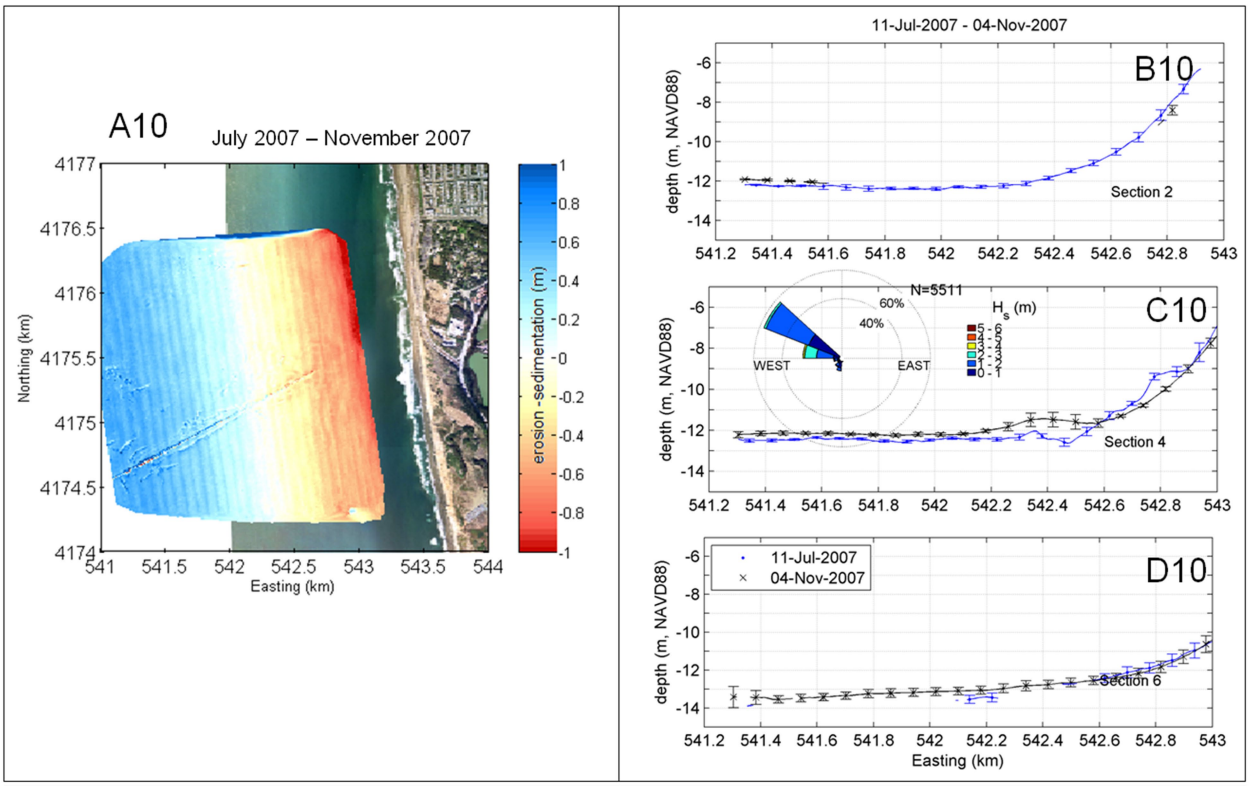
A10
July 2007 – November 2007
Northing (km)
Easting (km)
erosion -sedimentation (m)
11-Jul-2007 - 04-Nov-2007
B10
Section 2
C10
N=5511
Section 4
D10
11-Jul-2007
04-Nov-2007
Section 6
depth (m, NAVD88)
Easting (km)

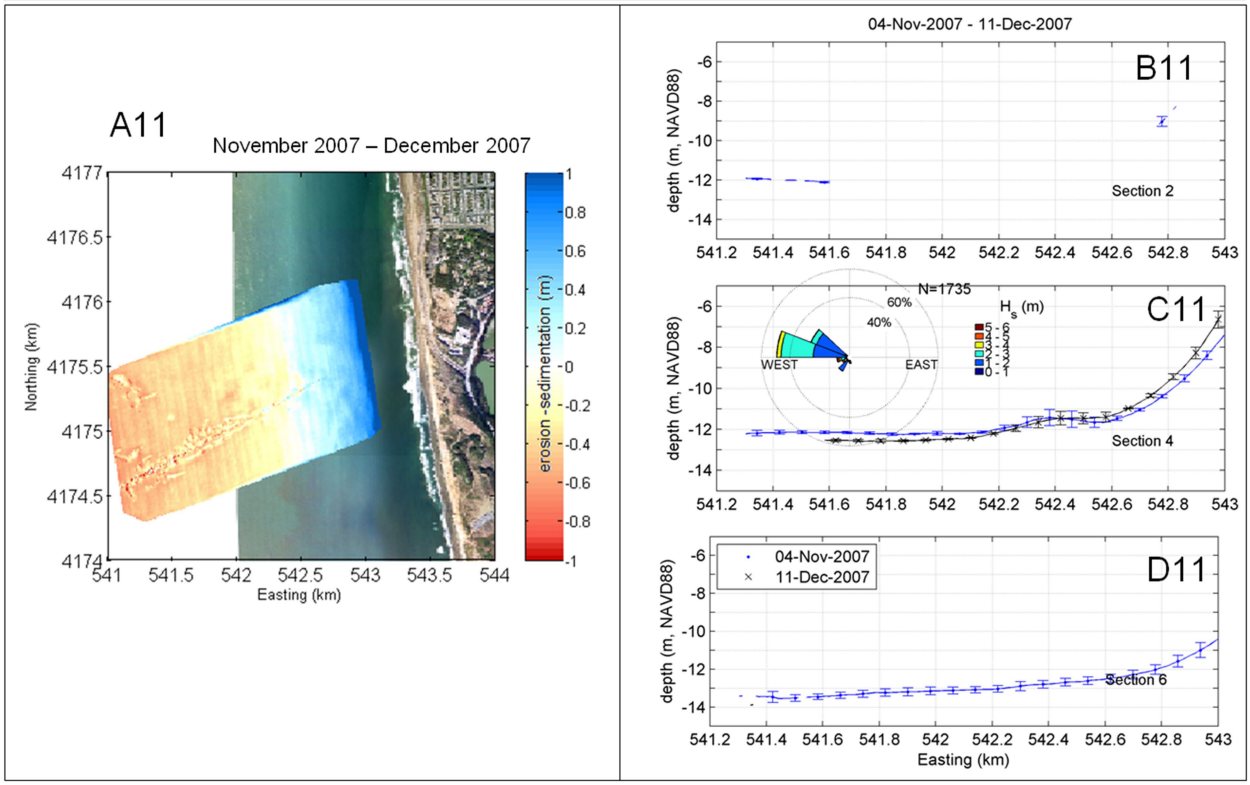
A11
November 2007 – December 2007
Northing (km)
Easting (km)
erosion -sedimentation (m)
04-Nov-2007 - 11-Dec-2007
B11
Section 2
C11
N=1735
Section 4
D11
04-Nov-2007
11-Dec-2007
Section 6
depth (m, NAVD88)
Easting (km)

others, 2007). Interaction between tides and waves are not included in the model-predicted wave conditions presented in the wave roses.

With the exception of difference maps following the nourishment (figs. 14*A*, *E*, and *J*), bathymetric change is small, with relatively greater changes at the shoreward extent of the multibeam measurements (about 6 m water depth). The placement of the dredge material is evident in figures 14*A*, *E*, and *J*.

Typically the cross-shore extent of the profile used to measure accretion or erosion is from the subaerial berm to the main breakpoint bar. However, because multibeam measurements were not possible in the shallow sections along the beach, only that portion extending from the 9 m depth contour to the landward most measured point was used as a proxy to determine if erosion or accretion had taken place between consecutive surveys. Based on this approach, and ignoring the profile changes immediately after nourishment, accretion occurred during 3 of the 8 measured time periods: Oct 2005 to May 2006, Dec 2006 to Jan 2007, and Nov 2007 to Dec 2007. These time periods are also the ones with the longest mean wave periods and greatest predicted mean significant wave heights (propagated to the 13 m contour and shown with the wave roses), indicating that the larger wave events of low wave steepness provide a mechanism for onshore transport of sediments.

The net accretion of the disposal region may be emphasized when comparing bathymetric measurements to the initial condition prior to any placement in June 2005. Figure 9 shows the bathymetric change in December 2007, associated with the dredge disposal, relative to the bathymetry measured in May 2005. The peak of the asymmetric disposal mound in June 2005 is about 1.75 m high and can be seen in figure 10. By October 2005, the peak location is largely unchanged, but the mound has greatly dissipated, and the overall volume within the focus area (indicated by the survey extent in fig. 9*A*) has been reduced by about 50 percent. Much of this volume loss is attributed to the summer seasonal, cross-shore sediment flux, that is, the natural cross-shore sediment transport trend toward the beach. A large portion of the dredge volume was placed in the vicinity of the exposed outfall pipe (fig. 14), and cross sections show that some accretion has occurred around severely exposed portions of the pipe at depths between 10 and 13 m, reducing the exposure and, thus, the scour potential (fig. 9*C*). However, much of the pipe remains exposed.

CPS Nearshore Surveys

CPS surveys in the vicinity of the disposal region suggest high rates of seasonal cross-shore sediment transport (fig. 15). Seasonal surveys show offshore bar migration and growth during the winter, with the reverse occurring in the summer. Three cycles of this migration have now been observed, with estimates per profile of 300 m^3/m/yr of cross-shore sediment transport. When applied to the entire seven kilometers of shoreline along Ocean Beach, the result is an approximate volume of 2.1 million m^3/yr of sand moving cross-shore (Barnard and others, 2007a, chapter 3). Therefore, it is not surprising that the cross-shore flux of sediment largely masks any dredge signal in this data set. The dredge-disposal mound is barely identifiable in depths >10 m along survey lines 15-16 in the target disposal area and is undetectable in lines 14 and 17, on the fringes of the target disposal area. CPS surveys in the southern portion of Ocean Beach indicate that detectable wave-induced cross-shore sediment transport (depth of closure) exists out to about 10 m of water depth in the southern portion of the beach, encompassing portions of the disposal area, and becomes significant in water depths <8 m.

A

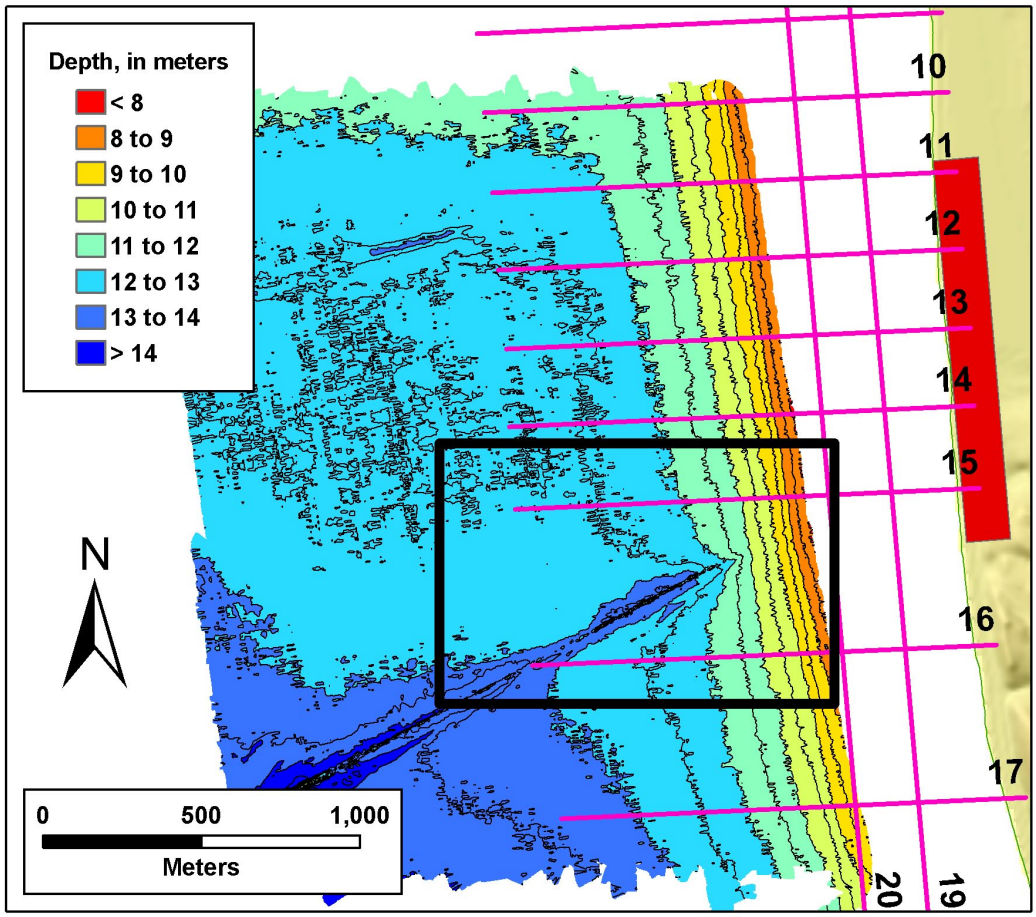
Depth, in meters
< 8
8 to 9
9 to 10
10 to 11
11 to 12
12 to 13
13 to 14
> 14
N
0
500
1,000
Meters
10
11
12
13
14
15
16
17
19
20

B

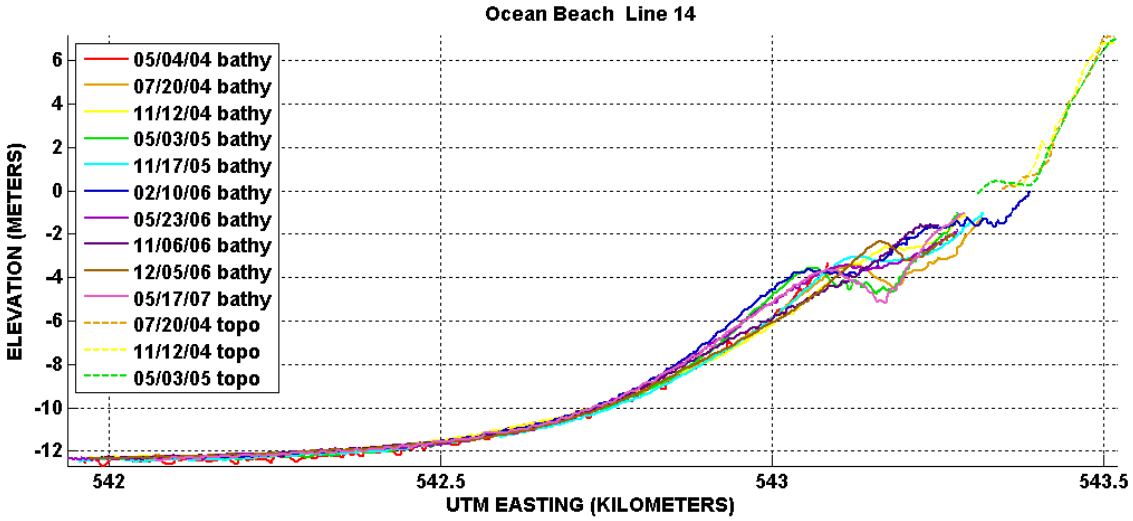
Ocean Beach Line 14
05/04/04 bathy
07/20/04 bathy
11/12/04 bathy
05/03/05 bathy
11/17/05 bathy
02/10/06 bathy
05/23/06 bathy
11/06/06 bathy
12/05/06 bathy
05/17/07 bathy
07/20/04 topo
11/12/04 topo
05/03/05 topo
ELEVATION (METERS)
6
4
2
0
-2
-4
-6
-8
-10
-12
542
542.5
543
543.5
UTM EASTING (KILOMETERS)

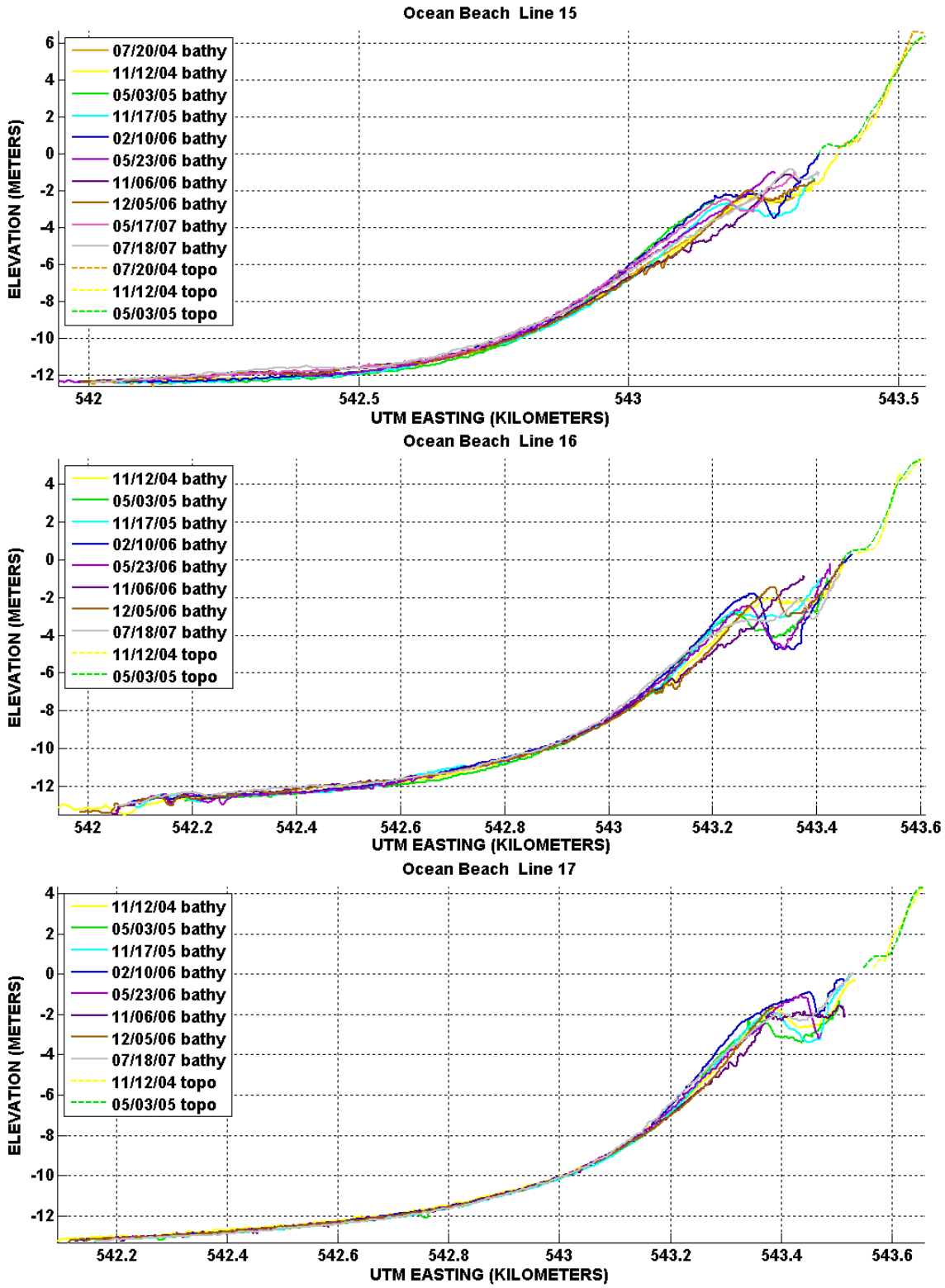

Figure 15. *A*, Cross-shore bathymetric profiles in the vicinity of the dredge-disposal area. *B*, CPS survey lines 14-17, in the vicinity of the dredge-disposal area, between May 2004 and July 2007.

In an attempt to estimate the sediment-transport pathways within the multibeam-survey area and into the surf zone, CPS and multibeam data were merged and compared for the May 2005 (prior to any nourishment) and May 2007 datasets. The PWC and multibeam data were not collected concurrently but were obtained within 11 and 8 days of each other for the 2005 and 2007 merged data sets, respectively. Data were interpolated by using a triangular –based linear interpolation method in Matlab™. The merged datasets are shown in the upper plots of figure 16.

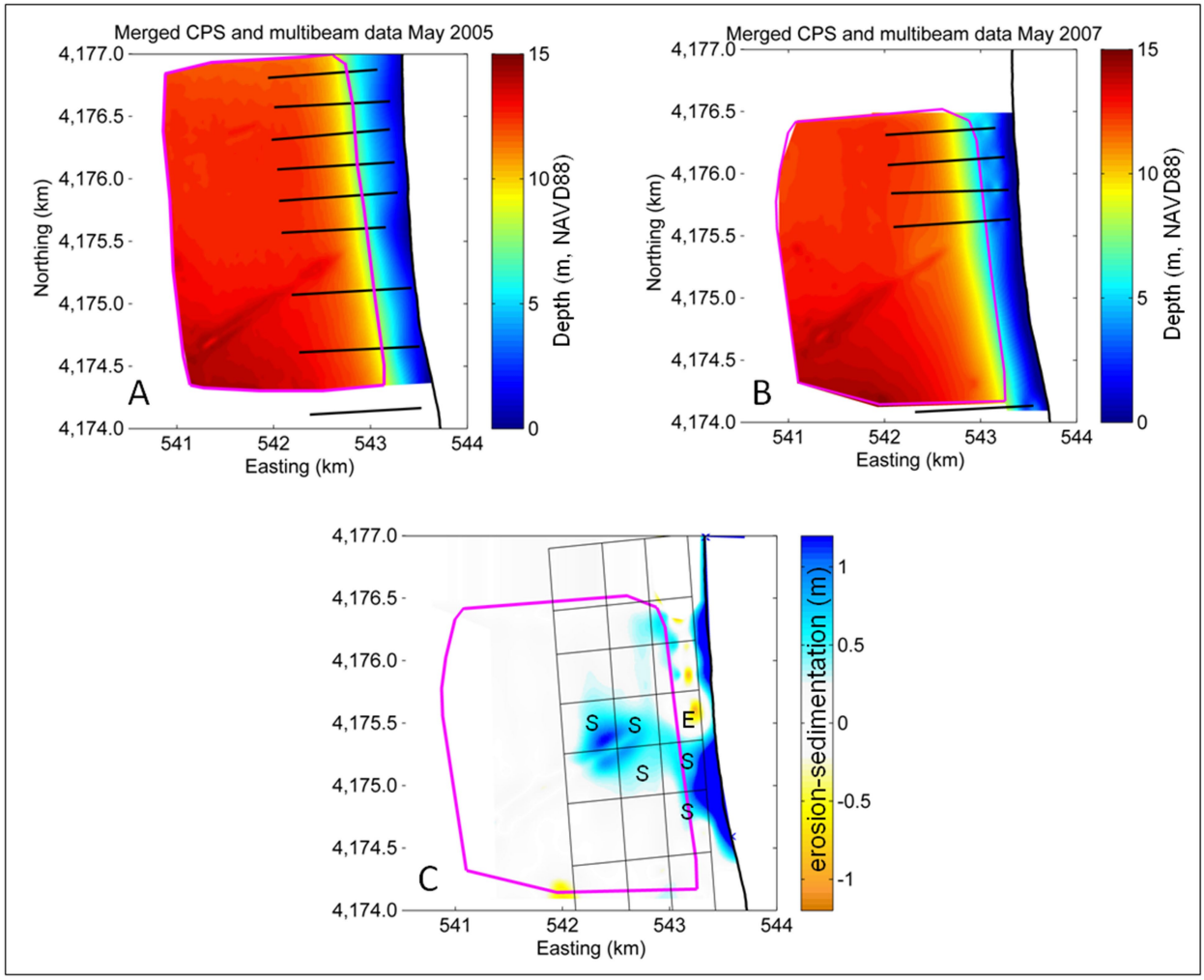

Figure 16. Bathymetry plots employing merged multibeam and CPS data gridded to 10 x 10 m for *A,* May 2005 and *B,* May 2007. Magenta boxes denote area of multibeam measurements. CPS data was collected along shown cross-shore transects (numbered). *C,* Bathymetric difference between the two merged datasets. Letters 'S' and 'E' denote total net sedimentation or erosion within overlaid sediment grid.

Surveyed multibeam areas are shown by using magenta boxes, and CPS cross-shore transects are shown by using solid lines. The alongshore distance between the CPS cross-shore transects (250 m or greater) do not make them ideal for data interpolation, but they do provide a rough indication of the outer and middle surf-zone bathymetry not captured with the multibeam. Field conditions limited the collection of data along CPS transects 16 and 17 in 2007. For the 2005 CPS survey, a significant longshore bar was measured at transect 16, but not at transect 15, resulting in some inconsistencies in the nearshore interpolation. A bathymetric difference plot between the May 2005 and 2007 datasets is shown in figure 16*C*, where sediment loss is represented by yellow and red shades and sediment accumulation is represented by blue shades. The grid overlay in figure 16 is the same as the grid presented in figure 7 and used for alongshore averaging of cross-shore profiles; total net sedimentation (S) or erosion (E) is shown within each cell. Notable accumulation of sediments is apparent in the region of the exposed outfall pipe and original nourishment location. With the exception of the northeast-southwest oriented accretion signal south and shoreward of the nourishment site (thought to be an erroneous signal related to the low alongshore resolution of the CPS data and interpolation method) sediment loss is apparent in the shoreward cells. Close inspection of the CPS transects (fig. 15) suggests that the difference is due to a slight difference in the position of the alongshore bar.

Subaerial Beach Change

The MSL shoreline position and volumetric change were examined in the area immediately onshore of the nourishment (profiles 115-120, fig. 2 and table 1). Data from 2004 (the year prior to the first offshore nourishment) provided the baseline for comparison. In order to minimize the effect of the highly variable wave conditions and beach response that occurs during the winter months, the subaerial analysis is focused on the annual change observed during the summer months (May, June, and July), which is also the time period of most extensive topographic-data coverage in the nourishment area. During the winter months, the beach at the heart of the erosion hot spot (fig. 1) often becomes so eroded as to not allow safe passage of the ATV to the southern portion of the beach, preventing data collection in the area for months at a time and creating large data gaps in the winter surveys.

Figure 17 shows the mean summer (May-July) position of the MSL shoreline in 2005, 2006, and 2007 relative to the 2004 location. Profiles 116-120 show a noticeable accretion signal in 2007, compared to 2004. Data from the summer of 2006 also show subaerial accretion, but the location of these signals, north and south of the nourishment site, is highly localized ($\leq$ 300 m alongshore) and provides little evidence that these "peaks" are related to the nourishment. Moreover, the data from 2007 shows that the 2006 shoreline-accretion signal has all but disappeared, and in all years erosion is prevalent throughout the region of interest (fig. 17*B*). Table 5 lists the 2007 shoreline-position change relative to 2004 in the area of the nourishment, as well as the percentage of the 2007 change relative to the maximum position difference of the MSL shoreline observed since surveys began in 2004. The maximum difference in position for each profile gives an idea of the variability observed in that portion of the beach, and calculation of the percentage of the maximum "normalizes" the change while providing a measure of the significance of any observed signal. Inspection of the profiles in the nourishment area indicates that the accretion signal shown in figure 17 only accounts for 13 - 32 percent of the largest variability. While not removing the possibility that the offshore nourishment is responsible for the observed accretion, the lower percentages indicate that the change in the shoreline position is

A

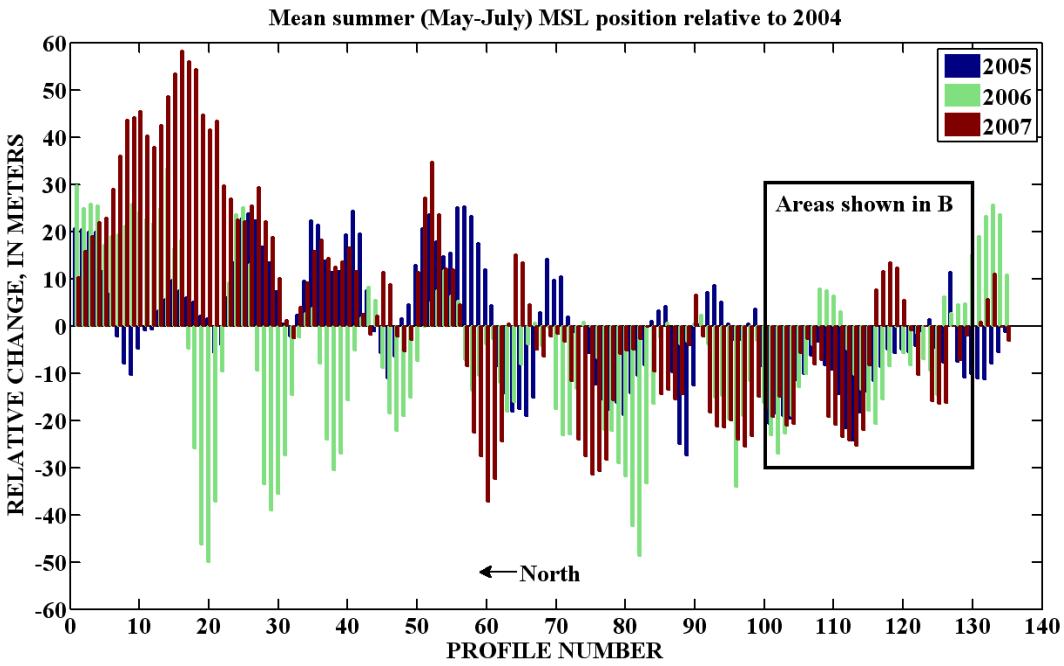

B Inset of box in A

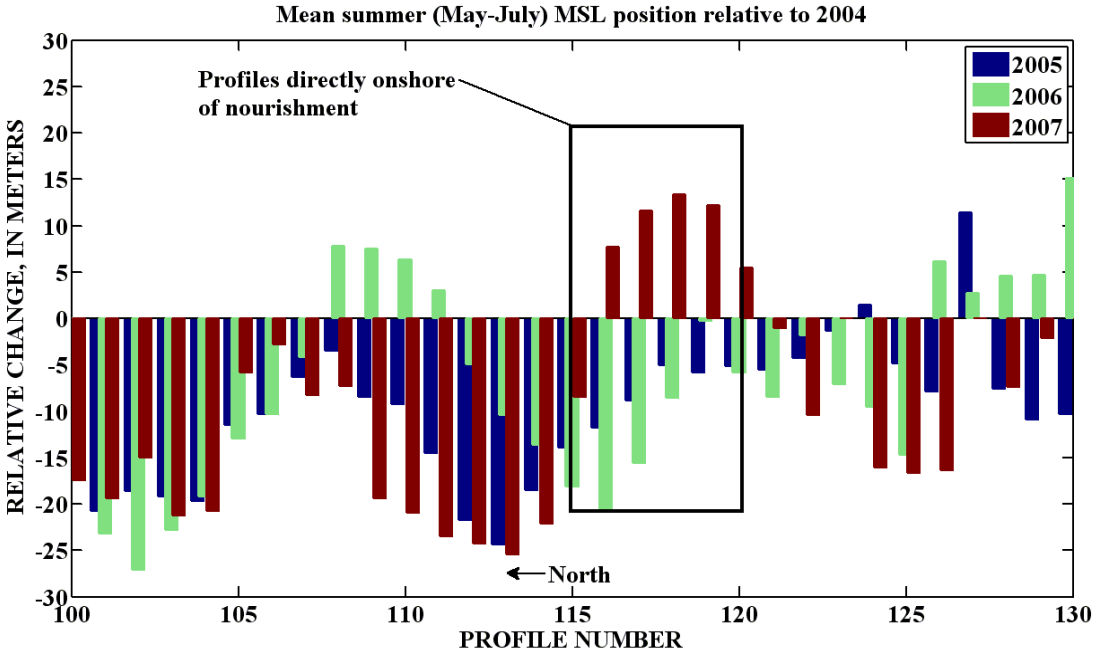

Figure 17. *A*, Bar plot showing the average summer (May-July) position of the MSL shoreline relative to its 2004 position. Note the accretion at the northern end of the beach and erosion of the middle and southern portion of the beach. The position of the shoreline south of profile 120 in 2007 is from only one survey, due to common data gaps in this area caused by inaccessibility or poor GPS and radio coverage. *B*, Inset view of the box plot A, highlighting the accretion signal onshore of the nourishment site at profiles 116-120.

Table 5. Change in position of the mean sea level (MSL) shoreline, the maximum change observed since 2004 for each profile, and the percentage of the 2007 change of the maximum observed. N/A indicates that there was no intersection of the ATV data and MSL. Bold numbers indicate location adjacent to nearshore disposal site.

Profile Number	Average MSL change summer 2007-2004, in meters	Largest difference between any two surveys (absolute value), in meters	Summer 2007-2004 percentage of largest difference
100	-17.49	33.64	52
101	-19.41	50.13	39
102	-15.05	34.09	44
103	-21.25	32.74	65
104	-20.80	30.81	67
105	-5.85	22.01	27
106	-2.79	18.72	15
107	-8.31	23.33	36
108	-7.34	21.15	35
109	-19.38	33.66	58
110	-20.99	43.48	48
111	-23.54	44.84	53
112	-24.30	53.47	45
113	-25.46	49.29	52
114	-22.16	48.46	46
115	-8.52	51.82	16
116	**7.69**	**45.08**	**17**
117	**11.57**	**36.70**	**32**
118	**13.36**	**44.17**	**30**
119	**12.23**	**46.78**	**26**
120	**5.49**	**42.66**	**13**
121	-1.08	49.16	2
122	-10.40	34.48	30
123	N/A	27.56	N/A
124	-16.05	33.74	48
125	-16.66	36.67	45
126	-16.39	30.79	53
127	N/A	60.13	N/A
128	-7.37	20.51	36
129	-2.16	24.29	9
130	-0.11	28.74	0

not particularly striking for that area of Ocean Beach and could be a result of coincidental positioning of alongshore topography.

The annual change in the position of the average summer MSL shoreline is shown in figure 18. In the summer of 2007, the MSL shoreline was more than 20 m seaward of its 2006 location for more than a 100 m stretch of beach (profiles 116-118), while immediately north of the nourishment area, there is considerable erosion (profiles 108-113). Inspection of the 2006 and 2007 data in figure 18*A* appears to indicate an annual oscillation between erosion and accretion along the entire length of the beach; in nearly all locations, the 2006 and 2007 data are out of phase. The oscillations suggest that the local position of the shoreline could be largely controlled by propagation of alongshore topography (for example, horns and cusps).

A

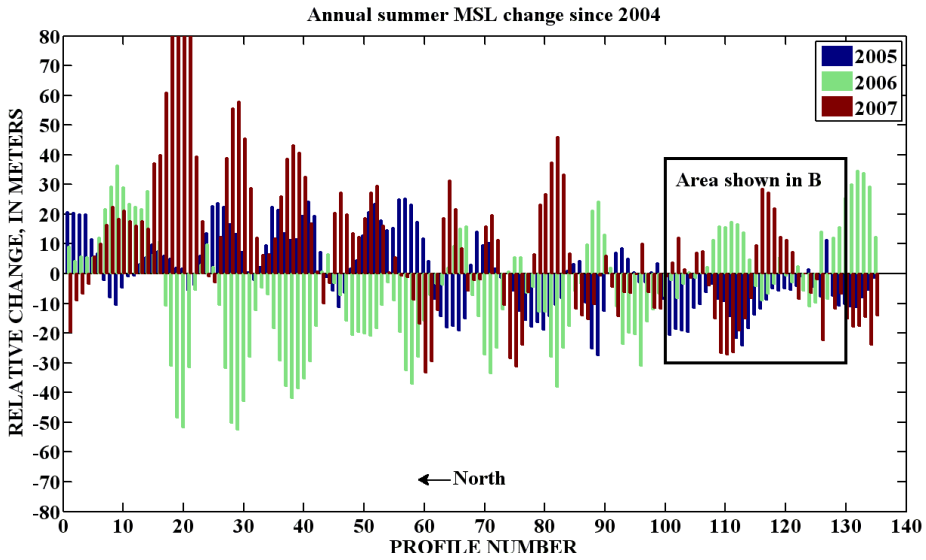

B **Inset of box in A**

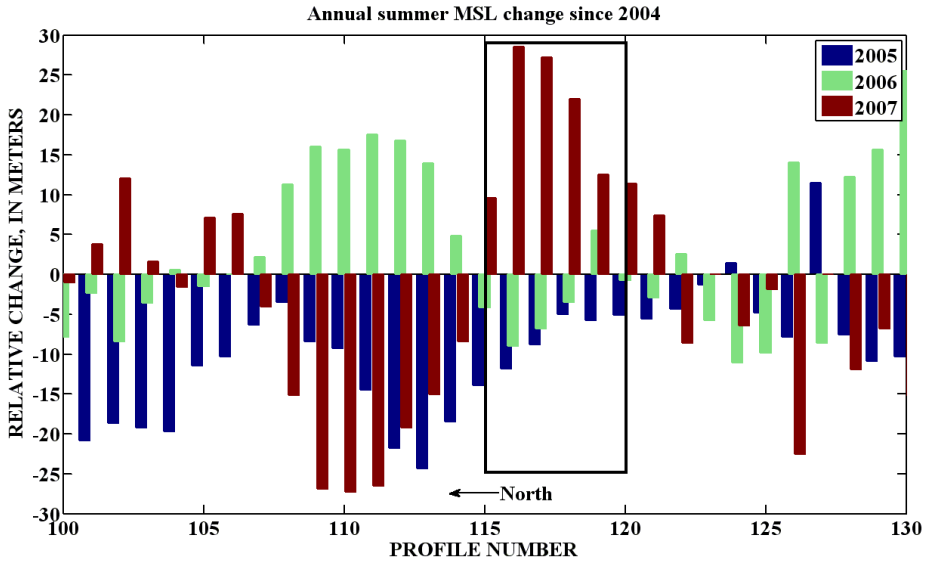

Figure 18. *A*, Annual change in the position of the MSL shoreline. *B*, Inset view of area next to the nourishment site. The profiles onshore of the nourishment site are indicated by the box in plot B.

Figure 19 shows the positions of the MSL shoreline on May 7, 2004, and May 21, 2007, adjacent to the nourishment. Accretion onshore of the nourishment site is visible along with erosion both north and south of the area. Figure 20 shows the subaerial beach-elevation difference between the two May surveys in the same area. Between profiles 115 and 120 there is a roughly 225 by 75 m swath of 0.5 m elevation gain.

To examine the volume difference between years, the summer grids for each year, 2004-2007, were averaged to produce a representative summer-topographic surface. Subtracting the average summer grids from one another gives the volume difference between the respective years. The averaged summer-volumetric difference, relative to 2004, between profiles 115 and 120 is summarized in table 6. In the nourishment area the subaerial beach contained about 2,400 m^3 more sediment in the summer of 2007 than in 2004. This volume corresponds to an increase in sediment of about 9 m^3/m of shoreline. Both 2005 and 2006 show volume loss relative to 2004, with the greatest erosion observed in 2006. In comparison to the CPS observed seasonal cross-shore transport of 300 m^3/m, and storm-induced subaerial beach changes which can erode the shoreline an average of 10 m (14 m^3/m; Barnard and others, 2007a; Hansen, 2007) the amount of accretion observed in table 6 is negligible.

Comparison of topographic surveys from 2004 through 2007 indicate that the subaerial beach has accreted immediately onshore of the nourishment site, but is only visible when comparing 2007 to 2004. The accretion signal, while noticeable in the data, cannot be definitively linked to the offshore nourishment. Several more years of offshore nourishment and topographic surveys will be required to conclusively determine if the nourishment is having the desired effect.

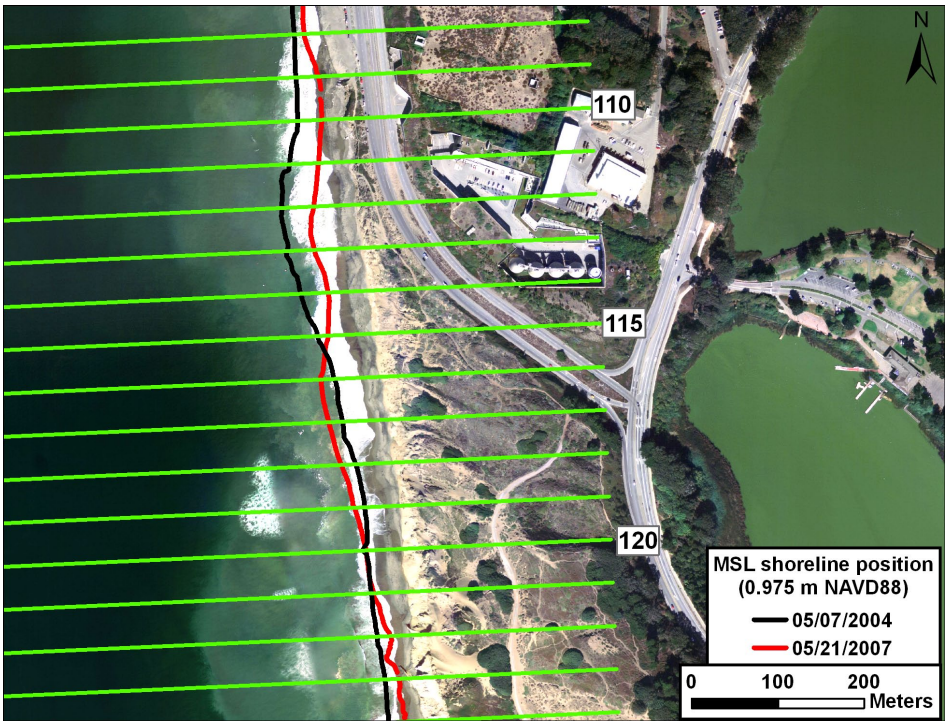

Figure 19. Position of the MSL shoreline on May 7, 2004, and May 21, 2007. Note accretion in 2007 survey onshore of nourishment site (located approximately 1,000 m offshore between profiles 115 and 120).

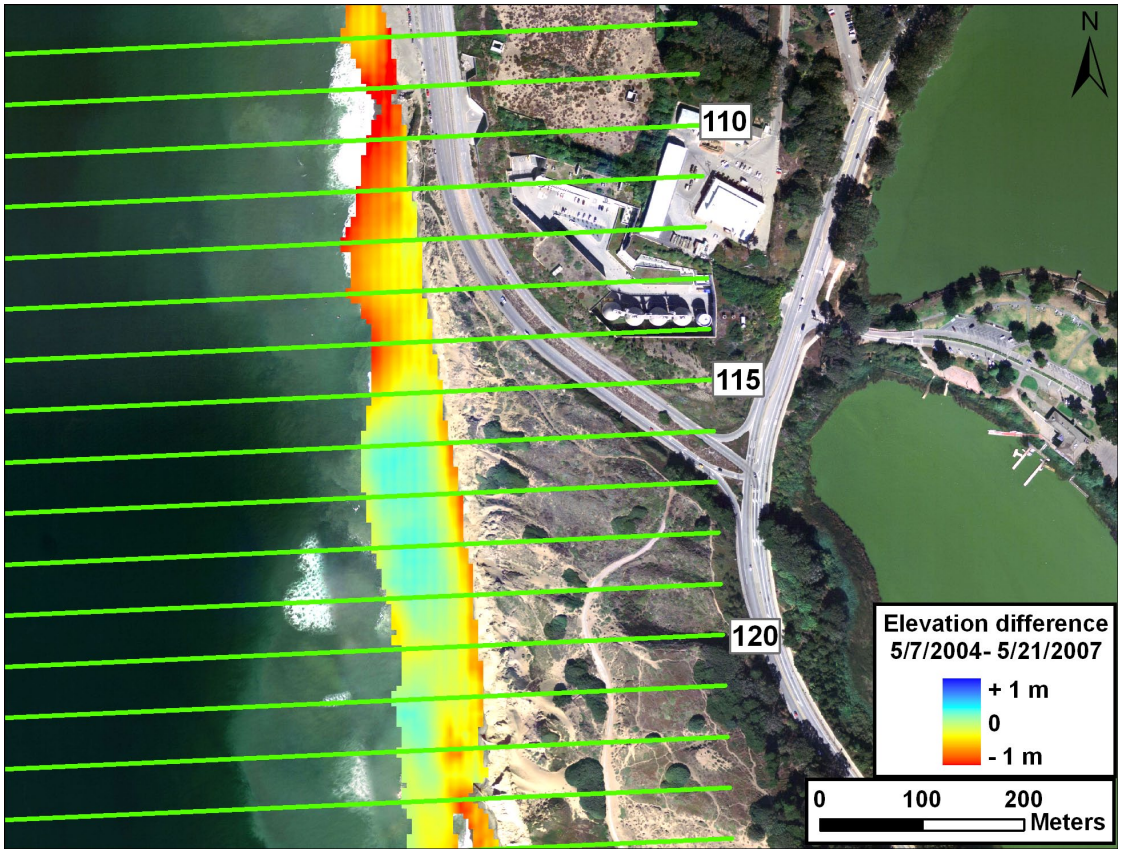

Figure 20. Elevation change of subaerial beach between May 7, 2004, and May 21, 2007. The light blue area between profiles 115 and 120 equates to approximately 0.5 m in accretion. Note the severe erosion at profile 109.

Table 6. Area, volume, and volume-difference statistics for average summer surveys from 2004 through 2007 for profiles 115 through 120. Note the area and volume statistics require the use of the common area between the various years, factors that cause variation in the surveyed area (for example, 2005 vs. 2007) include tide stage during surveys, GPS coverage, and shape of beach.

Year	Surveys averaged	Area* in square meters	Volume+ in cubic meters	Volume difference versus 2004 in cubic meters
2004	05/07/04, 06/07/04, 07/06/04	Varies	Varies	N/A
2005	05/02/05, 06/10/05, 06/27/05, 07,22/05	16,423	40,146	-1,633
2006	06/19/06, 06/30/06	6,559	19,061	-3,062
2007	05/21/07, 07/19/07	8,580	20,073	2,371

*In common with average of summer 2004 surveys.

+Calculated using common area with 2004 surveys.

Grain Size Analysis

Grain-size analysis shows a highly spatially variable sedimentological character at the mouth of San Francisco Bay (fig. 21). Median grain size varies from coarse sand and gravel in the inlet throat to a dominance of fine sand on the ebb-tidal delta. Detailed sampling in the nearshore-dredge disposal region indicates that surficial sediments consist primarily of fine sand (median grain size (d_{50}) = 0.18 mm), broadly consistent with nearshore bar and dune sediment found at Ocean Beach, but finer than beach sand (d_{50}= 0.28 mm). This sediment is, therefore, not ideally compatible to stay on the beach, but could build up the nearshore bars and help protect the beach from direct wave attack (Barnard and others, 2007a). Based on the results of the multibeam survey, at least half of this 0.18 mm sediment remains within the focus area after each full year of monitoring.

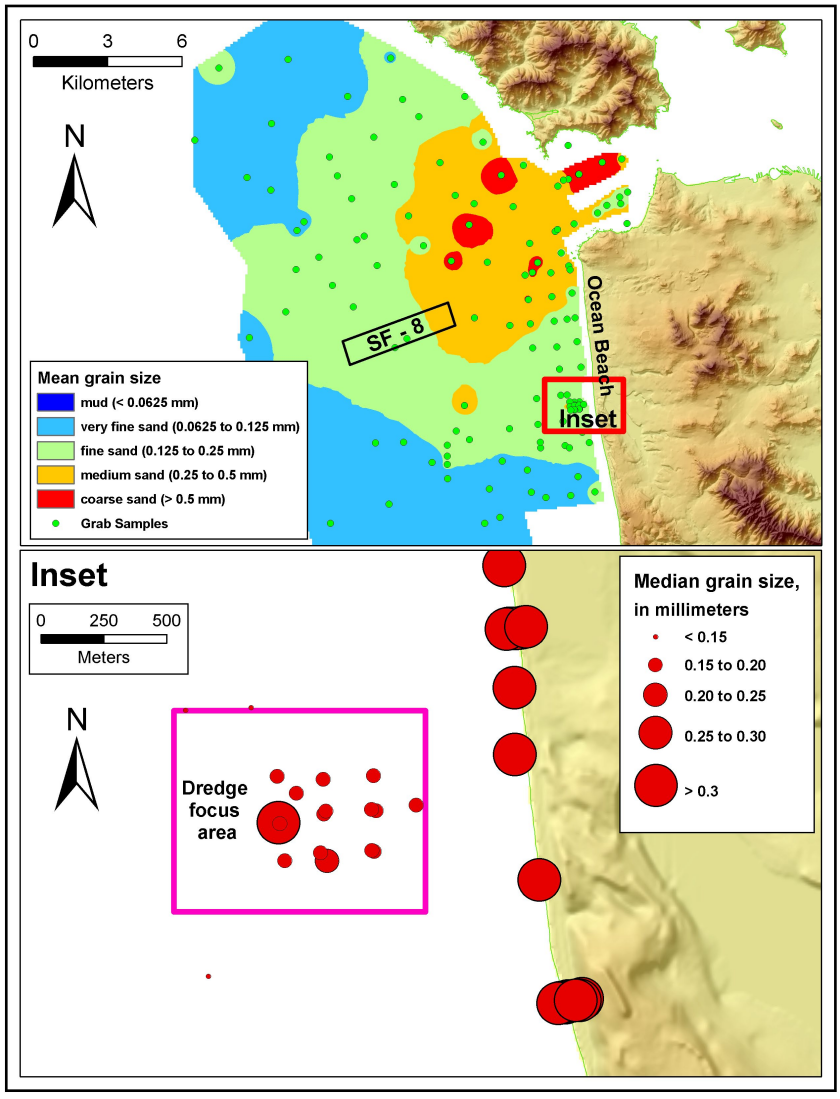

Figure 21. *A*, Gridded mean grain size from grab samples collected at the mouth of San Francisco Bay and *B*, individual samples of median grain size (D_{50}) collected in the dredge disposal region (inset).

Oceanographic Measurements

Principal axis plots of ADCP-measured currents at three distinct heights above the seabed (1.5 m above the bed, midway through the water column, and near the surface) are shown for the summer and winter measurements in figure 22. Currents are predominantly slightly west of north-south, following the orientation of the coastline. Both the summer and winter data show that the major orientation midway through the water column is rotated slightly clockwise, aligned with the north-south direction-this is most evident in summer measurements.

Depth-averaged currents ranged from 0.20 cm/s at slack tide and no waves to 80 cm/s during maximum ebb tide and wave heights greater than 2 m. Surface currents average 40 cm/s and are about twice as strong as near bottom currents (fig. 22*B*). Near-surface currents exceeding 1 m/s occurred on a few occasions during both winter- and summer- measurement periods and are primarily associated with ebb-tidal currents and significant wave heights exceeding 2 m. Near-bottom currents peaked at 60 cm/s during the winter deployment and at 50 cm/s during the summer deployment. The frequency of occurrence of near-bottom currents exceeding 40 cm/s was about 13 percent during the winter, which is 2-3 percent more frequently than during summer. Estimates of the critical Shields parameter (θ_c; Soulsby and Whitehouse, 1997) indicate that near-bottom currents on the order of 38 cm/s are capable of entraining and maintaining 18-mm sized sediment grains in suspension (assuming $\theta \geq 2\theta_c$, a Chezy friction coefficient of 65, and a relative sediment density of 2.58 g/cm^3 in seawater) under steady uniform currents. Based on empirical and theoretical relations presented by Hanson and Camenen (2007), it is estimated that 15 s waves producing currents on the order of 50 cm/s are necessary to entrain and transport sediments of 18-mm-median grain size. As such, measured currents suggest that transport of placed dredge material occurred during episodes of stronger tides and episodic storm events.

Wave roses for the summer and winter deployments are shown in figure 22*C*. Waves were predominantly from the west and northwest during the summer and from both the southwest and northwest during the winter deployment. Maximum measured significant-wave heights during the summer and winter were 2.4 m and 3.4 m, respectively. Peak wave periods (not shown) ranged from 3 s to 18 s and from 9 s to 18 s in summer and winter, respectively.

Numerical Modeling

In order to assess the behavior of nearshore-dredge disposal at Ocean Beach, processes affecting the hydro- and morphodynamics were investigated with numerical modeling. Two separate model approaches were applied: a cross-shore profile model and a coastal-area model. The cross-shore model was employed to assess the potential for onshore migration of sediments due to cross-shore processes, including the effect of mound volumes and proximity to the shoreline. The coastal-area model was used to investigate the effect of mound placement on nearshore-wave transformation, alongshore currents, and the transport of sediments in the alongshore direction. The coastal-area model was run in a vertically-averaged mode, thus eliminating any bottom return flow in the cross-shore direction and not accounting for cross-shore transport caused by wave asymmetry. Hence, any predicted cross-shore directed transport in the coastal-area model is expected to be less accurate than that predicted with the cross-shore model.

Cross-Shore Profile Modeling

Cross-shore profile modeling was done with the UNIBEST-TC model (Bosboom and others, 2000). A shore-normal profile through the centroid of the nourishment site in May 2006

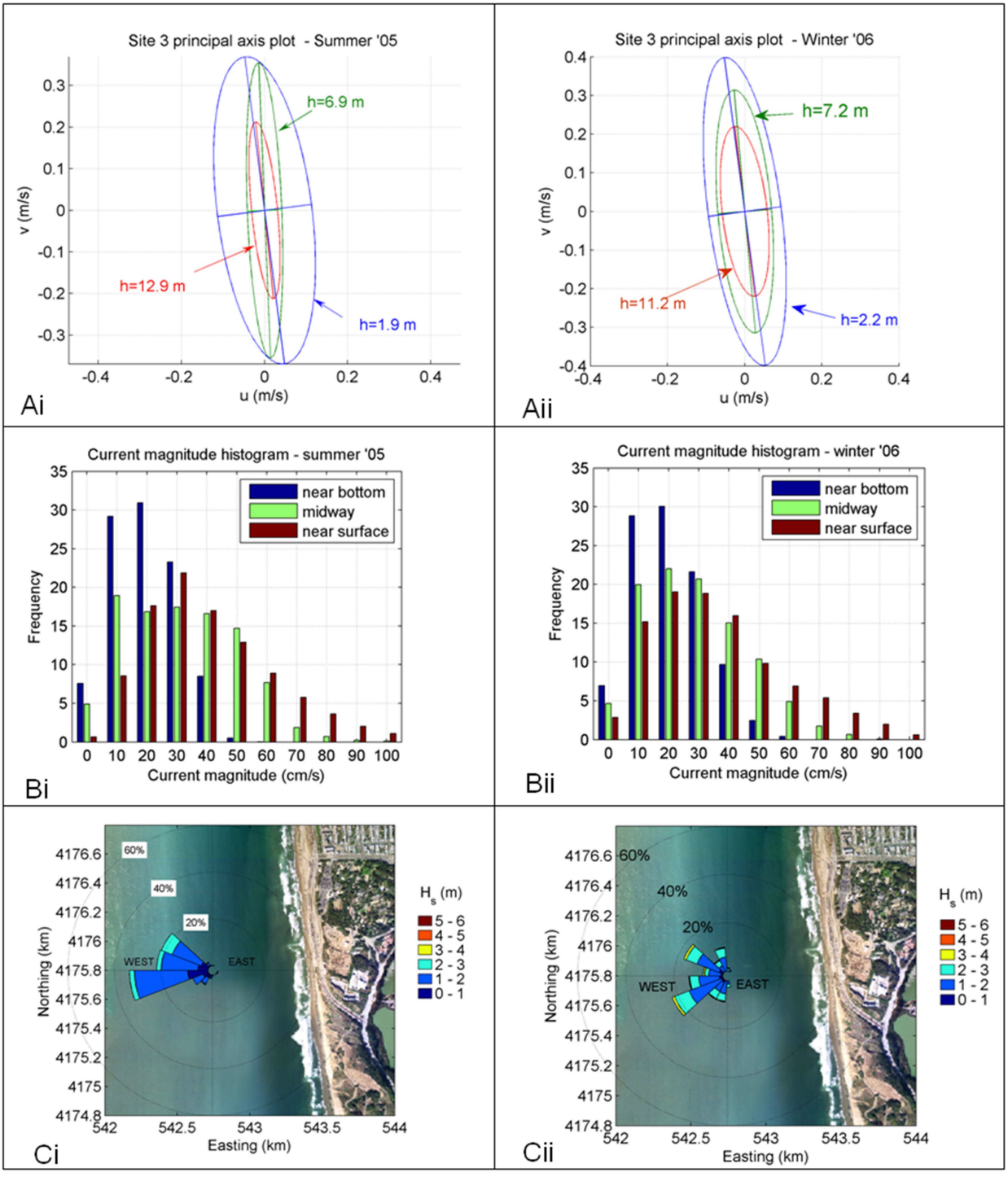

Figure 22. Field-measured currents and waves during summer 2005 at the onset of shoreface nourishment and winter 2006. Current principal-axis plots are shown for *Ai*, the summer, and *Aii*, winter deployments. *Bi-ii,* current magnitude histograms . *Ci-ii*, wave roses.

was extracted from the multibeam data, extrapolated to the shore, and used as initial bathymetry in the cross-shore model runs. The profile was assumed to be representative of typical cross-shore profile in the region of nourishment. Parameter settings used for the model simulations are mostly default values (table 7).

Table 7. UNIBEST model parameter settings.

Variable	Description	Units	Value
BETD	roller parameter	-	0.1
BVAR	varying beta switch (on/off: 1/0)		0
D50	D_{50} grain size	m	0.0002
D90	D_{90} grain size	m	0.00025
DSS	suspended grain diameter	m	0.00018
DT	time step	days	0.5
DVAR	varying grain size switch (on/off:1/0)	-	1
FCVISC	viscosity coefficient	-	0.1
FWEE	friction factor	-	0.01
GAMMA	breaking parameter	-	B & S
RC	friction factor for currents	-	0.055935
RKVAL	friction factor	-	0.045
RW	friction factor for waves	-	0.045
SALIN	salinity	psu	33
TEMP	temperature	°C	10

Model-Predicted Sediment Transport Modes

In order to assess the potential for onshore migration of sediments and the relative contribution of alongshore-directed tidal currents on the total transport, results from two simulations, one with tides and one without tides, were compared. The simulations were run by using the UNIBEST model and consisted of realistic tide and wave conditions (encompassing the time-period between July through Dec 2006) were compared. Wave conditions at the open boundary were estimated with a time-series of deep-water waves (CDIP buoy p029) and a look-up-table of SWAN model results for the region (Eshleman and others, 2007). Offshore deep-water measured wave heights and peak directions are plotted in figure 23*A* along with the model-predicted conditions at the cross-shore model open boundary. Long ($O(Tp$=20 s)) high waves (significant wave height often greater than 4 m) from the northwest are typical for the area during winter months and result in a high degree of refraction and energy dissipation over the shelf, emphasizing the need to account for these processes prior to applying forcing at the nearshore model boundary. Water levels and tidal currents were estimated with outputs from a calibrated depth-averaged Delft3D model of the region including San Francisco Bay (Barnard and others, 2007a). Water levels ranged from -0.31 to 2.1 m, relative to NAVD88, with maximum tidal currents peaking at 0.53 m/s.

Figure 23*B* summarizes the mean sediment transport rates by type and direction of transport as predicted with the UNIBEST cross-shore model. Predicted bed-level changes for cases with and without tidal currents show little difference for the given sediment grain size (D_{50}=0.20 mm) and time period (July 2006 - Dec 2006). Outside the breaker zone, in the region of mound placement (at about 1,200 m), south-directed suspended-load transport dominates. In

the cross-shore direction within the surf zone, offshore-directed suspended transport dominates onshore directed cross-shore transport, resulting in a net decrease of the beach slope.

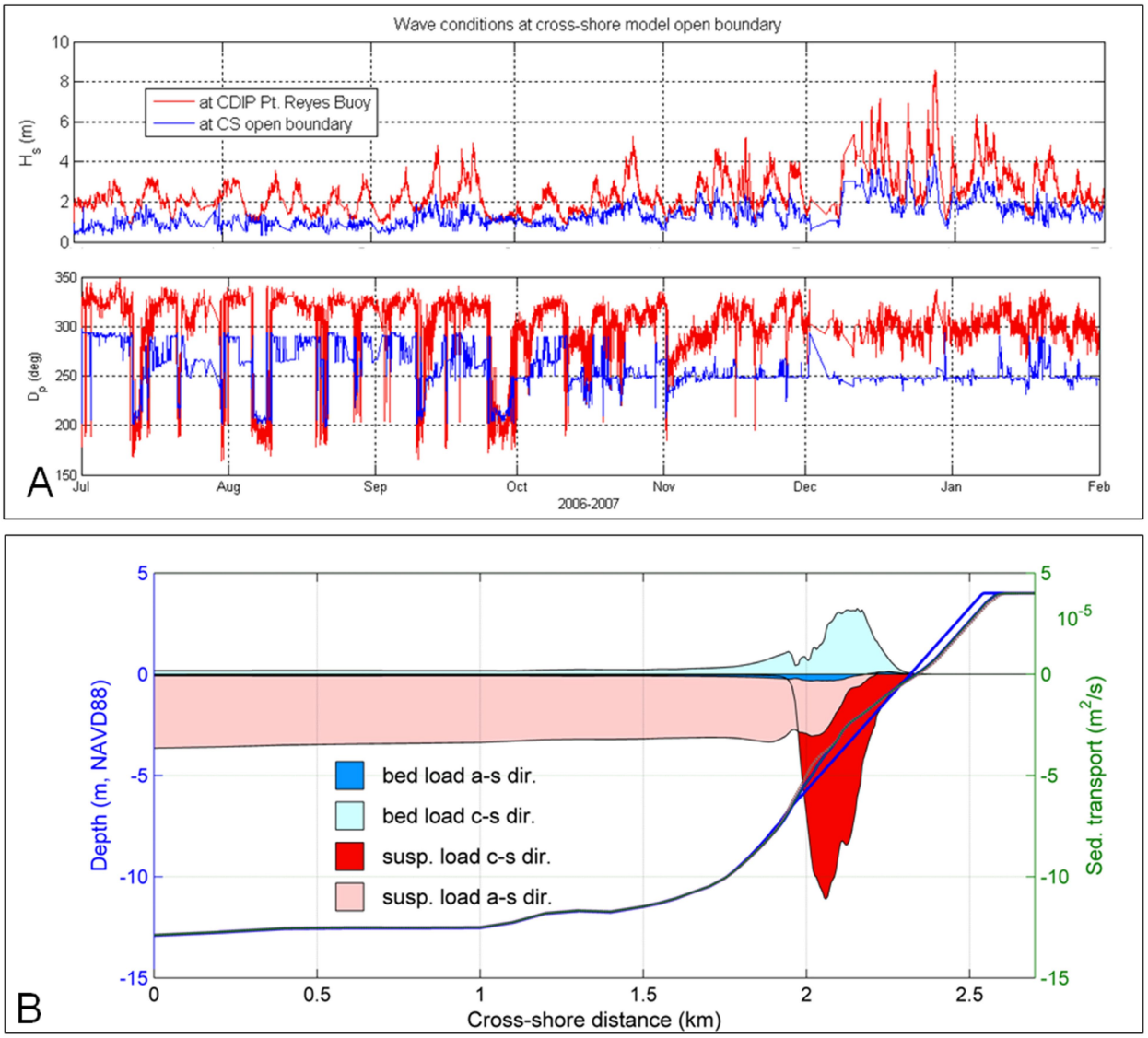

Figure 23. Wave-forcing conditions and model-predicted sediment-transport modes. *A*, Wave height and peak direction measured at the offshore CDIP Pt. Reyes buoy (red) and corresponding modeled conditions at the open boundary of the UNIBEST cross-shore model at 13 m water depth (blue). Note the high degree of wave-energy lost due to refraction and shoaling. *B*, Mean transport rates and modes predicted with the UNIBEST cross-shore model. Transport modes are shown with filled in areas with mean rates shown on the right-hand abscissa. Initial and final profiles are shown with solid blue and black lines and referenced to left abscissa. Suspended load in the along-shore (a-s) direction dominates in the region of dredge placement (~1,200 m in the cross-shore direction (c-s)).

Model-Predicted Shoreline Change

The potential for onshore movement of shoreface nourishment was tested by including various mound configurations in three distinct water depths. Figure 24 shows three hypothetical mound locations and quantities used in the model. Wave and tide conditions were the same as for the simulation described in the previous section.

Predicted volumetric shoreline change is plotted against the three different placement locations. The active shoreline was defined as the maximum tidal range predicted at Ocean Beach for years 2005 through 2006. The predicted volumes plotted on the abscissa of (fig. 24*A*) were normalized by the predicted volume change for the same simulation time period (summer 2006 - winter 2007) without any placement (32 m^3/m). Model results indicate that placement must occur in shallow water (about 5 m) in order for the cross-shore driven transport to dominate the alongshore suspended sediment transport. However, the combination of alongshore currents and onshore-driven bed-load transport from waves may aid in downdrift and shoreward transport not captured in the cross-shore model.

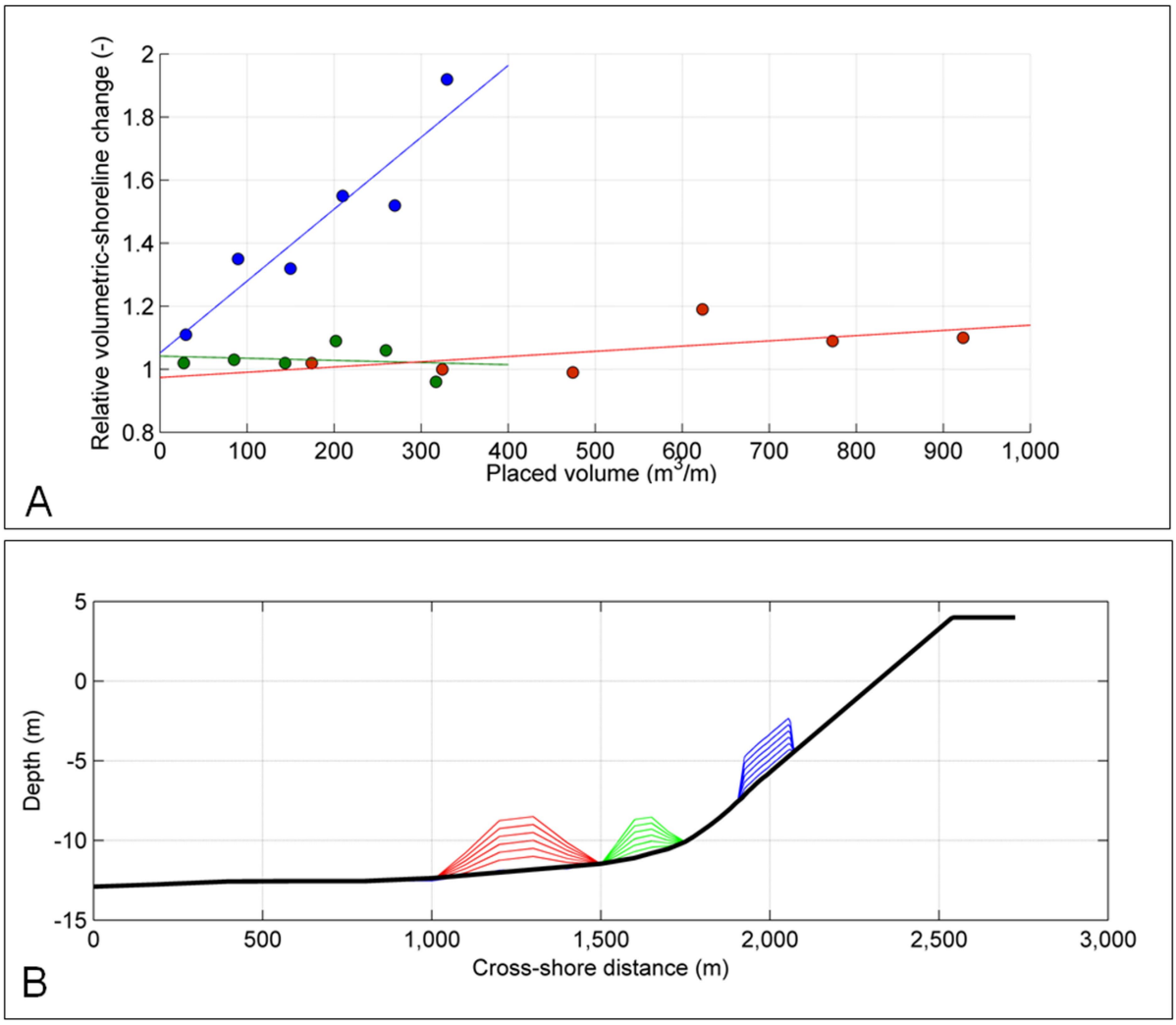

Figure 24. Relative volumetric-shoreline change as a function of amount placed (*A*) for three different hypothetical water depths (*B*) as predicted with the cross-shore UNIBEST model.

Coastal-Area Model

Coastal-area modeling of Ocean Beach was done with the Delft3D numerical-modeling system (Roelvink and van Banning, 1994; Lesser and others, 2004). A curvilinear FLOW grid, extending from central San Francisco Bay in the east to about 35 m of water depth in the west, and from Pacifica in the south to Bolinas in the north, was used to calculate tidal currents (fig. 25). The large FLOW grid was chosen in order to account for influence of the tidal inlet on flows at the study site (about 6 km south of the inlet). Tidal constituents, obtained from a previously calibrated larger model encompassing the entire San Francisco Bay, and from Half Moon Bay in the south to Pt. Reyes in the north out to 80 m water depth, were used to force the model at its open boundaries. Grid resolution was 220 m in the alongshore direction and 95 m in the cross-shore direction in the vicinity of the study site.

A coarse-wave grid and a finer, nested rectangular-wave grid were used to simulate the propagation of waves from offshore to the nourishment area. Resolution of the coarse-wave grid was 500 m^2, while the nested-wave grid measured 250 m in the alongshore direction and 100 m in the cross-shore direction in the vicinity of the study site. Multibeam bathymetry measurements obtained as part of this study (table 2) were used to generate model input bathymetry data at the study site. The remaining bathymetry was derived from nearshore Ocean Beach depth data collected under the auspices of the Ocean Beach Coastal Processes Study (Barnard and others 2007a; http://pubs.usgs.gov/of/2007/1217/). This bathymetry includes CPS data from May 2004, multibeam measurements of the seaward end of the Golden Gate inlet including the ebb tidal shoal (Barnard and others, 2006a), multibeam measurements of central San Francisco Bay (Dartnell and Gardner, 1999), and National Ocean Service (NOS) soundings from 1956 (NOAA, 2008a).

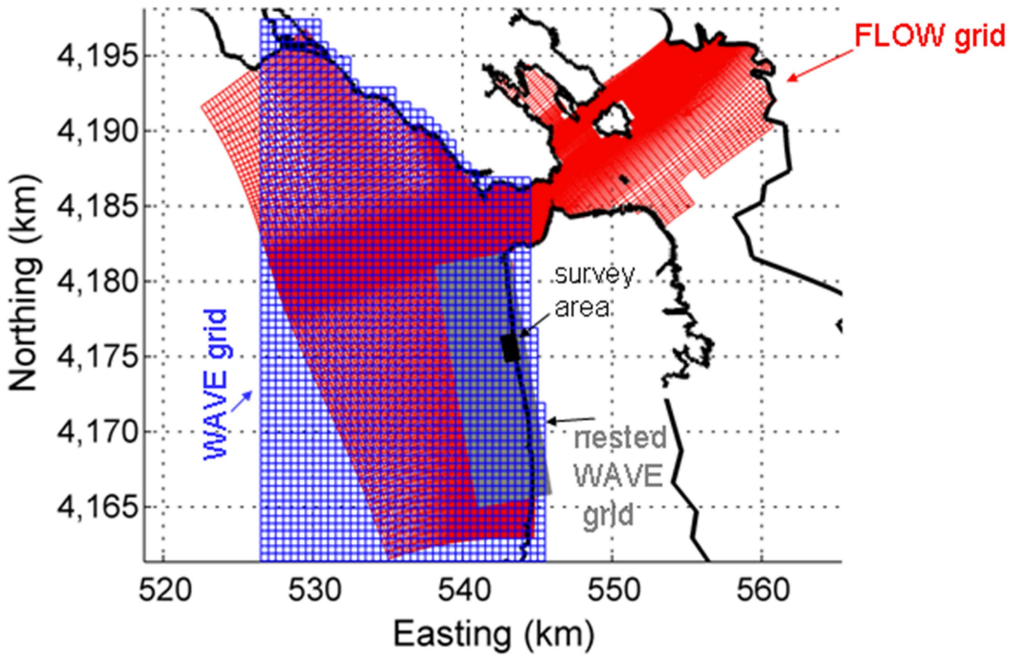

Figure 25. Delft3D grids employed in the coastal-area model. Resolution of FLOW grid (red) is 220 x 95 m in the along- and cross-shore directions, respectively. Resolutions of the WAVE grids are 500 x 500 m for the larger (blue) grid and 250 x 100 m for the smaller, nested (gray) grid – both in the along- and cross-shore directions, respectively.

Model parameter settings are listed in table 8 and are based on measurements (for example, temperature) and calibration results of the larger San Francisco Bight model. The van Rijn (1993) formulation for suspended- and bed-load sediment transport due to tidal- and wave-induced currents was employed with the multiplication factor for bed-load transport from currents set to 1 (default) and the wave related suspended- and bed-load transport factors set to 0.3 (default is 1).

Table 8. Delft3D parameter settings.

Variable	Description	Units	Value
WAVE module			
α/γ	Battjes and Janssen (1978) bore based model for depth induced breaking	[-]	1 / 0.73
	Spectral peak enhancement factor (Jonswap)	[-]	3.3
	Min/max/number bins in freq. space	[-]	0.05 / 1.0 / 36
α / β	Non-linear triad wave-wave interactions	[-]	0.1 / 2.2
	Bottom friction (Jonswap)	m^2/s^3	0.067
R	Water density	kg/m^3	1,025
Te	Temperature	°C	11
FLOW module			
ρ_w / ρ_a	Water/air density (kg/m^3)		1,025 / 1
ν	Horizontal eddy viscosity	(m^2/s)	1
S	Salinity	psu	31
δ	Threshold depth	(m)	0.1
	Bottom stress formulation due to wave forces	[-]	Fredsoe, 1984
C_h	Bottom roughness (Chezy coeff.)	[-]	*65
Transport and morphology			
ρ_s	Sediment density (sand/dredge material)	kg/m^3	2,650/2,650
D_{50}	grain size (sand/dredge material)	μm	280/200
MorFac	Morphologic scale factor	[-]	10
z	van Rijn's reference height factor	[-]	1
Sus	Current-related suspended transport factor	[-]	1
Bed	Current-related bed load transport factor	[-]	1
SusW	Wave-related suspended transport factor	[-]	0.3
BedW	Wave-related bed-load transport factor	[-]	0.3

*At the study site

Effect of Mound Placement on Nearshore-Wave Transformation

Placement of an offshore mound can alter wave heights and propagation direction as the waves shoal, refract, and diffract around a mound. The altered wave field has the potential to change local sediment-transport gradients, causing some areas to experience a reduction in longshore transport and other areas to increase. The magnitude and significance of the change at the shoreline is expected to depend upon the wave climate, surrounding bathymetry, and size and location of mound placement.

The influence of two different-sized mounds subjected to two constant offshore wave conditions approaching directly from the west (fig. 26). Offshore significant wave heights of 4 m

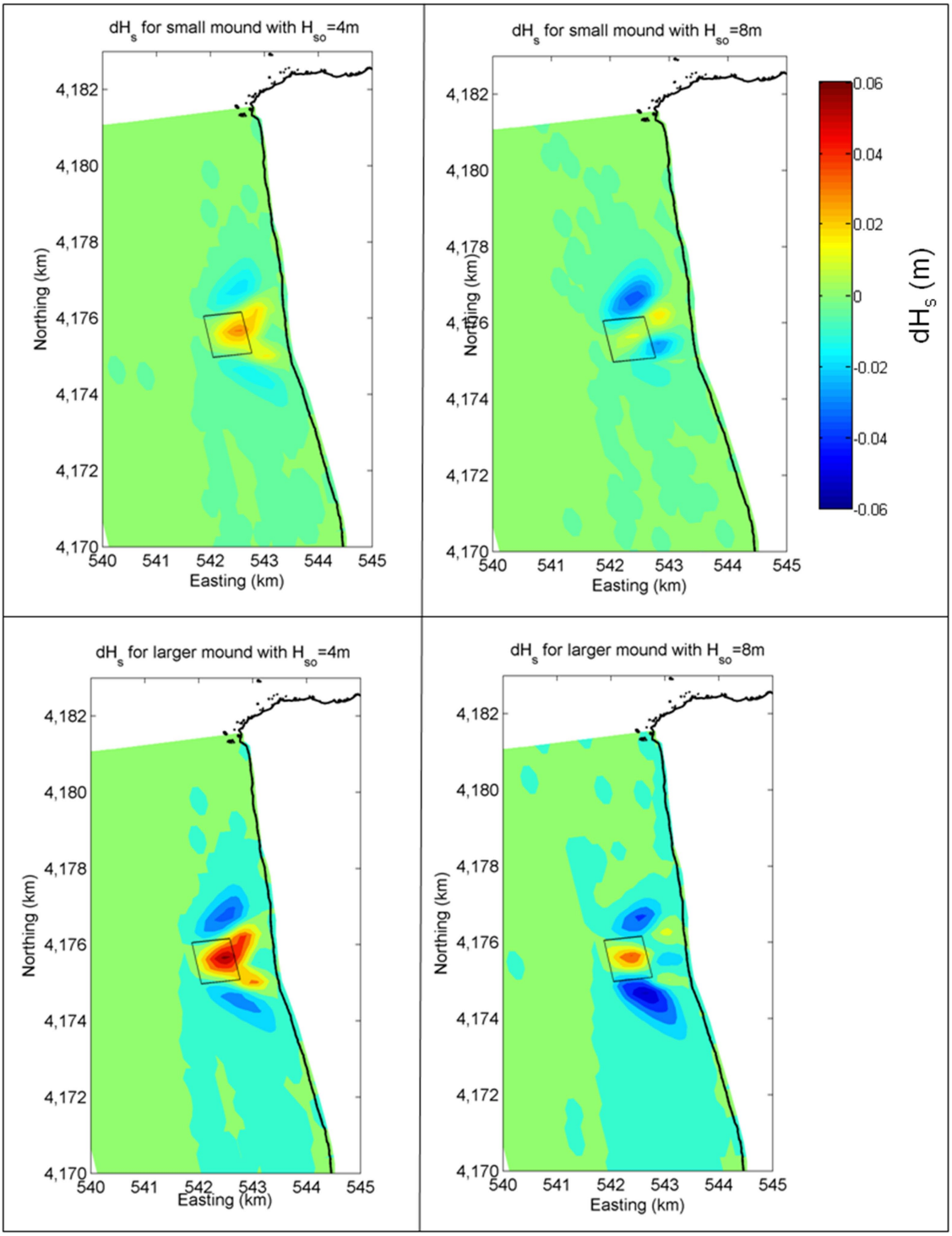

Figure 26. The influence of mound size on nearshore wave-height transformation. Colors depict wave-height differences (H_s with mound – H_s without mound) for varying mound volumes and incident wave conditions.

represent low-end storm conditions based on analysis and a qualitative assessment of ten years of historical data measured at the CDIP Pt. Reyes buoy [mean winter (October-March) significant wave height 2.8 m and peak period 13.0 s]. The 8 m wave height represents extreme cases. Following refraction and shoaling across the shelf, wave heights (H_s) immediately seaward of the nourishment are predicted to be 3.3 m and 4.3 m for the 4 m and 8 m offshore conditions, respectively. The colors indicate the difference in wave heights for cases with and without dredge mounds (H_s with mound – H_s without mound) exposed to the same offshore forcing conditions during the same lower low tide. The snapshots represent conditions one day after placement and include small differences in mound volumes due to previous transport. The mound footprint is indicated by the black box that approximates the region in which dredge material has been placed during the last three years. The upper two figures are for a total mound volume of 280,000 m^3 with an approximate 0.5 m height. The lower two figures are for a mound of twice the volume and height. In all cases, the influence of the mound extends slightly more than one km in the alongshore direction both to the south and north. With the mound in place, the model predicts that wave heights increase due to shoaling in the immediate location of the mound and that the waves refract toward more shallow water along the edges creating regions of wave focusing and energy loss further out. Although the nearshore placement of the mound does affect wave propagation and transformation just outside the surf zone, the overall difference is small with a maximum wave height difference of ± 6 cm.

Alongshore Flow Velocities

Variations in alongshore flow velocities were estimated for two separate wave conditions for cases with and without a nourishment. A 2-m-thick nourishment placed at the centroid of the 2005 nourishment was assumed. Resulting alongshore velocities are shown in figure 27 for a longshore transect shoreward of the nourishment and through shore parallel sections a2-a7 in figure 7. The instantaneous depth-averaged velocities are for maximum ebb tide under conditions of northwest (D_p=315°) high (H_{so}=7.7 m) and low waves (H_{so}=1.9 m). Wave periods were 16 s for both cases. The model results indicate that the nourishment mound has little effect on the longshore velocities independent of wave height, but that greater wave heights induce a stronger alongshore directed current, except in the region north of the nourishment. This reduction in flow

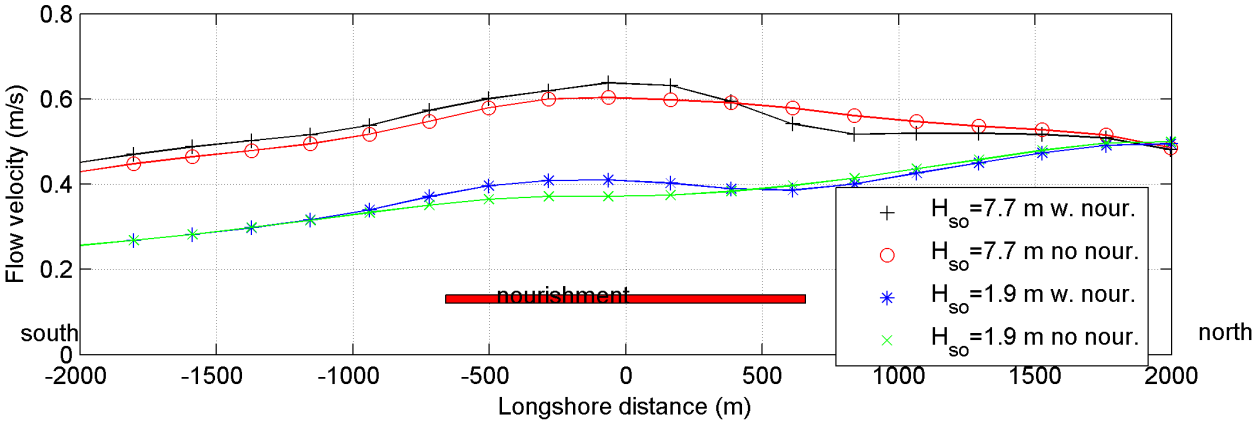

Figure 27. Model-predicted along-shore currents at the 10 m contour shoreward of the nourishment at maximum ebb-tide with high (7.7 m) and low (1.9 m) waves from the northwest (D_p=315°) and for the case with and without a shoreface nourishment.

velocity for the higher wave condition and increase in flow velocity for the lower wave condition at the lee side and north of the nourishment are thought to be related to increased wave dissipation of the larger waves as they break further offshore compared to the smaller waves. The net effect may be that the presence of the nourishment reduces flow velocities, allowing some sediment to settle out north and lee of the mound.

Overall Sediment-Transport Patterns

Model-predicted sediment-transport patterns are shown in figure 28. The left-hand panels (A and D) show predicted magnitudes without nourishment, and the right-hand panels (B and E) show the same simulation, but with 340,000 m^3 nourishment at the centroid of the 2005 placement. For the sediment-transport simulations, 24 distinct wave cases were run during a representative diurnal tide. Transport magnitudes were then multiplied by the probability of occurrence of the given wave condition based on 11 years of measurements at the offshore Pt. Reyes CDIP (p029) buoy (table 9). As with the previous simulations, wave forcing from the CDIP buoy was first propagated with a larger domain model (not shown) to the boundaries of the larger wave grid (fig. 25), allowing boundary wave conditions to vary in both space and time.

Resulting transport patterns in the alongshore direction are shown, for the greater part of Ocean Beach (figs. 28*A*-*B*). Alongshore transport rates are averaged at model grid points (fig. 28*F*). As such, transport both inside and outside the surf zone are included, and in most cases, magnitudes and directions are weighted by transport seaward of the surf zone. As a result, the southerly predicted transport at the northern end of the beach is primarily due to currents exiting the Bay during ebb. Although not explicitly shown, alongshore transport in the inshore region is to the north at the northern end of Ocean Beach.

Overall, the predicted cross-shore averaged alongshore transport rates are similar whether nourishment is present or not. In particular, there are two regions of alongshore sediment transport divergence (fig. 28C), where the alongshore sediment transport gradient ($\delta S/\delta y$) is plotted on the abscissa: one at about N4,175 km at the nourishment area and point of pipe outfall scour, and a second slightly smaller point (about 0.32 m^3/year/m) at about N 4,172 km. An area of convergence is apparent north of N4,176 km, south of the observed attachment of the ebb tidal shoal with the shore (about N4,178 km). A detail of the model-predicted sediment transport vectors in the cross- and alongshore directions for the case with and without the nourishment are shown for the immediate vicinity of the nourishment site in figures 28*D*-*E*, respectively. The location of the dredge mound is indicated by the black solid rectangle. The red grid is the sediment grid shown in figure 7, and, it is used to calculate measured and modeled sediment-transport patterns. Sediment-transport directions and magnitudes (units of 0.001 m^3/yr) are indicated by the red arrows across grid boundaries. Overall, the net transport within the sediment-grid area is significantly greater in the cross-shore direction as compared to the alongshore direction for both cases. However, because the coastal-area model was run in a vertically depth-averaged mode, offshore-directed sediment transport in the nearshore region is not expected to be as accurate as that predicted by using the cross-shore model.

In the cross-shore direction, transport is predicted to be larger outside the disposal region when no mound is present, and greater across the mound in the presence of dredged material. Onshore transport across the grid, closest to the shore, is greater in the case of no mound, except immediately shoreward of the center portion of the mound where the onshore transport is

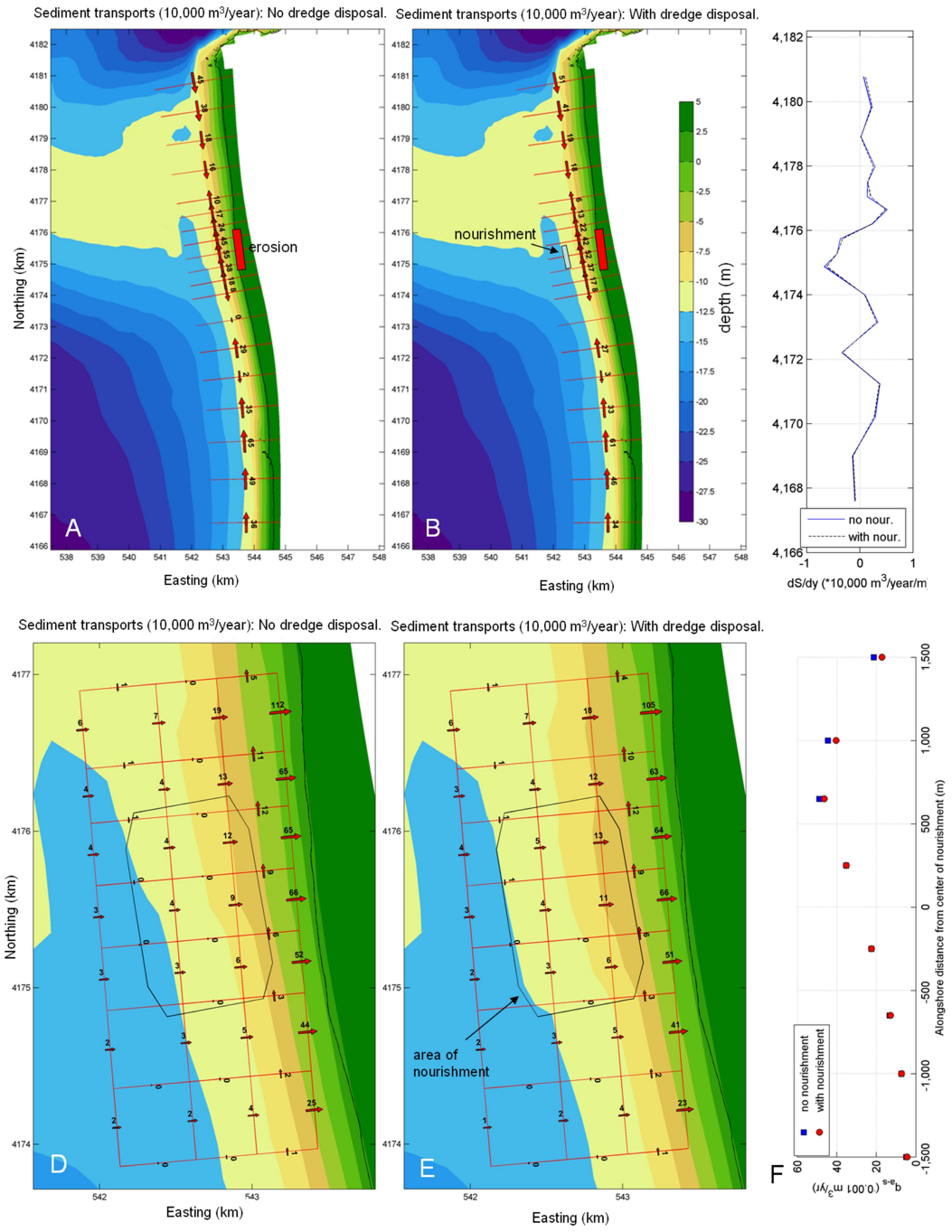

Figure 28. Model-predicted sediment-transport patterns. The left panels (*A* and *D*) represent simulations without a nourishment, while panels B and E are for simulations with a nourishment centered at the centroid of the 2005 dredge placement. Alongshore transport patterns for the greater Ocean Beach area (*A*, *B*, and *C*) show points of divergence in the region of the hotspot and south thereof, and a point of convergence where the ebb-tidal shoal attaches to the shore. A detail of the along- and cross-shore directed sediment transport magnitudes in the region of the nourishment are shown in *D* and *E* followed by along-shore transport rates just shoreward of the mound placement in *F*.

Table 9. Offshore wave conditions employed for sediment transport model simulations. The wave parameters are mean significant wave height (Hs), peak period (Tp), and wave direction (Dp).

	Offshore			Mid-point of wave grid west boundary			
Wave conditions	Hs (m)	Tp (s)	Dp (o) offshore	Hs (m)	Tp (s)	Dp (o) offshore	Probability (0 -1)
1	1.5	13.5	183	1.4	13.9	188	3.04E-02
2	1.5	14.1	203	1.4	13.9	205	2.46E-02
3	1.6	11.8	230	1.5	11.9	233	8.50E-03
4	1.8	10.9	258	1.8	10.0	257	2.10E-02
5	1.9	12.7	283	1.7	12.0	277	1.07E-01
6	1.9	10.7	306	1.5	10.1	302	1.98E-01
7	1.9	8.0	325	1.1	8.3	315	1.71E-01
8	1.6	6.5	346	0.4	6.6	320	9.00E-04
9	3.5	8.2	179	2.9	8.4	180	7.20E-03
10	3.4	8.5	203	2.9	8.4	201	4.10E-03
11	3.3	9.1	232	3.1	9.8	229	3.30E-03
12	3.4	11.7	259	3.0	12.0	256	1.05E-02
13	3.4	14.1	284	2.8	14.0	277	8.92E-02
14	3.4	12.6	305	2.4	12.0	298	1.82E-01
15	3.3	9.1	324	2.2	10.2	307	1.12E-01
16	5.7	10.1	177	4.5	10.3	182	4.00E-04
17	5.3	10.3	205	4.5	10.3	212	1.00E-04
18	5.4	11.2	234	4.8	12.1	229	2.00E-04
19	5.9	14.1	260	5.0	14.1	253	5.00E-04
20	5.7	15.9	283	4.2	16.1	261	6.10E-03
21	5.7	14.8	304	3.7	14.0	294	1.04E-02
22	5.5	11.2	324	3.2	12.1	302	3.40E-03
23	7.9	16.5	282	5.8	16.1	261	1.00E-04
24	7.7	16.7	302	4.7	16.0	293	1.00E-04

predicted to be similar (661 m^3/yr). The differences might be attributed to wave dissipation due to breaking, which is expected to be a direct result of the presence of the nourishment.

In the alongshore direction the effect of what appears to be a north-south directed eddy can be seen in the transport directions for both cases with and without nourishment (figs. 28*D-E*). Alongshore transport is directed southward in the offshore cells, with little to no transport in the middle cells, and northward in the shoreward cells. The major difference between the two scenarios is that transport magnitudes north of the mound taper off for both scenarios with and without a mound, but they do so more for the case with the nourishment (fig. 28*F*). The presence of the mound appears to cause a slightly calmer wave climate shoreward and north of the nourishment, slowing sediments transported by alongshore currents, possibly allowing them to settle out in the lee of the nourishment.

Considering the contribution of both the alongshore and cross-shore transport paths, the model does predict some onshore transport of sediments. Inspection of single-wave cases suggests that it is the larger waves from the northwest and the smaller waves from the west or southwest that contribute to the transport of sediments from the mound onshore (fig. 29). Because the probability of occurrence of the larger waves is small compared to the occurrence of smaller wave heights from the west or southwest, the lower west to southwest incident waves contribute more to the onshore-directed sediment transport. Although the trend of onshore transport from west and southwest waves cannot be clearly ascertained in the measured field data, the model indicates that a small amount of onshore transport from an enlarged mound might be expected.

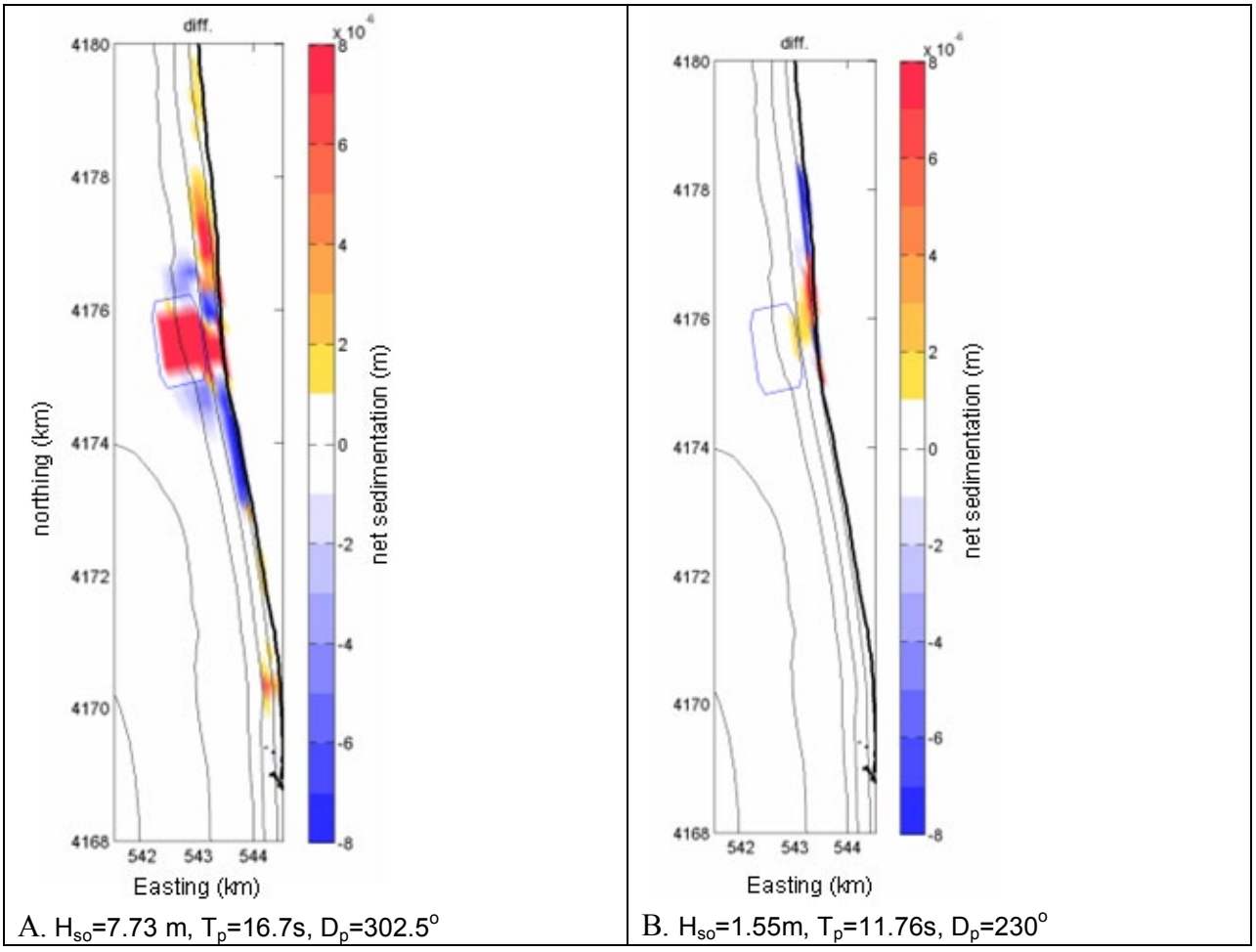

Figure 29. Difference plots of sediment transport (m^3) with and without a shoreface nourishment including contributions from both cross- and along-shore directed transports over one tidal cycle. The contribution of onshore transport appears to be primarily due to *A*, large waves out of the northwest and *B*, smaller waves from the southwest or west .

Conclusions

- Approximately half of the sediment that has been placed in the nearshore dredge-disposal site during the 2.5 years of this study remains within the dredge focus area.
- In the winter of 2006-7, large waves transported the dredge-mound material onshore.
- High rates of seasonal cross-shore sediment transport mask any potential profile change in the Coastal Profiling System data due to dredge placement.
- Pockets of accretion have been recorded by topographic surveying adjacent to the dredge site, but it is unclear if the accretion is linked to the nourishment.
- Cross-shore profile modeling suggests that dredge material must be placed in water depths no greater than 5 m to drive a positive shoreline response.
- Area modeling demonstrates that the new dredge site increases wave dissipation and modifies local sediment-transport patterns, although the effect on the nearshore morphology is largely negligible.
- Any increase in beach width or wave energy-dissipation related to the nourishment is likely to be realized only in the vicinity directly onshore of the nourishment site, which is several hundred meters south of the area of critical erosion.
- Larger waves from the northwest and smaller waves from the west or southwest contribute most to the sediment transport from the dredge mound onshore.

Acknowledgments

Thanks to the USGS Coastal and Marine Geology Team, particularly the Coastal Evolution: Process-Based, Multi-Scale Modeling Project for the generous support of this project. The United States Army Corps of Engineers, San Francisco District, funded a portion of this study. Peter Mull, in particular, has been extremely supportive. The National Park Service provided site permits and other logistical support. The San Francisco Public Utilities Commission generously granted us access to their secure Oceanside Water Pollution Control Plant to establish a permanent base station for our survey work at Ocean Beach. Peter Ruggiero provided PWC survey support and data analysis along with Jodi Eshleman, who also performed instrument data analysis. Thomas Reiss provide GPS support for CPS and beach topographic surveys. Gerry Hatcher assisted with the sediment sampling. Joanne Ferreira directed instrument deployments and recovery. Cheryl Hapke and Kate Dallas for provided constructive internal reviews.

References Cited

Barnard, P.L., 2005, Modern processes at the mouth of San Francisco Bay: San Francisco, American Shore and Beach Preservation Association, 23 p.

Barnard, P.L., Eshleman, J.L., Erikson, L.H., and Hanes, D.M., 2007, Coastal processes study at Ocean Beach, San Francisco, CA: summary of data collection 2004-2006: U.S. Geological Survey Open-File Report 2007-1217, 165 p., [http://pubs.usgs.gov/of/2007/1217/, 2008].

Barnard, P.L, and Hanes, D.M., 2005, Integrating field research, modeling and remote sensing to quantify morphodynamics in a high-energy coastal setting, Ocean Beach, San Francisco, California: 5th International Conference on Coastal Dynamics 2005 Conference Proceedings, Barcelona, Spain, American Society of Civil Engineers, CD-ROM, 14 p.

Barnard, P.L., and Hanes, D.M., 2006, Coastal monitoring of the May 2005 dredge disposal offshore of Ocean Beach, San Francisco, California: U.S. Geological Survey, Open-File Report 2006-1140, 27 p., [http://pubs.usgs.gov/of/2006/1140/, 2008].

Barnard, P.L., and Hanes, D.M., 2007, Cover photograph-San Francisco Bay, California, U.S.A.: Journal of Coastal Research, cover photograph w/ extended caption, v. 23, no. 3, p. ii.

Barnard, P.L., Hanes, D.M., Kvitek, R.G., and Iampietro, P.J., 2006, Sand waves at the mouth of San Francisco Bay, California: U.S. Geological Survey, Scientific Investigations Map 2006-2944, 5 map sheets, [http://pubs.usgs.gov/sim/2006/2944/, 2008].

Barnard, P.L., Hanes, D.M, Rubin, D.M., and Kvitek, R.G., 2006, Giant sand waves at the mouth of San Francisco Bay: Eos Transactions of the American Geophysical Union, v. 87, no. 29, p. 285, 289.

Barnard, P.L., Hanes, D.M., Lescinski, J., and Elias, E., 2007, Monitoring and modeling nearshore dredge disposal for indirect beach nourishment, Ocean Beach, San Francisco *in* Smith, J.M., ed., Coastal Engineering 2006: Proceedings of the 30th International Conference, Conference Proceedings, San Diego, CA, USA, 3-8 September 2006, v 4, p. 4192-4204.

Battjes, J.A., and Janssen, J.P.F.M., 1978, Energy loss and set-up due to breaking of random waves: Proceedings of the 16th International Conference on Coastal Engineering, ASCE, p. 569-587.

Bosboom, J., Aarninkhof, S.G.J., Reniers, A.J.H.M., Roelvink, J.A., and Walstra, D.J.R., 2000, Unibest-TC 2.0. Overview of model formulations, 49 p.

Dartnell, P., and Gardner, J.V., 1999, Sea-Floor Images and Data from Multibeam Surveys in San Francisco Bay, Southern California, Hawaii, the Gulf of Mexico, and Lake Tahoe, California-Nevada: USGS Digital Data Series, DDS-55, CD-ROM [http://pubs.usgs.gov/dds/dds-55/, 2008].

Delft University of Technology, 2008. SWAN Cycle III Version 40.51A User Manual, Delft, The Netherlands, 111 p, http://www.fluidmechanics.tudelft.nl/swan/index.htm.

Duin, M.J.P. van, Wiersma, N.R., Walstra, D.J.R., van Rijn, L.C., and Stive, M.J.F., 2004, Nourishing the shoreface: observations and hindcasting of the Egmond case, The Netherlands: Coastal Engineering, v. 51, no, 8/9, p. 813-837.

Erikson, L., Hanes, D.M., Barnard, P.L., and Gibbs, A.E., 2007, Swash zone characteristics at Ocean Beach *in* Smith, J.M., ed., Coastal Engineering 2006: Proceedings of the 30th International Conference, Conference Proceedings, San Diego, CA, USA, 3-8 September 2006, v. 1, p. 909-921.

Eshleman, J. L., Barnard, P. L., Erikson, L. H., and Hanes, D. M., 2007, Coupling alongshore variations in wave energy to beach morphologic change using the SWAN wave model at Ocean Beach, San Francisco, CA *in* 10th International Workshop on Wave Hindcasting and Forecasting, Oahu, Hawaii, http://www.waveworkshop.org/10thWaves/Papers/ Eshlemanetal_Waves2007_final.pdf.

Farris, A.S., and List, J.H., 2007, Shoreline change as a proxy for subaerial beach volume change: Journal Of Coastal Research, v. 23, no. 3, p. 740-748.

Hanes, D.M., and Barnard, P.L., 2007, Morphological Evolution in the San Francisco Bight: Journal of Coastal Research, Special Issue 50, Proceedings of the 9th International Coastal Symposium, Gold Coast, Australia, p. 469-473.

Hansen, J.E., 2007, Quantifying Beach response to Episodic Large Wave Events, Ocean Beach, San Francisco, CA [unpublished M.S. thesis], San Francisco State University, 118 p.

Hapke, C.J., Reid, D., Richmond, B.M., Ruggiero, P., and List, J., 2006, National Assessment of Shoreline Change Part 3: Historical Shoreline Change and Associated Coastal Land Loss Along Sandy Shorelines of the California Coast: U.S. Geological Survey Open-File Report 2006-1251, 79 p., [http://pubs.usgs.gov/of/2006/1251, 2008].

Hanson, H., and Camenen, B., 2007, Closed form solution for threshold velocity for initiation of motion under waves: Proceedings of Coastal Sediments '07, Reston, VA, p. 15-27.

Lesser, G.R., Roelvink, J.A., van Kester, J.A.T.M., and Stelling, G.S., 2004, Development and validation of a three-dimensional morphological model: Coastal Engineering, v. 51, no. 8/9, p. 883-915.

Magellan Navigation, Inc., 2006, Z-Extreme Survey System Data Sheet. http://pro.magellangps.com/en/.

National Oceanic and Atmospheric Administration (NOAA), 2008, NOS Hydrographic Survey Viewer: http://map.ngdc.noaa.gov/website/mgg/nos_hydro/viewer.htm.

National Oceanic and Atmospheric Administration (NOAA), 2008, Tides & Currents: Center of Operational Products and Services, http://tidesandcurrents.noaa.gov/.

Rijn, L.C. van, 1993, Principles of Sediment Transport in Rivers, Estuaries and Coastal Seas. Aqua Publications, Amsterdam.

Roelvink, J.A., and van Banning, G.K.F.M., 1994, Design and development of Delft2/3D and application to coastal morphodynamics: Proceedings of Hydroinformatics'94 Conference, Delft, The Netherlands.

SCRIPPS Institution of Oceanography, 2008, The Coastal Data Information Program: San Diego, Integrative Oceanography Division, Scripps Institution of Oceanography, http://cdip.ucsd.edu

Soulsby, R., and Whitehouse, R., 1997, Threshold of sediment motion in coastal environment: Proceedings of Pacific Coasts and Ports '97 Conference, University of Canterbury, Christchurch, New Zealand, p. 149-154.

Thieler, E.R., Himmelstoss, E.A., Zichichi, J.L., and Miller, T.L., 2005, Digital Shoreline Analysis System (DSAS) version 3.0: An ArcGIS extension for calculating shoreline change: U.S. Geological Survey Open-File Report 2005-1304.

Walstra, D.J., and Roelvink, J.A., 2000, 3D calculation of wave-driven cross-shore currents: Proceedings of the 27th International Conference on Coastal Engineering, July 16-21, 2000, Sydney, ASCE, p. 1050-1063.

Appendix

Field Activity IDs and Web Links

ATV Survey List

Survey no.	Field Activity ID	Survey date	URL For Field Activity ID
1	O-B1-04-CA	04/07/04	http://walrus.wr.usgs.gov/infobank/o/ob104ca/html/o-b1-04-ca.meta.html
2	O-B2-04-CA	05/07/04	http://walrus.wr.usgs.gov/infobank/o/ob204ca/html/o-b2-04-ca.meta.html
3	O-B3-04-CA	06/07/04	http://walrus.wr.usgs.gov/infobank/o/ob304ca/html/o-b3-04-ca.meta.html
4	O-B4-04-CA	07/06/04	http://walrus.wr.usgs.gov/infobank/o/ob404ca/html/o-b4-04-ca.meta.html
5	O-B5-04-CA	10/13/04	http://walrus.wr.usgs.gov/infobank/o/ob504ca/html/o-b5-04-ca.meta.html
6	O-B6-04-CA	11/15/04	http://walrus.wr.usgs.gov/infobank/o/ob604ca/html/o-b6-04-ca.meta.html
7	O-B7-04-CA	12/10/04	http://walrus.wr.usgs.gov/infobank/o/ob704ca/html/o-b7-04-ca.meta.html
8	O-B1-05-CA	01/11/05	http://walrus.wr.usgs.gov/infobank/o/ob105ca/html/o-b1-05-ca.meta.html
9	O-B2-05-CA	02/07/05	http://walrus.wr.usgs.gov/infobank/o/ob205ca/html/o-b2-05-ca.meta.html
10	O-B3-05-CA	03/08/05	http://walrus.wr.usgs.gov/infobank/o/ob305ca/html/o-b3-05-ca.meta.html
11	O-B4-05-CA	03/11/05	http://walrus.wr.usgs.gov/infobank/o/ob405ca/html/o-b4-05-ca.meta.html
12	O-B5-05-CA	05/02/05	http://walrus.wr.usgs.gov/infobank/o/ob505ca/html/o-b5-05-ca.meta.html
13	O-B6-05-CA	06/10/05	http://walrus.wr.usgs.gov/infobank/o/ob605ca/html/o-b6-05-ca.meta.html
14	O-B7-05-CA	06/27/05	http://walrus.wr.usgs.gov/infobank/o/ob705ca/html/o-b7-05-ca.meta.html
15	O-B8-05-CA	07/12/05	http://walrus.wr.usgs.gov/infobank/o/ob805ca/html/o-b8-05-ca.meta.html
16	O-B9-05-CA	07/22/05	http://walrus.wr.usgs.gov/infobank/o/ob905ca/html/o-b9-05-ca.meta.html
17	O-BA-05-CA	08/22/05	http://walrus.wr.usgs.gov/infobank/o/oba05ca/html/o-ba-05-ca.meta.html
18	O-BB-05-CA	11/17/05	http://walrus.wr.usgs.gov/infobank/o/obb05ca/html/o-bb-05-ca.meta.html
19	O-BC-05-CA	12/15/05	http://walrus.wr.usgs.gov/infobank/o/obc05ca/html/o-bc-05-ca.meta.html
20	O-BD-05-CA	12/22/05	http://walrus.wr.usgs.gov/infobank/o/obd05ca/html/o-bd-05-ca.meta.html

21	O-BE-05-CA	12/29/05	http://walrus.wr.usgs.gov/infobank/o/obe05ca/html/o-be-05-ca.meta.html
22	O-B1-06-CA	01/16/06	http://walrus.wr.usgs.gov/infobank/o/ob106ca/html/o-b1-06-ca.meta.html
23	O-B2-06-CA	01/24/06	http://walrus.wr.usgs.gov/infobank/o/ob206ca/html/o-b2-06-ca.meta.html
24	O-B3-06-CA	01/26/06	http://walrus.wr.usgs.gov/infobank/o/ob306ca/html/o-b3-06-ca.meta.html
25	O-B4-06-CA	01/30/06	http://walrus.wr.usgs.gov/infobank/o/ob406ca/html/o-b4-06-ca.meta.html
26	O-B5-06-CA	02/10/06	http://walrus.wr.usgs.gov/infobank/o/ob506ca/html/o-b5-06-ca.meta.html
27	O-B6-06-CA	02/13/06	http://walrus.wr.usgs.gov/infobank/o/ob606ca/html/o-b6-06-ca.meta.html
28	O-B7-06-CA	02/21/06	http://walrus.wr.usgs.gov/infobank/o/ob706ca/html/o-b7-06-ca.meta.html
29	O-B8-06-CA	02/26/06	http://walrus.wr.usgs.gov/infobank/o/ob806ca/html/o-b8-06-ca.meta.html
30	O-B9-06-CA	03/05/05	http://walrus.wr.usgs.gov/infobank/o/ob906ca/html/o-b9-06-ca.meta.html
31	O-10-06-CA	03/23/06	http://walrus.wr.usgs.gov/infobank/o/o1006ca/html/o-10-06-ca.meta.html
32	O-11-06-CA	04/06/06	http://walrus.wr.usgs.gov/infobank/o/o1106ca/html/o-11-06-ca.meta.html
33	O-12-06-CA	04/21/06	http://walrus.wr.usgs.gov/infobank/o/o1206ca/html/o-12-06-ca.meta.html
34	O-13-06-CA	05/08/06	http://walrus.wr.usgs.gov/infobank/o/o1306ca/html/o-13-06-ca.meta.html
35	O-14-06-CA	05/22/06	http://walrus.wr.usgs.gov/infobank/o/o1406ca/html/o-14-06-ca.meta.html
36	O-15-06-CA	06/19/06	http://walrus.wr.usgs.gov/infobank/o/o1506ca/html/o-15-06-ca.meta.html
37	O-16-06-CA	06/30/06	http://walrus.wr.usgs.gov/infobank/o/o1606ca/html/o-16-06-ca.meta.html
38	O-17-06-CA	08/13/06	http://walrus.wr.usgs.gov/infobank/o/o1706ca/html/o-17-06-ca.meta.html
39	O-18-06-CA	10/23/06	http://walrus.wr.usgs.gov/infobank/o/o1806ca/html/o-18-06-ca.meta.html
40	O-19-06-CA	11/06/06	http://walrus.wr.usgs.gov/infobank/o/o1906ca/html/o-19-06-ca.meta.html
41	O-20-06-CA	11/20/06	http://walrus.wr.usgs.gov/infobank/o/o2006ca/html/o-20-06-ca.meta.html
42	O-21-06-CA	11/24/06	http://walrus.wr.usgs.gov/infobank/o/o2106ca/html/o-21-06-ca.meta.html
43	O-22-06-CA	12/05/06	http://walrus.wr.usgs.gov/infobank/o/o2206ca/html/o-22-06-ca.meta.html
44	O-23-06-CA	12/10/06	http://walrus.wr.usgs.gov/infobank/o/o2306ca/html/o-23-06-ca.meta.html

45	O-24-06-CA	12/29/06	http://walrus.wr.usgs.gov/infobank/o/o2406ca/html/o-24-06-ca.meta.html

PWC Survey List

Survey No.	Field Activity ID	Survey date	
1	O-B2-04-CA	05/04/04	http://walrus.wr.usgs.gov/infobank/o/ob204ca/html/o-b2-04-ca.meta.html
2	O-B4-04-CA	07/20/04	http://walrus.wr.usgs.gov/infobank/o/ob404ca/html/o-b4-04-ca.meta.html
3	O-B6-O4-CA	11/12/04	http://walrus.wr.usgs.gov/infobank/o/ob604ca/html/o-b6-04-ca.meta.html
4	O-B5-05-CA	05/05/05	http://walrus.wr.usgs.gov/infobank/o/ob505ca/html/o-b5-05-ca.meta.html
5	O-B8-05-CA	07/05/05	http://walrus.wr.usgs.gov/infobank/o/ob805ca/html/o-b8-05-ca.meta.html
6	O-BB-05-CA	11/17/05	http://walrus.wr.usgs.gov/infobank/o/obb05ca/html/o-bb-05-ca.meta.html
7	O-BA-06-CA	02/01/06	http://walrus.wr.usgs.gov/infobank/o/oba06ca/html/o-ba-06-ca.meta.html
8	O-BB-06-CA	02/10/06	http://walrus.wr.usgs.gov/infobank/o/obb06ca/html/o-bb-06-ca.meta.html
9	O-BC-06-CA	05/23/06	http://walrus.wr.usgs.gov/infobank/o/obc06ca/html/o-bc-06-ca.meta.html
10	O-BD-06-CA	05/23/06	http://walrus.wr.usgs.gov/infobank/o/obd06ca/html/o-bd-06-ca.meta.html
11	O-BD-06_CA	11/06/06	http://walrus.wr.usgs.gov/infobank/o/obd06ca/html/o-bd-06-ca.meta.html
12	*O-22-06-CA*	11/21/06	http://walrus.wr.usgs.gov/infobank/o/o2206ca/html/o-22-06-ca.meta.html
13	*O-B2-04-CA*	12/05/06	http://walrus.wr.usgs.gov/infobank/o/ob204ca/html/o-b2-04-ca.meta.html

Beach Eyeball Survey List

Survey No.	Field Activity ID	Survey date	
1	O-B1-04-CA	04/07/04	http://walrus.wr.usgs.gov/infobank/o/ob104ca/html/o-b1-04-ca.meta.html
2	O-B2-04-CA	05/07/04	http://walrus.wr.usgs.gov/infobank/o/ob204ca/html/o-b2-04-ca.meta.html
3	O-B4-04-CA	08/03/04	http://walrus.wr.usgs.gov/infobank/o/ob404ca/html/o-b4-04-ca.meta.html
4	O-B3-05-CA	03/07/05	http://walrus.wr.usgs.gov/infobank/o/ob305ca/html/o-b3-05-ca.meta.html
5	O-BB-05-CA	11/17/05	http://walrus.wr.usgs.gov/infobank/o/obb05ca/html/o-bb-05-ca.meta.html
6	O-B3-06-CA	01/26/06	http://walrus.wr.usgs.gov/infobank/o/ob

			306ca/html/o-b3-06-ca.meta.html
7	O-19-06-CA	11/06/06	http://walrus.wr.usgs.gov/infobank/o/o1906ca/html/o-19-06-ca.meta.html

Sediment Sampling Offshore

Survey No.	Field Activity ID	Survey date	
1	S-1-05-NC	06/21/05	http://walrus.wr.usgs.gov/infobank/s/s105nc/html/s-1-05-nc.meta.html
2	S-1-05-NC	06/22/05	http://walrus.wr.usgs.gov/infobank/s/s105nc/html/s-1-05-nc.meta.html
3	S-1-05-NC	06/23/05	http://walrus.wr.usgs.gov/infobank/s/s105nc/html/s-1-05-nc.meta.html
4	S-2-05-NC	07/25/05	http://walrus.wr.usgs.gov/infobank/s/s205nc/html/s-2-05-nc.meta.html
5	*S-2-05-NC*	07/27/05	http://walrus.wr.usgs.gov/infobank/s/s205nc/html/s-2-05-nc.meta.html

Instrument Deployments/ Recovery

Survey No.	Field Activity ID	Survey date	
1	S-1-05-NC	06/21/05	http://walrus.wr.usgs.gov/infobank/s/s105nc/html/s-1-05-nc.meta.html
2	S-2-05-NC	07/26/05	http://walrus.wr.usgs.gov/infobank/s/s205nc/html/s-2-05-nc.meta.html
3	none	07/28/05	
4	none	08/16/05	
5	S-1-06-NC	01/12/06	http://walrus.wr.usgs.gov/infobank/s/s106nc/html/s-1-06-nc.meta.html
6	*D-1-06-NC*	01/23/06	http://walrus.wr.usgs.gov/infobank/d/d106nc/html/d-1-06-nc.meta.html
7	none	01/27/06	
8	none	02/01/06	
9	*S-1-05-NC*	07/28/05	http://walrus.wr.usgs.gov/infobank/s/s105nc/html/s-1-05-nc.meta.html
10	*S-2-05-NC*	08/16/05	http://walrus.wr.usgs.gov/infobank/s/s205nc/html/s-2-05-nc.meta.html

Multibeam Surveys Survey	Field Activity ID	Survey date	
Mouth of SF Bay #1	V-2-04-NC	09/15/04	http://walrus.wr.usgs.gov/infobank/v/v204nc/html/v-2-04-nc.meta.html

Mouth of SF Bay #2	none	09/17/05
Dredge Monitoring #1	none	05/16/05
Dredge Monitoring #2	none	06/07/05
Dredge Monitoring #3	none	07/09/05
Dredge Monitoring #4	none	10/19/05
Dredge Monitoring #5	none	05/13/06
Dredge Monitoring #6	none	06/02/06
Dredge Monitoring #7	none	11/30/06

Bathymetry and Shaded Relief Maps

The following are 2-m gridded bathymetry and shaded-relief maps for each of the 12 multibeam surveys conducted as part of this study. In each map, the solid red box onshore indicates the beach area experiencing chronic erosion. Contours lines are drawn every 0.5 m. Depth is relative to the North American Vertical Datum (NAVD88). See the Methods section and Barnard and others (2007a) for more information on multibeam processing and gridding procedures.

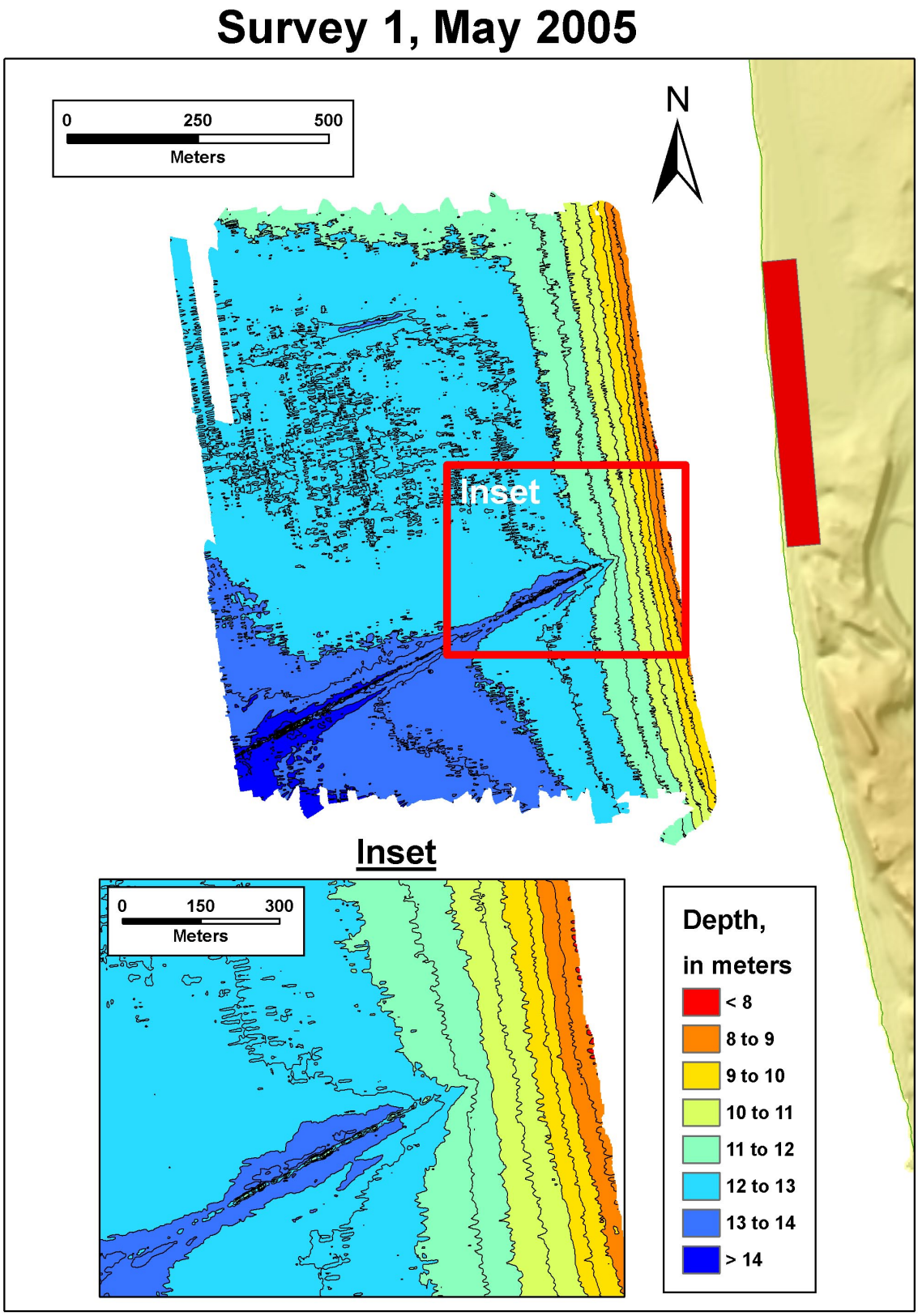

Figure A1. Bathymetry for Survey 1.

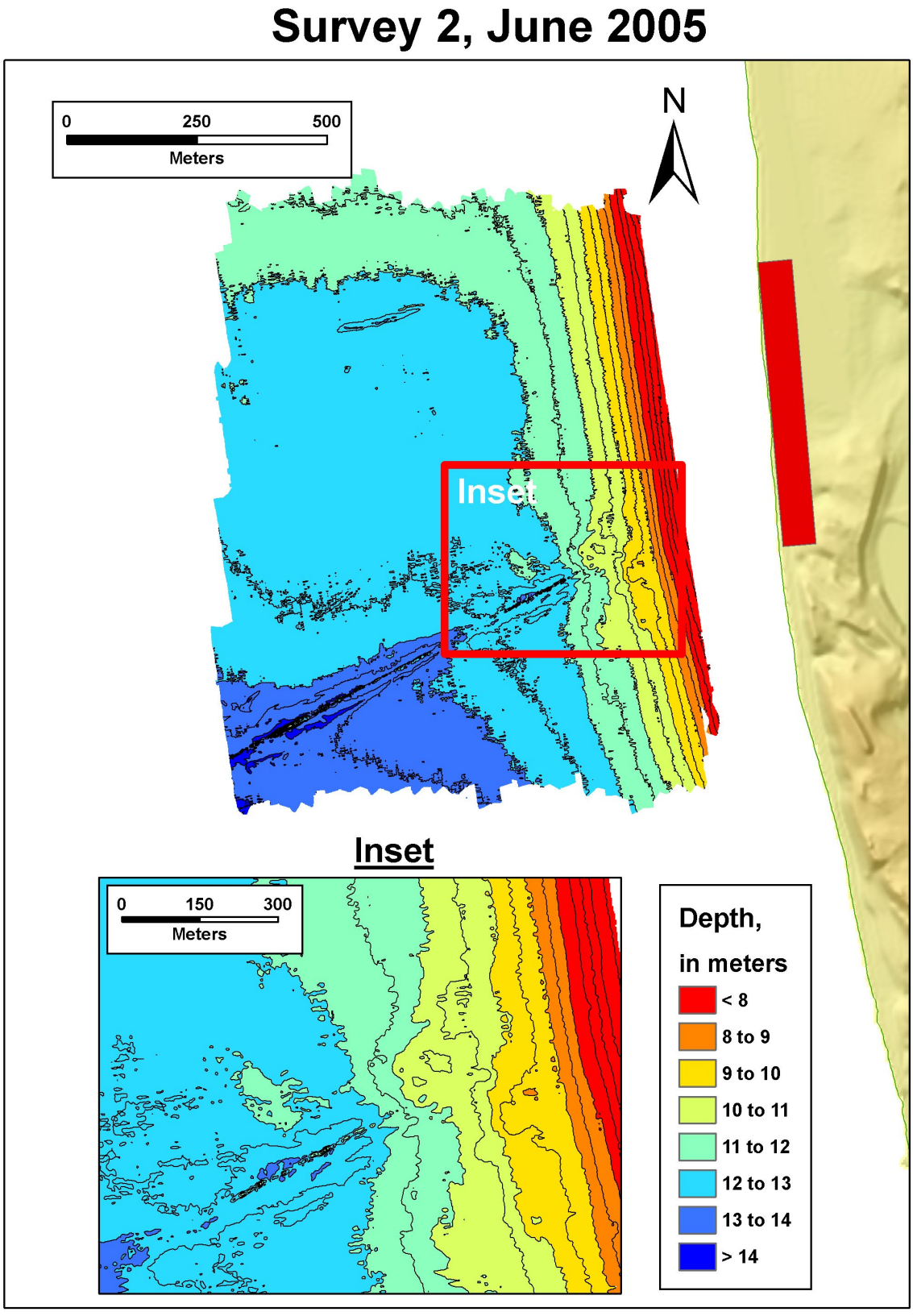

Figure A2. Bathymetry for Survey 2.

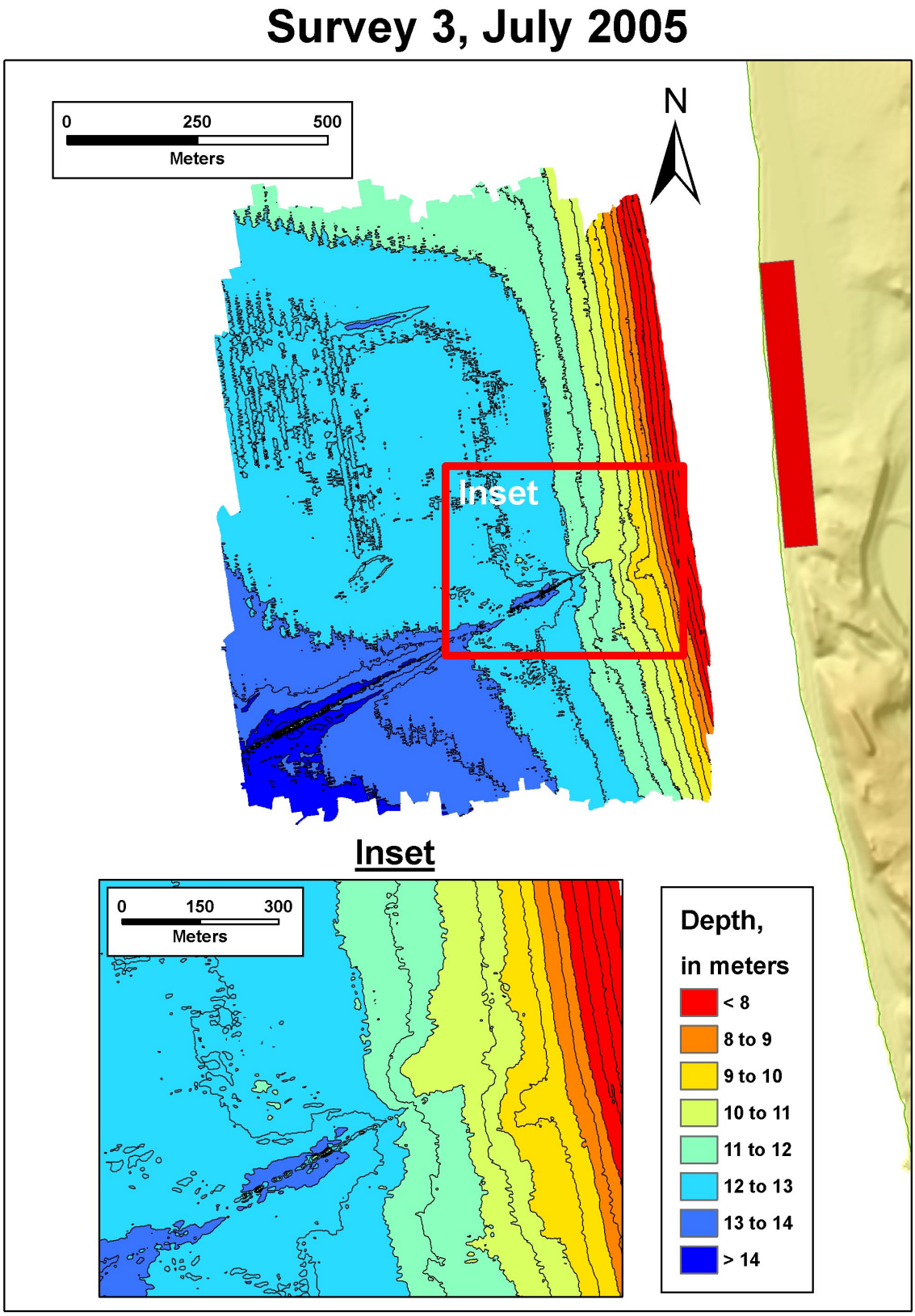

Figure A3. Bathymetry for Survey 3.

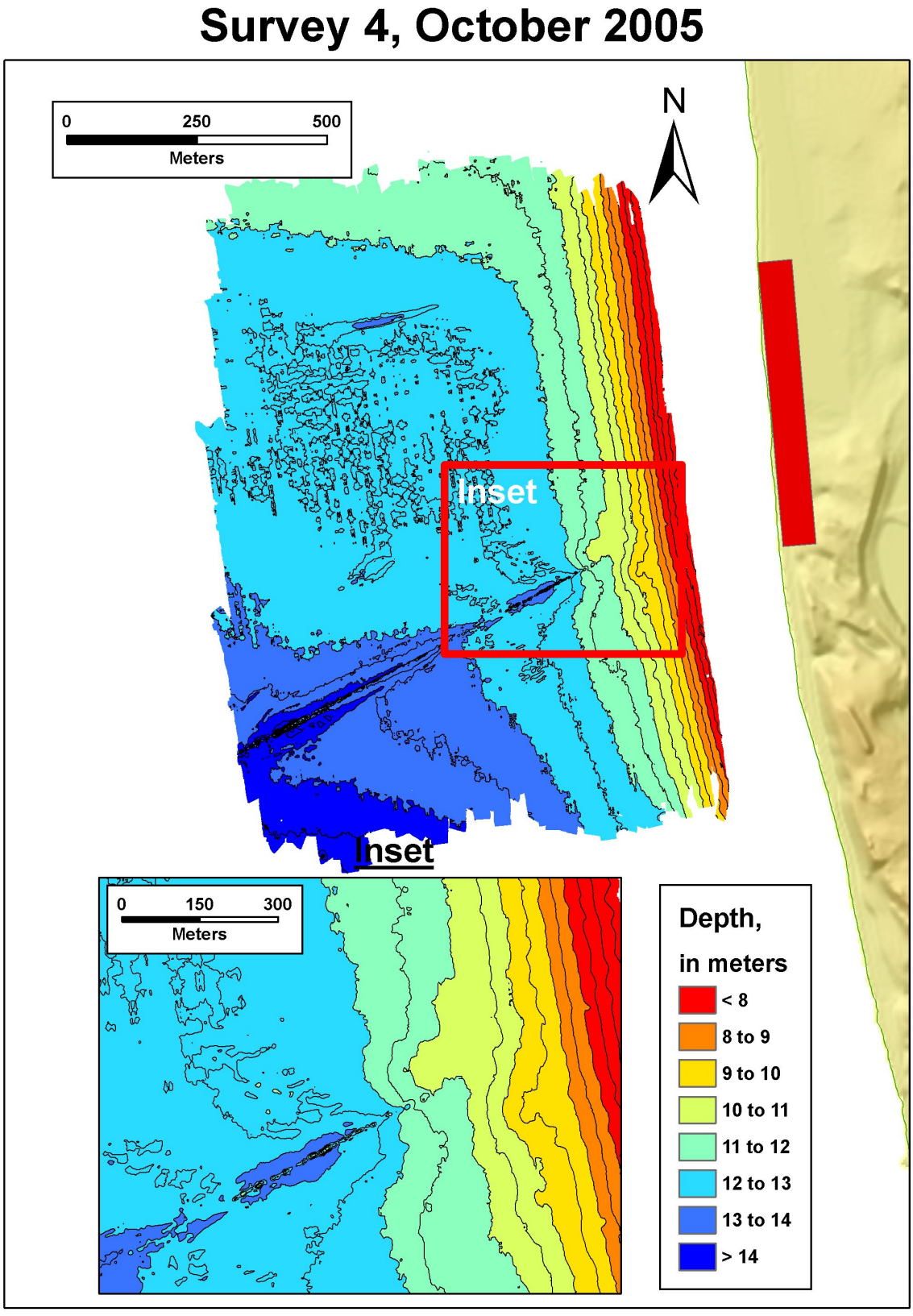

Figure A4. Bathymetry for Survey 4.

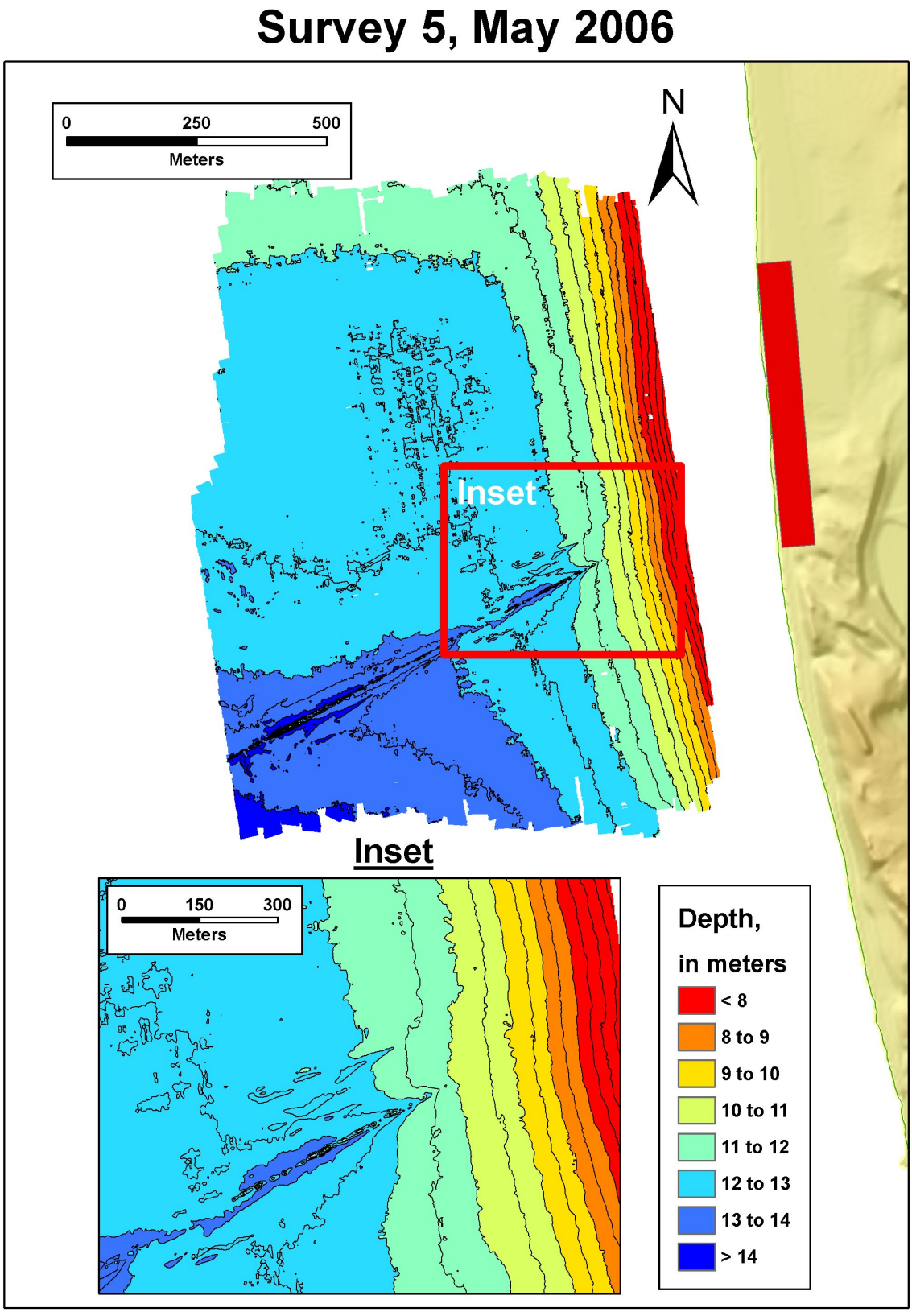

Figure A5. Bathymetry for Survey 5.

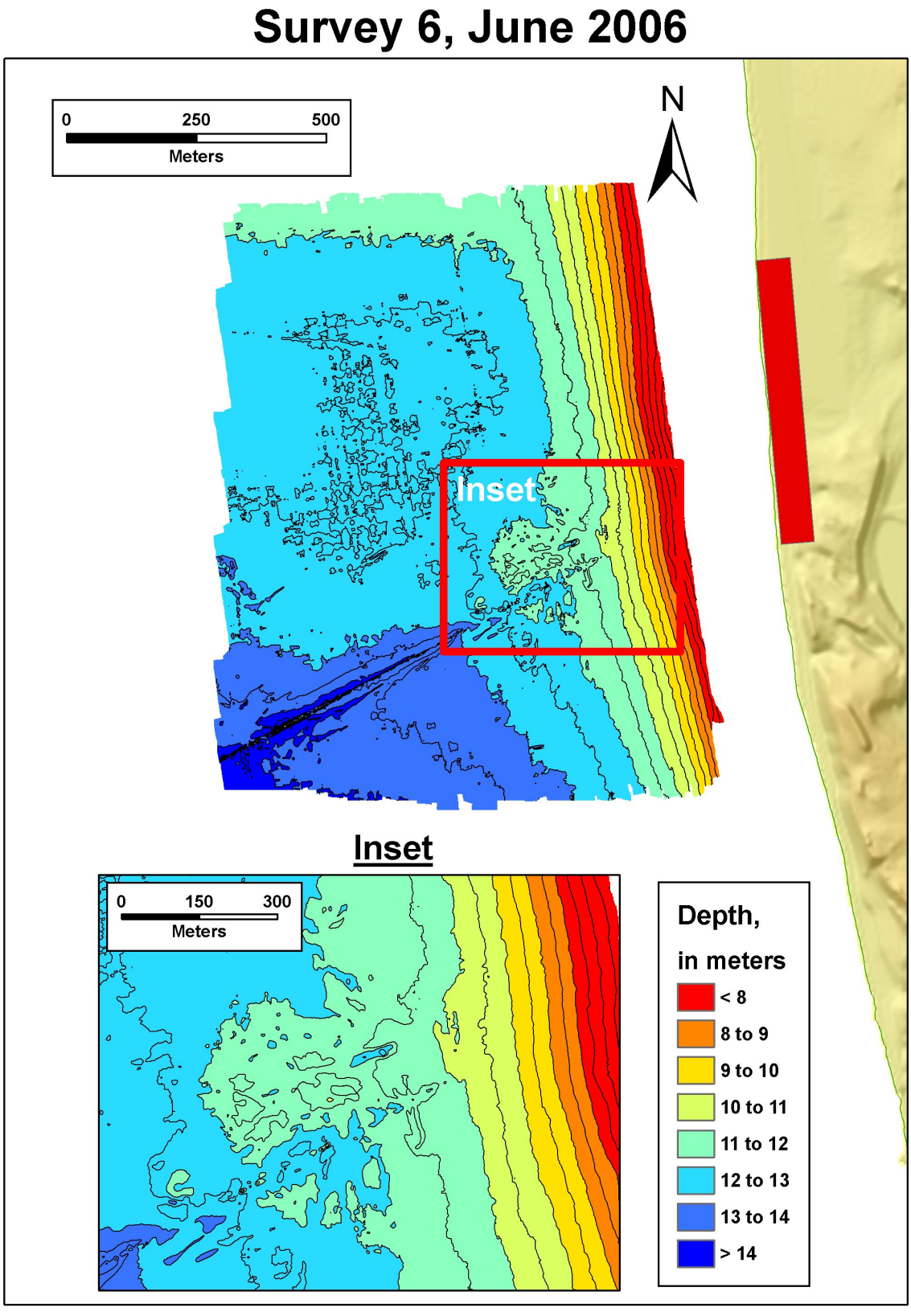

Figure A6. Bathymetry for Survey 6.

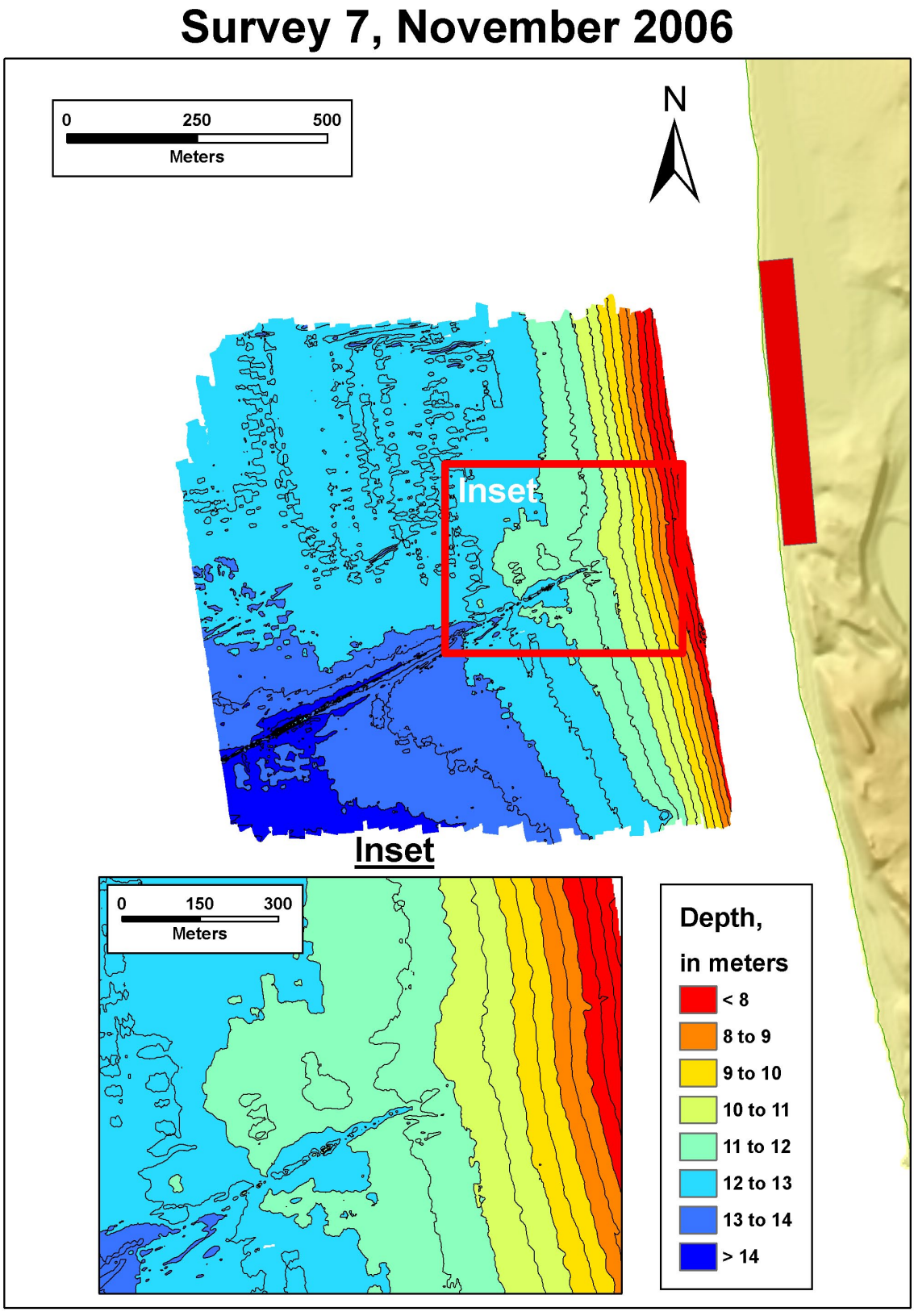

Figure A7. Bathymetry for Survey 7.

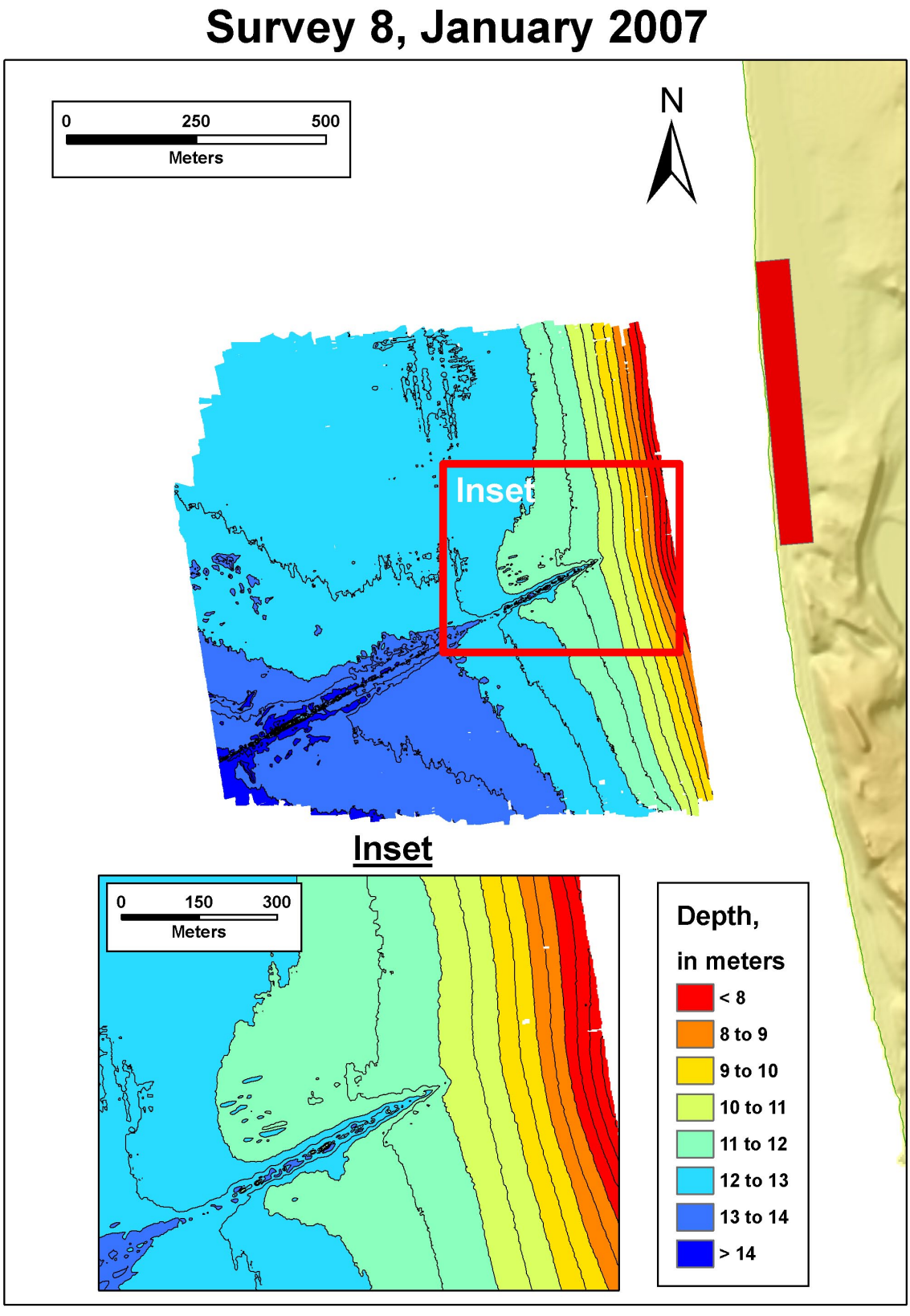

Figure A8. Bathymetry for Survey 8.

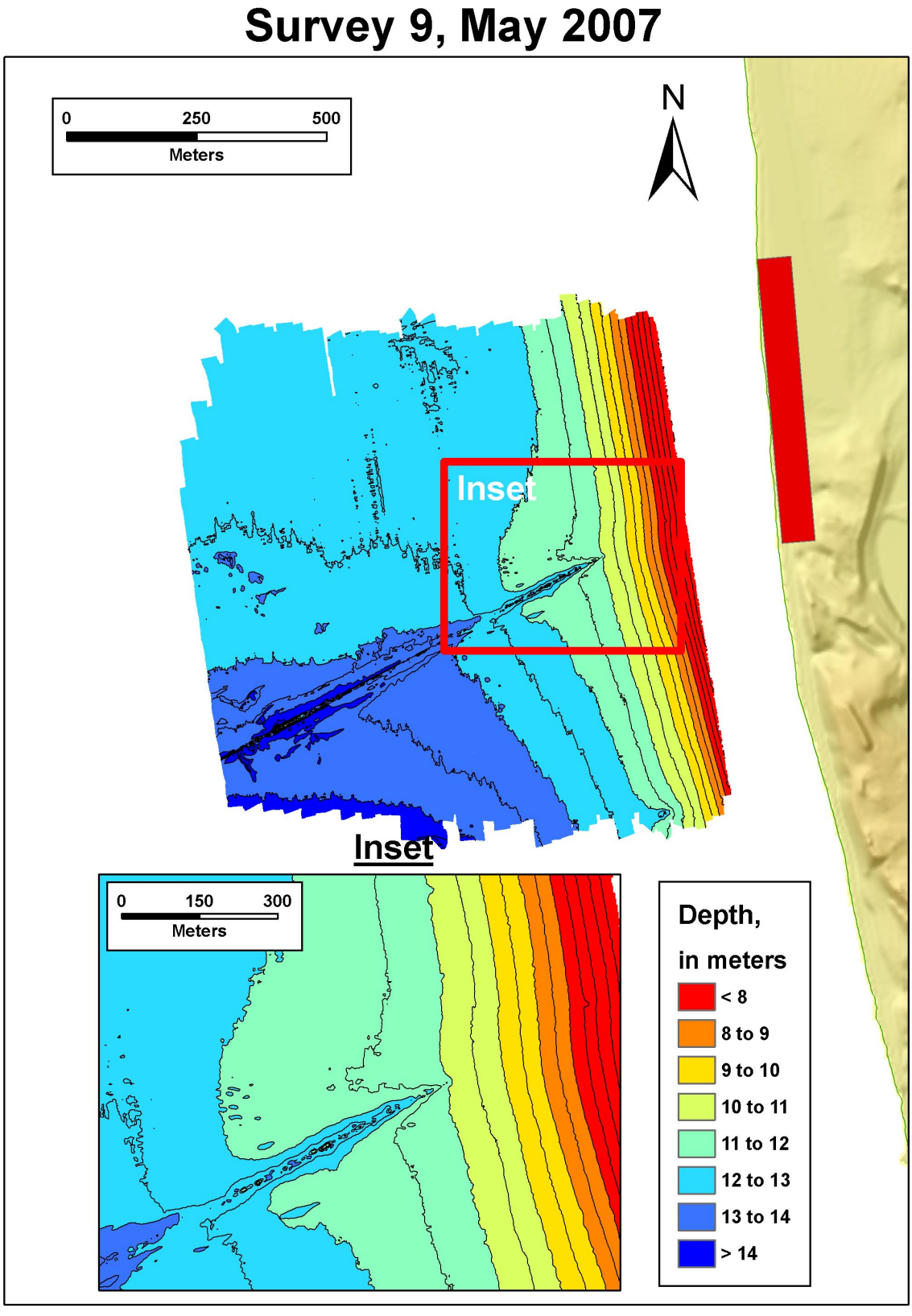

Figure A9. Bathymetry for Survey 9.

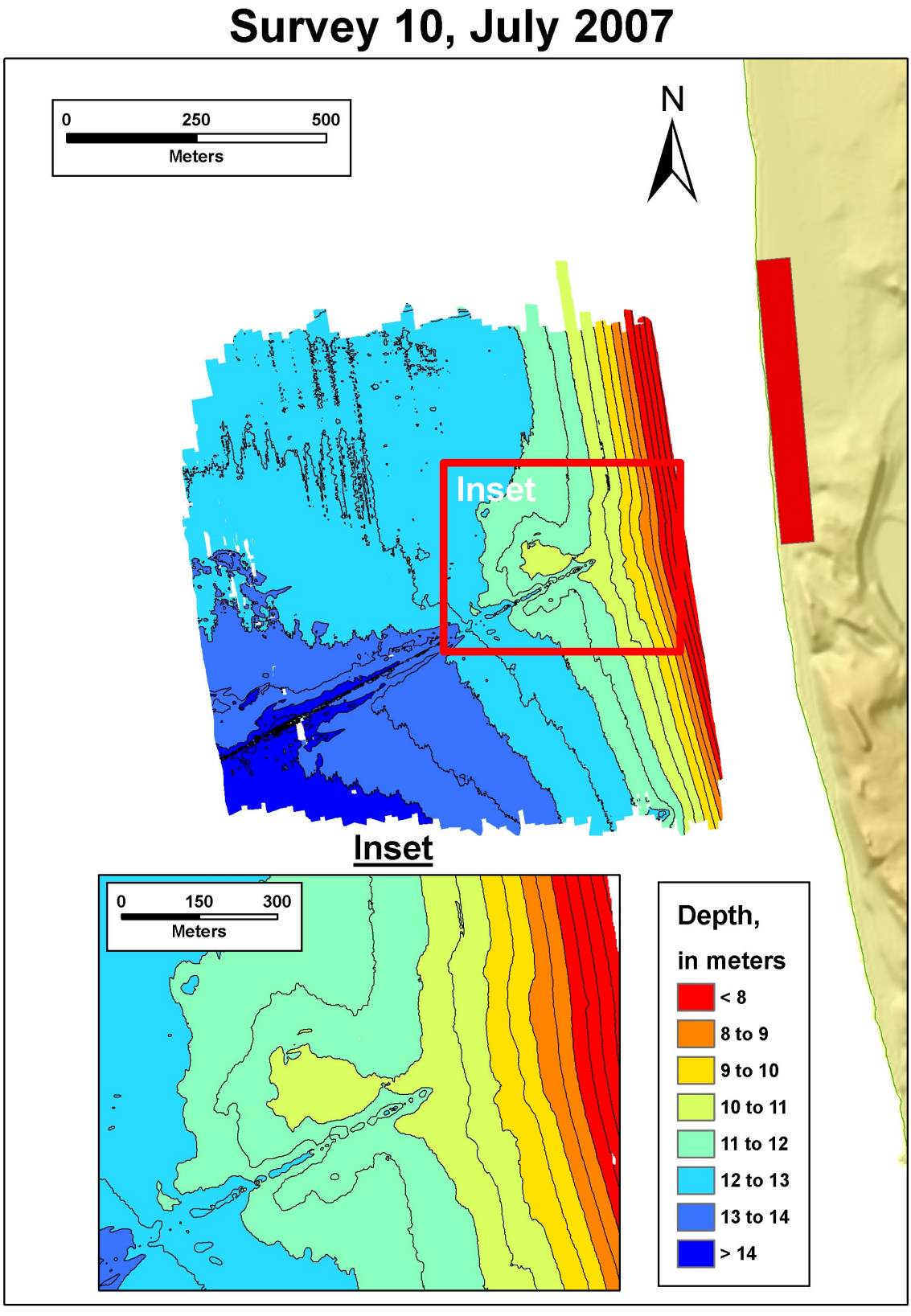

Figure A10. Bathymetry for Survey 10.

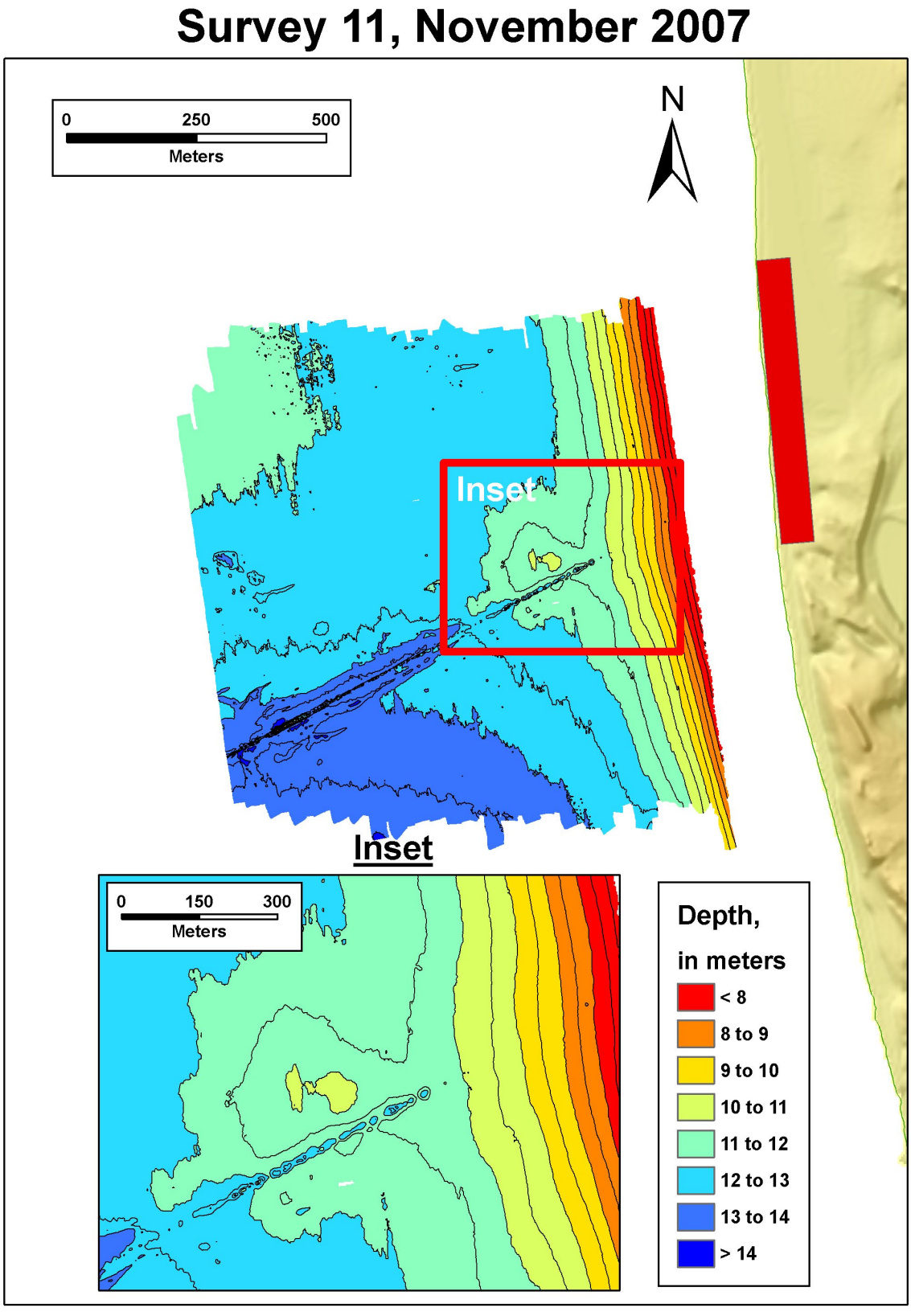

Figure A11. Bathymetry for Survey 11.

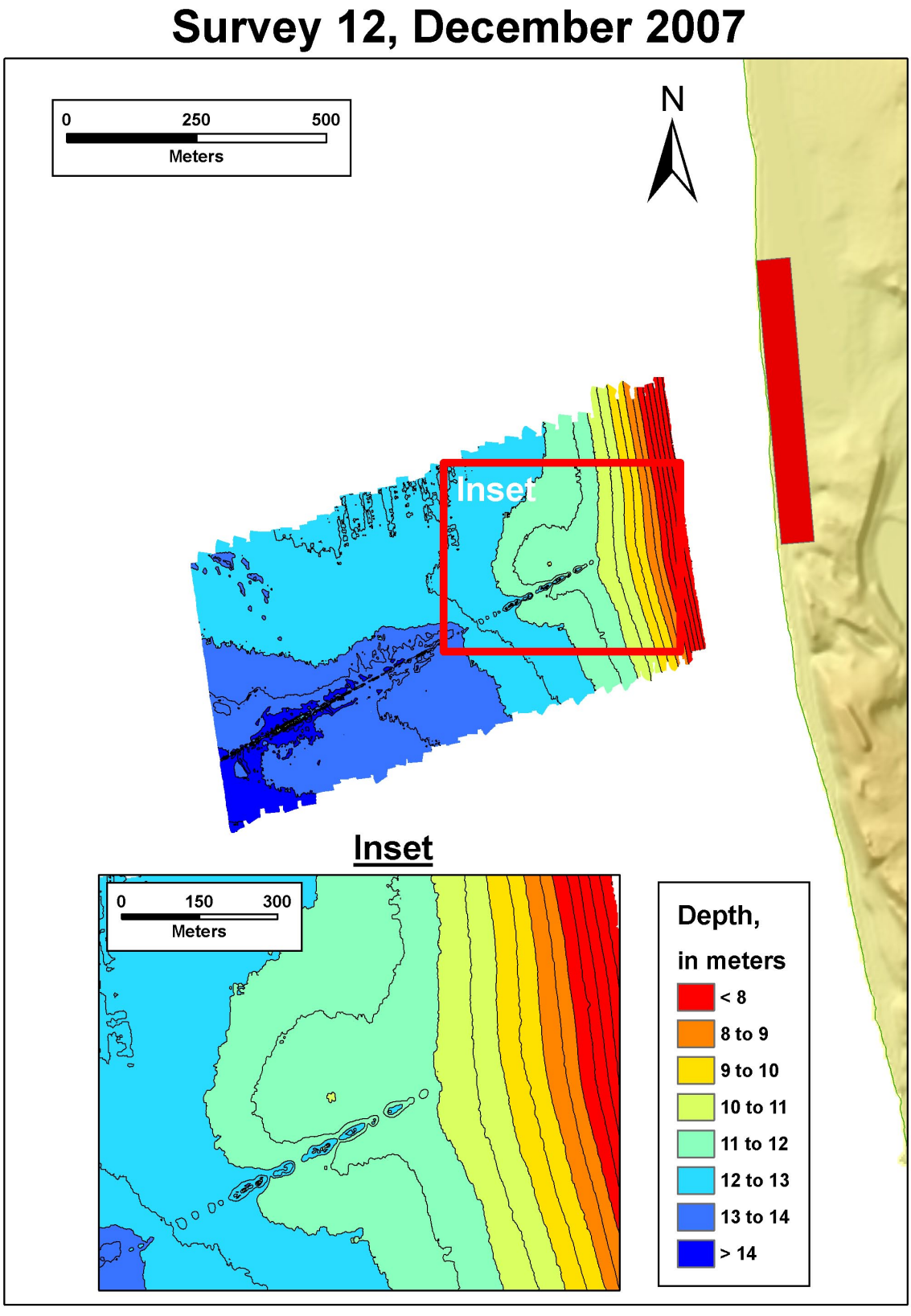

Figure A12. Bathymetry for Survey 12.

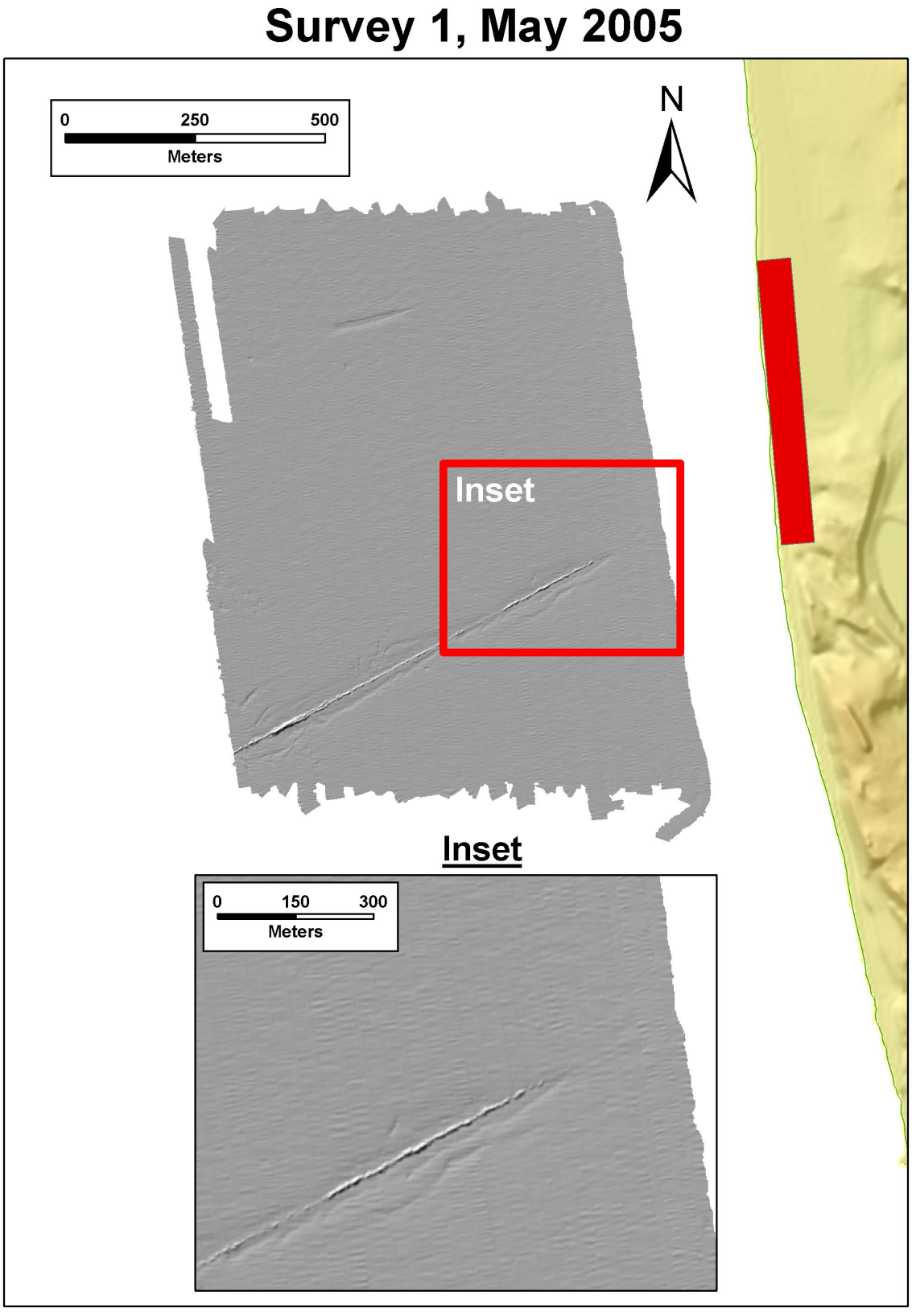

Figure A13. Shaded relief for Survey 1.

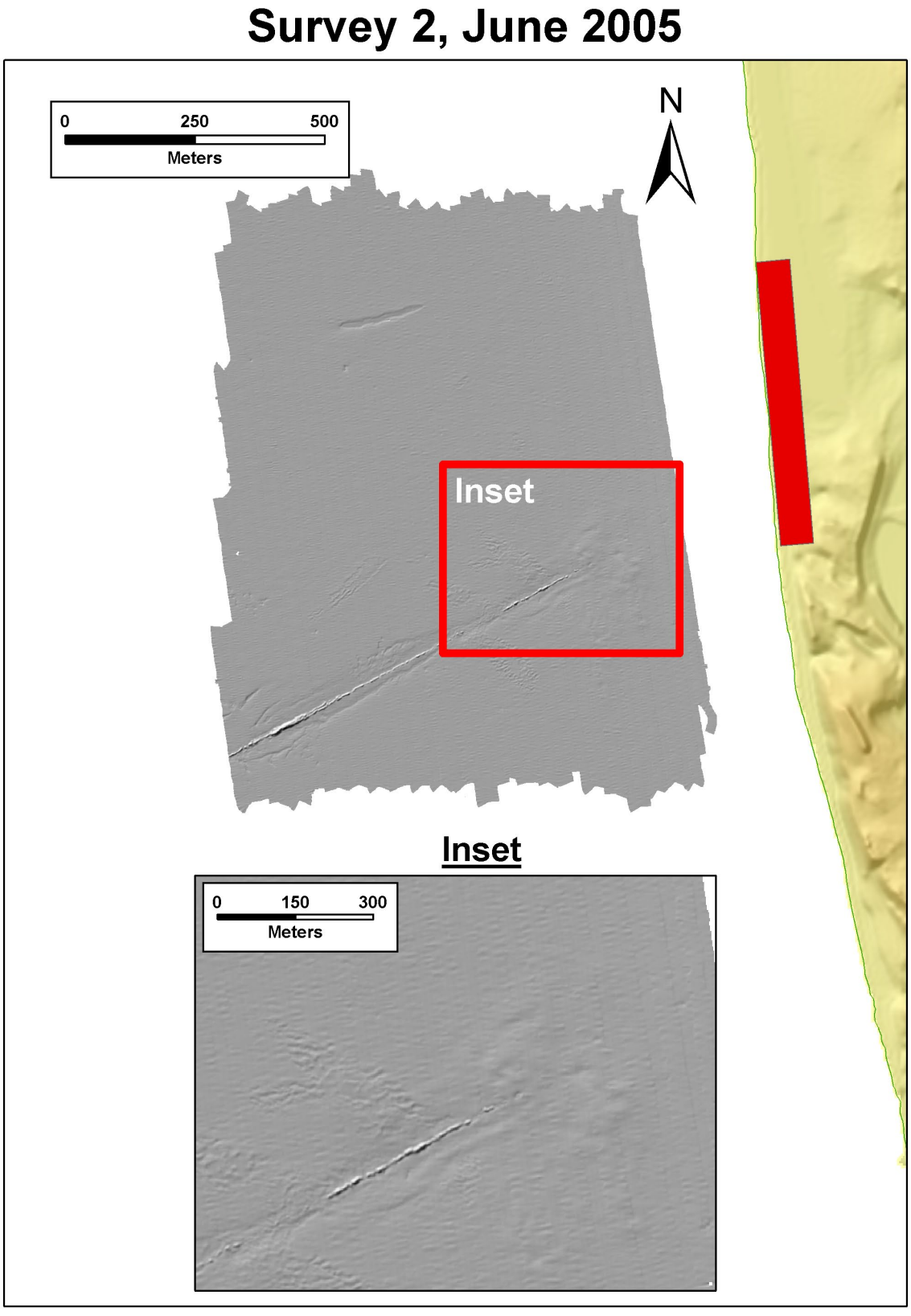

Figure A14. Shaded relief for Survey 2.

Figure A15. Shaded relief for Survey 3.

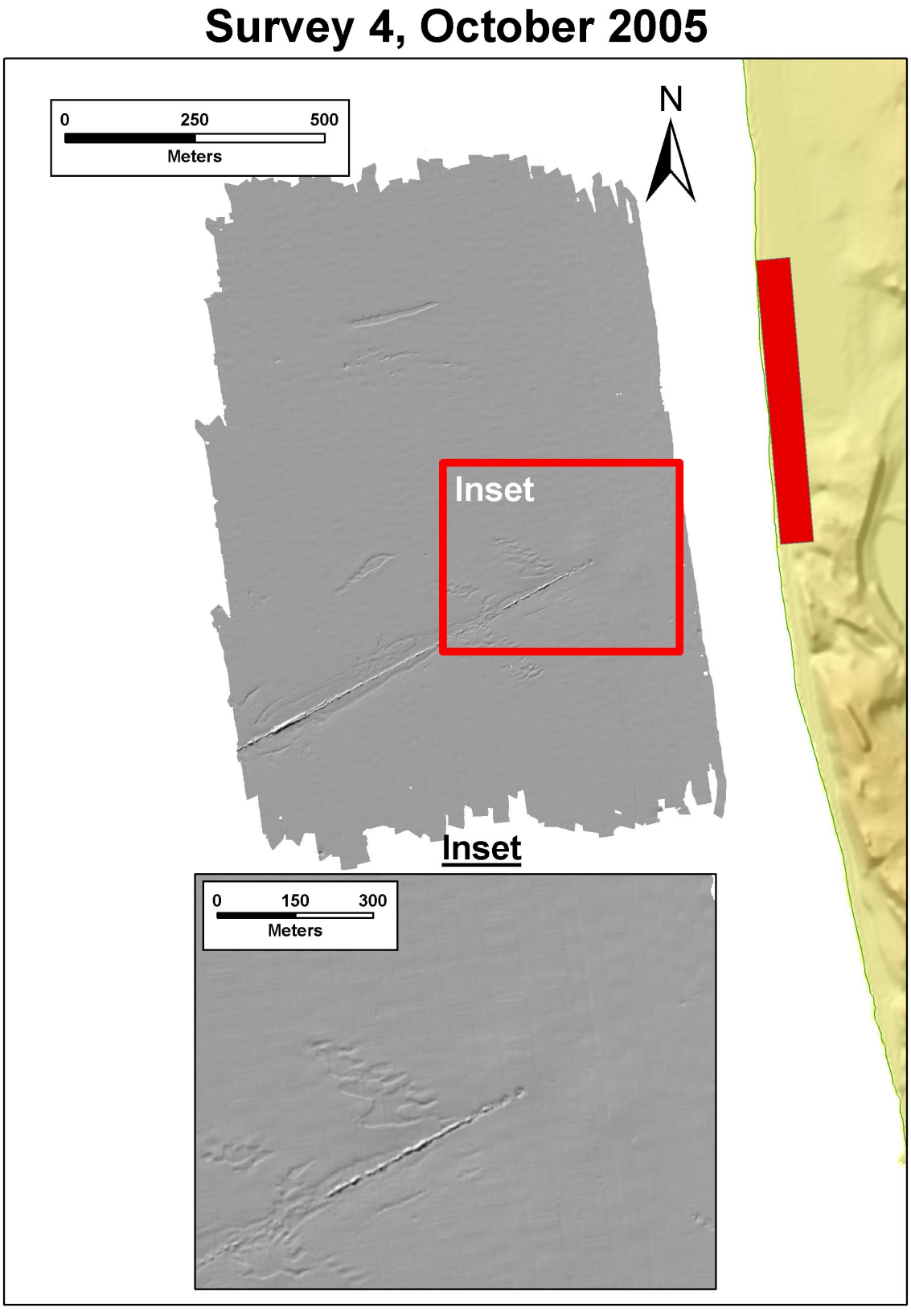

Figure A16. Shaded relief for Survey 4.

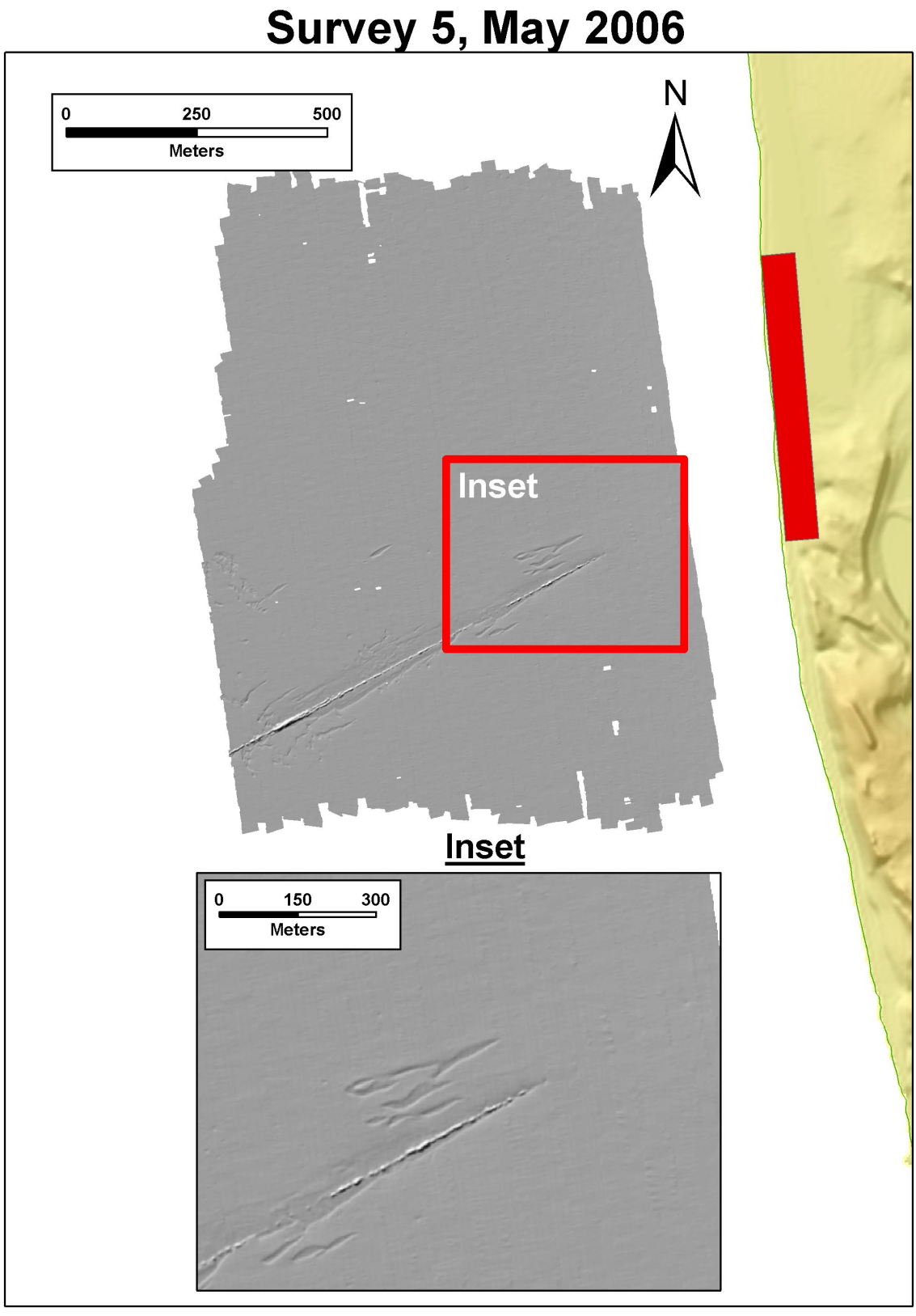

Figure A17. Shaded relief for Survey 5.

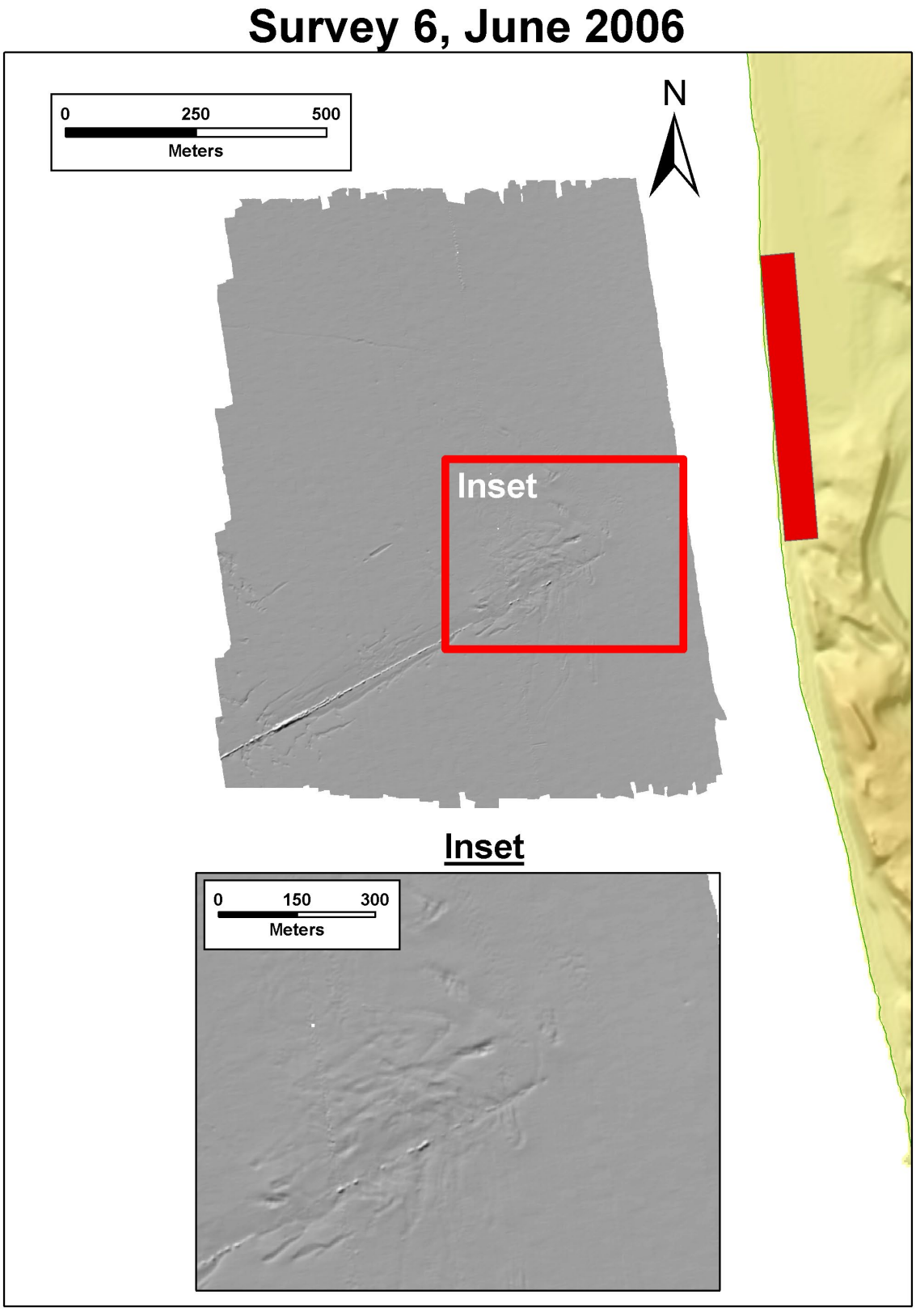

Figure A18. Shaded relief for Survey 6.

Figure A19. Shaded relief for Survey 7.

Figure A20. Shaded relief for Survey 8.

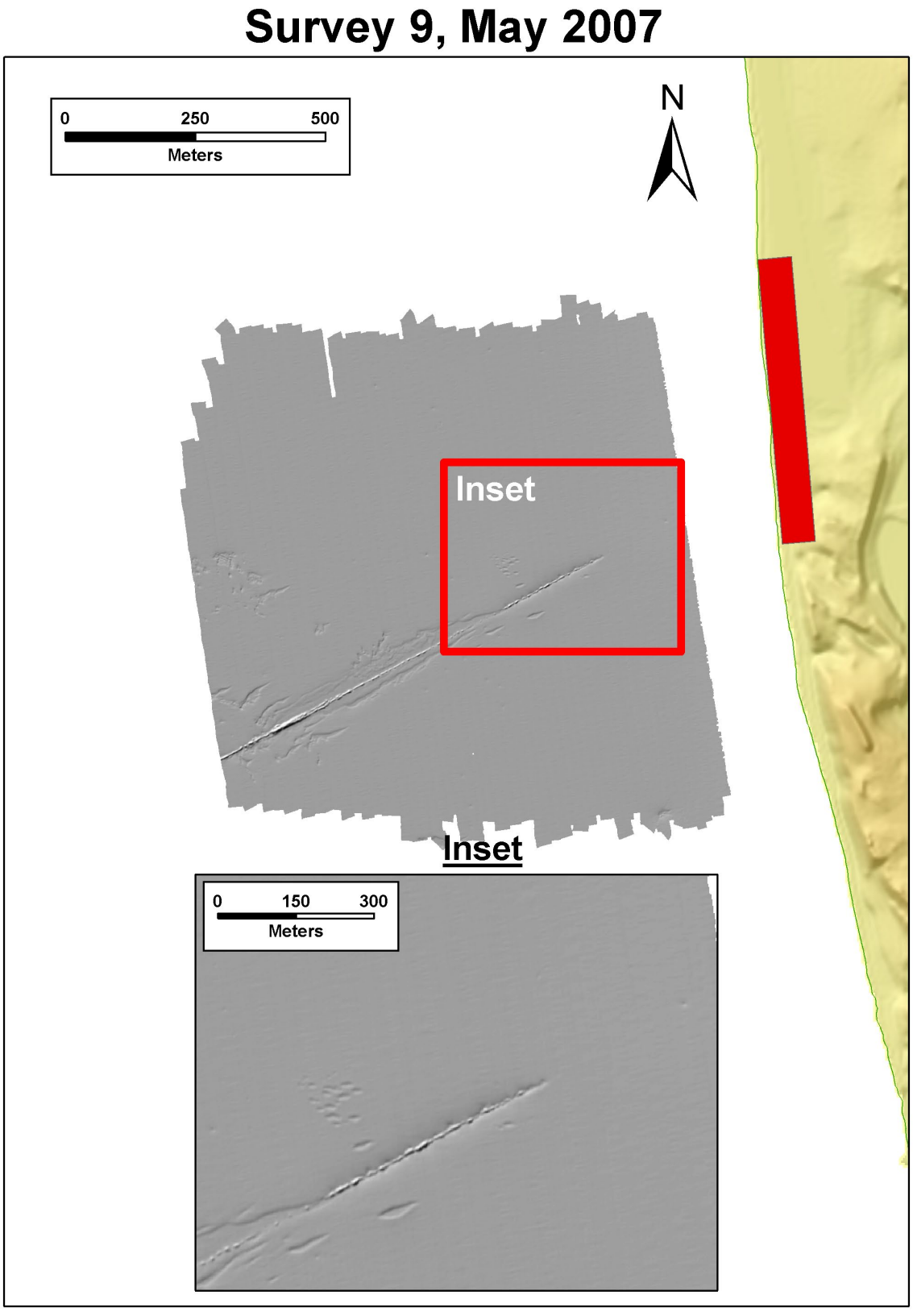

Figure A21. Shaded relief for Survey 9.

Figure A22. Shaded relief for Survey 10.

Figure A23. Shaded relief for Survey 11.

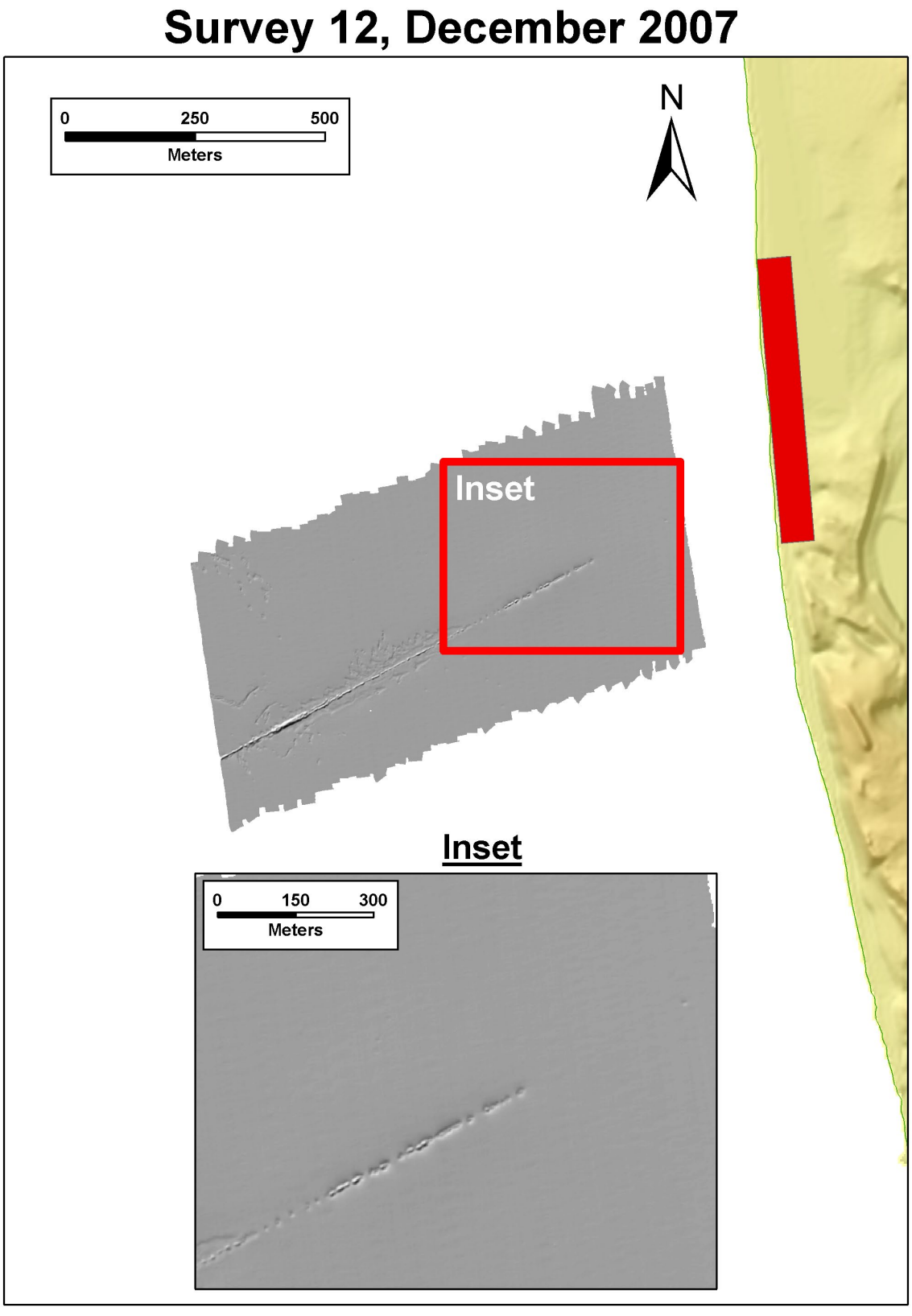

Figure A24. Shaded relief for Survey 12.

Survey Error and Uncertainty

There is inherent error in each data point collected due to GPS error (for example, due to atmospheric conditions, instrument precision), measurement error (for example, due to bumps on land, waves and salinity variations in the nearshore), and human error. The following is a brief section to demonstrate the steps taken to ensure that any error introduced in this research is primarily random, with little systematic error that would significantly alter the results and conclusions.

Topographic Surveys

Ashtech© Z-Extreme receivers were used for both ATV and CPS surveys and have manufacturer reported accuracies of approximately ±1 cm + 1ppm in the horizontal and approximately ±2 cm + 2ppm in the vertical while operating in RTK surveying mode (Magellan Navigation, Inc., 2006). These reported accuracies are, however, additionally subject to multi-path, satellite obstructions, poor satellite geometry and atmospheric conditions, which result in a total vertical uncertainty of 5 cm. Data points are discarded based on a quality rating which refers to the current satellite configuration, number of satellites, and rms error.

To detect non-GPS related error, cross-tracks of collected data points are compared for each survey conducted. An example is shown in figure A25, where 162 co-located (< 1 m apart) points are compared for the July 19, 2007, ATV survey. The plots show that although the greatest positional uncertainty was about 15 cm, the standard deviation is only 4.2 cm; there is no significant systematic offset (median < 0.5 cm), and the point pairs are extremely well correlated ($r^2 = 0.999$).

Error introduced by gridding is assessed by analyzing co-located (< 1 m apart) survey points and resulting grid points. Three examples are shown below to illustrate the range of random and systematic error introduced in this process (figs. A26-A28). Typical systematic error introduced by gridding is typically < 2 cm (for example, figs. A26-A27), with occasional values up to 4 cm (for example, fig. A28). In all cases the histogram is peaked near 0 (high kurtosis values) with minimal spread (low standard deviation) and excellent correlation ($r^2 > 0.99$). With typical beach slopes of 1:25, and a total mean elevation uncertainty of 10 cm (5 cm GPS + 1 cm measurement + 4 cm gridding), the shoreline position uncertainty would be 2.5 m, in the worst-case scenario.

CPS Profiles

While the horizontal and vertical uncertainty of individual data points is approximately 5 cm, the CPS operators cannot stay “on line”, in waves and currents, to this level of accuracy. Typically, mean offsets are less than 2.0 m from the preprogrammed track lines and maximum offsets along the approximately 1.5 km long transects are typically less than 10.0 m. Erroneous soundings are eliminated through manual editing and a mean filter based on all soundings within a 5 m search radius.

Measurement uncertainty is assessed in two different ways: (1) Consistency within the survey (cross-tracks, fig. A29), and (2) consistency between the 2 CPS vessels (duplicate lines, fig. A30). Both analyses demonstrate that the CPS depth point measurement error is insignificant. The soundings are extremely precise with a median error in both cases of 0 cm, high correlation, and low standard deviation.

Multibeam

For the multibeam surveys, a Trimble® 4700 GPS receiver logged position and attitude data with differential corrections provided by a Trimble® ProBeacon receiver. Horizontal positional accuracy of this system is typically ±1-2 m. Attitude (pitch, roll, yaw, and heave) data were recorded at 200 Hz by a TSS Position and Orientation System, Marine Vessel (POS-MV). Attitude accuracy for the POS/MV pitch, roll and yaw measurements averaged +/-0.03°, while heave accuracy was maintained at ±5 percent or 5 cm. Sonar, position, and attitude data were logged in XTF format using a Triton Elics Isis data acquisition system running Isis Sonar software. Multibeam data were monitored in real-time by using the 8101 Sonar Processor control interface and 2-D and 3-D display windows in the Isis Sonar and DelphMap software. In robust testing of the system, the total vertical uncertainty is ±12 cm (R. Kvitek, pers. comm.).

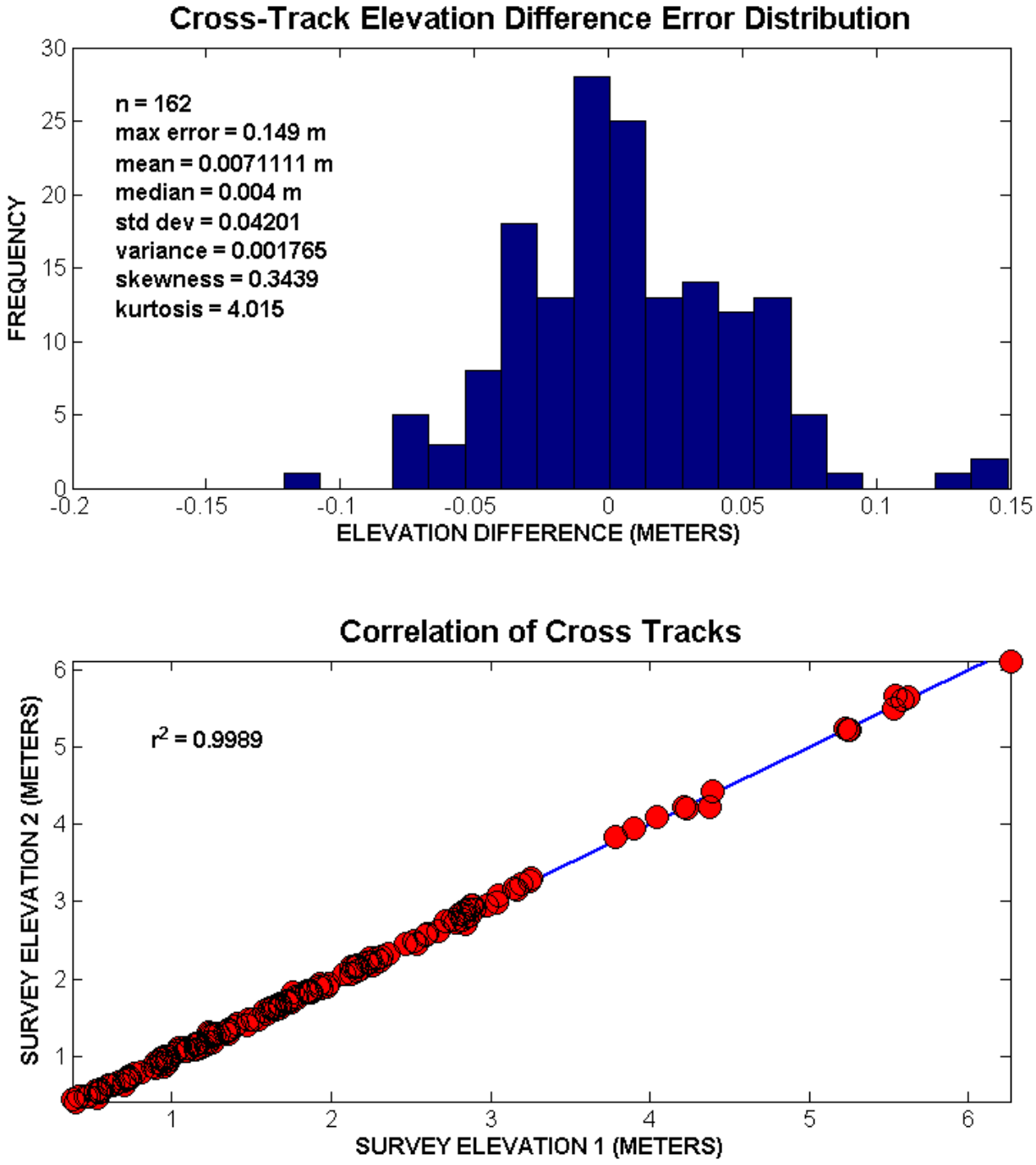

Figure A25. Error analysis of cross-tracks from the Ocean Beach ATV survey of July 19, 2007 (Survey 50).

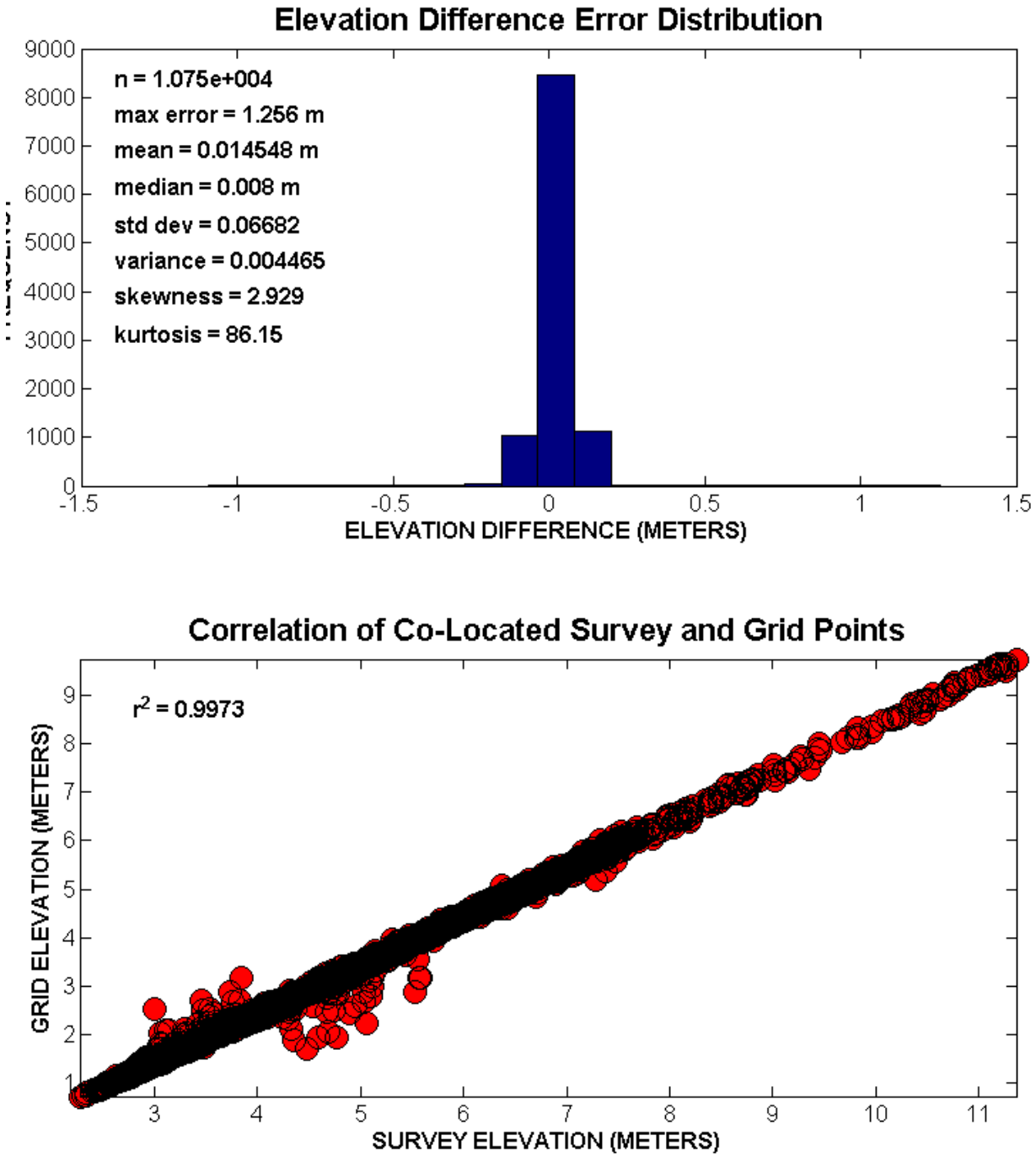

Figure A26. Error analysis of co-located survey points and grid points for the Ocean Beach ATV survey of December 22, 2005 (Survey 20).

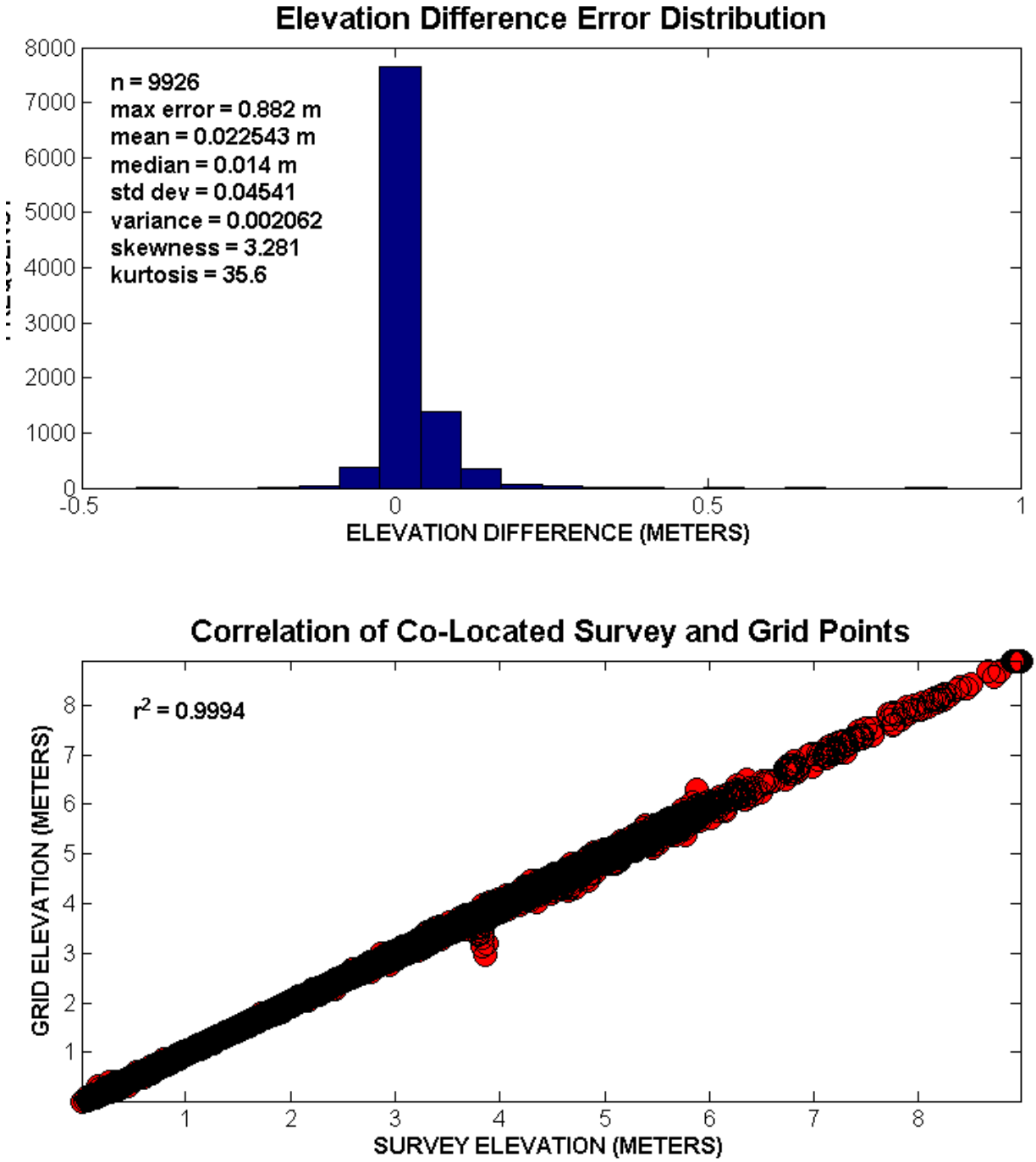

Figure A27. Error analysis of co-located survey points and grid points for the Ocean Beach ATV survey of March 5, 2006 (Survey 30).

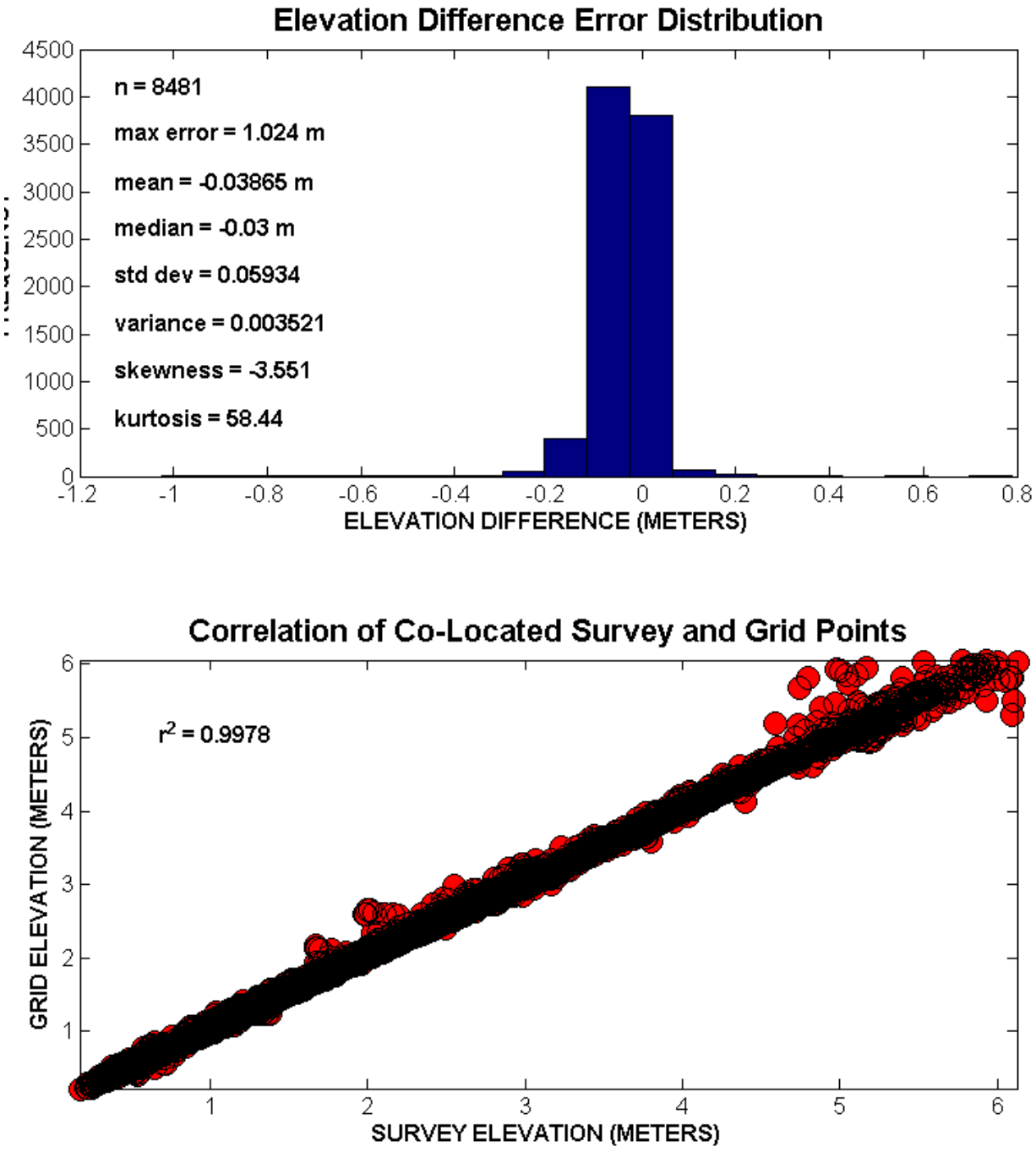

Figure A28. Error analysis of co-located survey points and grid points for the Ocean Beach ATV survey of July 19, 2007 (Survey 50).

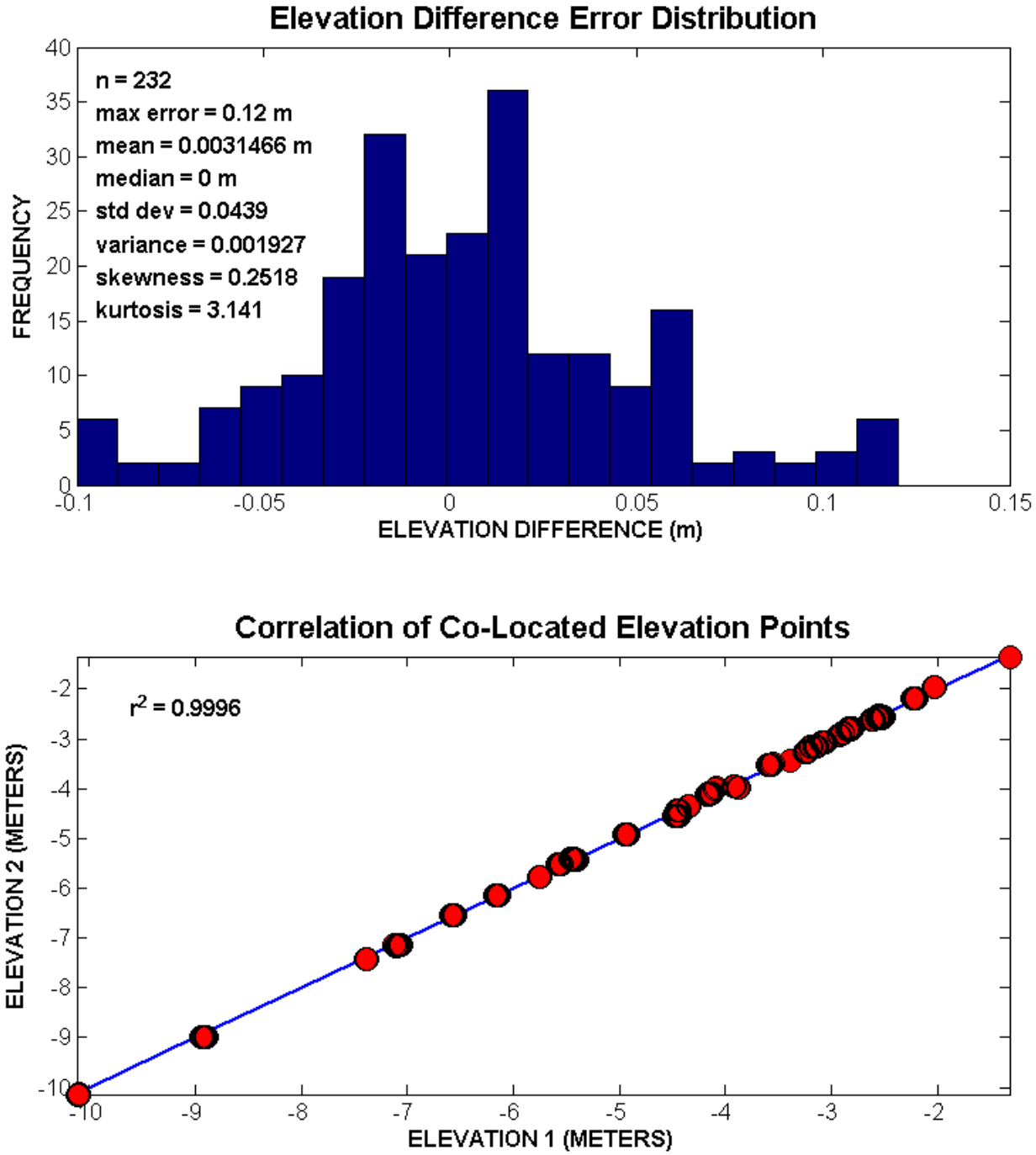

Figure A29. Error analysis of cross-tracks from the Ocean Beach CPS survey of October 24, 2007.

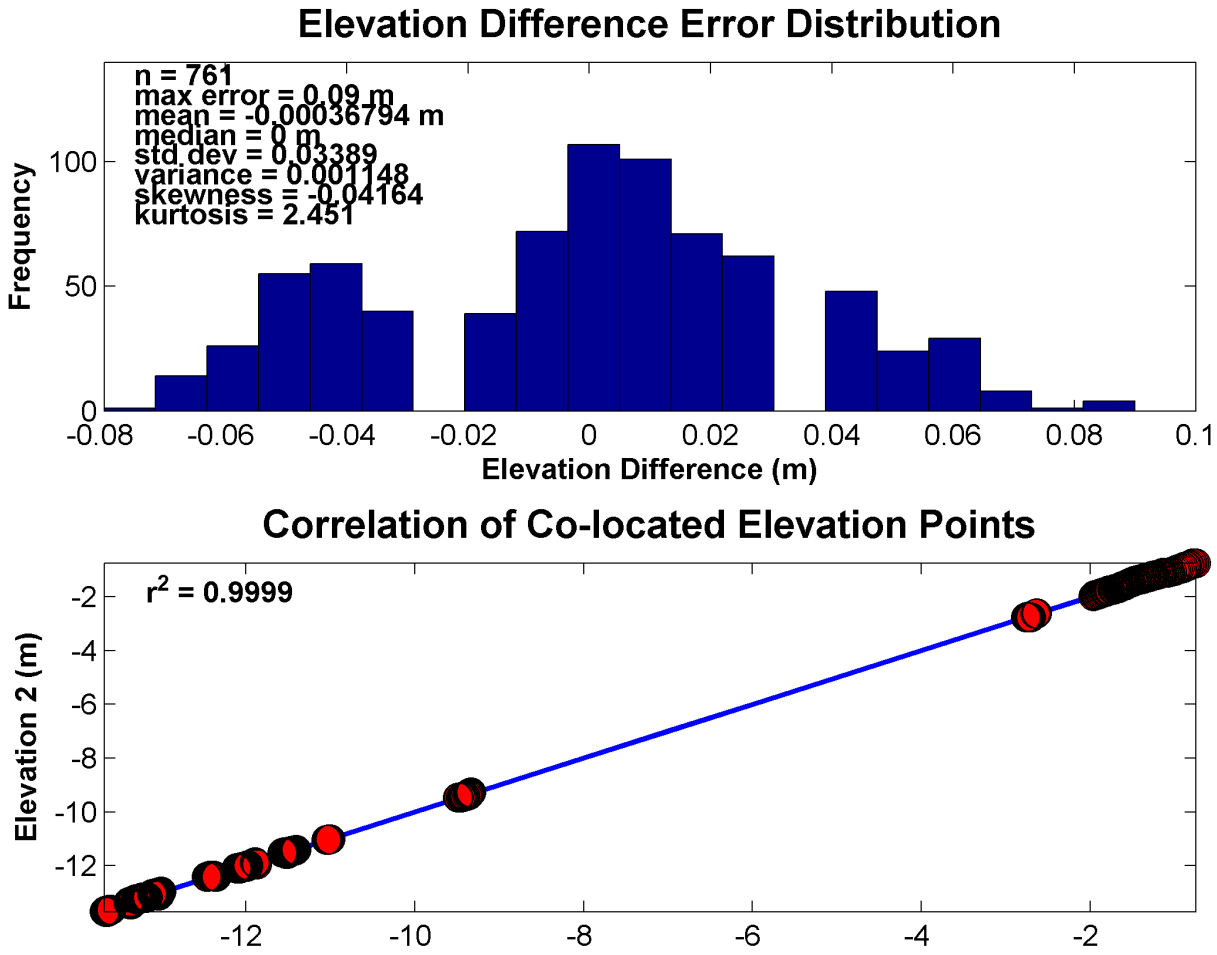

Figure A30. Error analysis of duplicate lines from the Ocean Beach CPS survey of October 24, 2007.

Publications and Other Resources

Below is a list of resources released to date and other links related to the Ocean Beach Coastal Processes Study:

Publications

Barnard, P.L., Eshleman, J.L., Erikson, L.H., and Hanes, D.M., 2007, Coastal processes study at Ocean Beach, San Francisco, CA: summary of data collection 2004-2006: U.S. Geological Survey Open-File Report 2007-1217, 165 p., http://pubs.usgs.gov/of/2007/1217/.

Barnard, P.L., Hanes, D.M., Lescinski, J., and Elias, E., 2007, Monitoring and modeling nearshore dredge disposal for indirect beach nourishment, Ocean Beach, San Francisco *in* Smith, J.M., ed., Coastal Engineering 2006: Proceedings of the 30th International Conference, v. 4, p. 4192-4204, http://walrus.wr.usgs.gov/coastal_processes/pubs.html.

Erikson, L., Hanes, D.M., Barnard, P.L., and Gibbs, A.E., 2007, Swash zone characteristics at Ocean Beach *in* Smith, J.M., ed., Coastal Engineering 2006: Proceedings of the 30th International Conference, Conference Proceedings, San Diego, CA, USA, 3-8 September 2006, v. 1, p. 909-921, http://walrus.wr.usgs.gov/coastal_processes/pubs.html.

Eshleman, J.L., Barnard, P.L., Erikson, L.H., and Hanes, D.M., 2007, Coupling alongshore variations in wave energy to beach morphologic change using the SWAN wave model at Ocean Beach, San Francisco, CA, *in* 10th International Workshop on Wave Hindcasting and Forecasting, Oahu, Hawaii, http://walrus.wr.usgs.gov/coastal_processes/pubs.html.

Barnard, P.L., and Hanes, D.M., 2006. Coastal monitoring of the May 2005 dredge disposal offshore of Ocean Beach, San Francisco, California: U.S. Geological Survey, Open-File Report 2006-1140, 27 p., http://pubs.usgs.gov/of/2006/1140/.

Barnard, P.L., Hanes, D.M., Kvitek, R.G, and Iampietro, P.J., 2006, Sand waves at the mouth of San Francisco Bay, California: U.S. Geological Survey, Scientific Investigations Map 2006-2944, 5 map sheets, http://pubs.usgs.gov/sim/2006/2944/.

Barnard, P.L., Hanes, D.M, Rubin, D.M., and Kvitek, R.G., 2006. Giant sand waves at the mouth of San Francisco Bay: EOS Transactions, v. 87, no. 29, p. 285, 289, http://walrus.wr.usgs.gov/coastal_processes/pubs.html.

Dartnell, P., Barnard, P.L., Chin, J.L., Hanes, D.M., Kvitek, R.G, Iampietro, P.J., and Gardner, J.V., 2006, Under the Golden Gate Bridge-views of the seafloor near the entrance to San Francisco Bay, California: United States Geological Survey, Scientific Investigations Map 2917, 1 map sheet http://pubs.usgs.gov/sim/2006/2917/.

Barnard, P.L., 2005, Modern processes at the mouth of San Francisco Bay: American Shore and Beach Preservation Association, 2005 Conference Field Trip Guide, 21 p., http://walrus.wr.usgs.gov/coastal_processes/pubs.html.

Barnard, P.L., and Hanes, D.M., 2005. Integrating field research, modeling and remote sensing to quantify morphodynamics in a high-energy coastal setting, Ocean Beach, San Francisco, California *in* 5th International Conference on Coastal Dynamics 2005 Conference Proceedings, Barcelona, Spain, American Society of Civil Engineers, CD-Rom, 14 p., http://walrus.wr.usgs.gov/coastal_processes/pubs.html.

Online Resources

- San Francisco Bight Coastal Processes Study Project Website: http://walrus.wr.usgs.gov/coastal_processes/sfbight/

- Coastal Evolution Modeling Project Website: http://walrus.wr.usgs.gov/research/projects/CEM.html

- Ocean Beach webcam: http://www.evsboca.com/usgs/default.htm

- USGS Online Reports
    - Ocean Beach Coastal Processes Study Summary http://pubs.usgs.gov/of/2007/1217/

    - Dredge Disposal Monitoring
      http://pubs.usgs.gov/of/2006/1140/

    - Sand Wave Maps
      http://pubs.usgs.gov/sim/2006/2944/

- Multibeam Data:
  http://seafloor.csumb.edu/SFMLwebDATA.htm